Université Mohamed Boudiaf - M'sila

FACULTE DE TECHNOLOGIE

DEPARTEMENT

Numéro de série……..…

Numéro d'inscription. **D.E/3C/01/17**

Thèse

Présentée pour l'obtention du diplôme de

DOCTORAT LMD

Filière : Electronique

Spécialité : Electronique et Télécommunications

THEME

Contribution à l'analyse et à la conception d'antennes microstrip à ondes millimétriques pour les réseaux de communication sans fil

Présentée Par

KHEZZAR Djamel

Soutenue le : 19 / 06 / 2022

Devant le jury composé de :

Nom & Prénom	Grade	Etablissement	Qualité
MEZACHE Amar	**Professeur**	Univ.de **M'sila**	Président
KHEDROUCHE Djamel	**Professeur**	Univ.de **M'sila**	Rapporteur
DENIDNI Ahmed Tayeb	**Professeur**	Univ.de **Quebec**	Co-Rapporteur
HOCINI Abdesselam	**Professeur**	Univ.de **M'sila**	Examinateur
LIDJICI Hamza	**Professeur**	Univ.de **Laghouat**	Examinateur

Année Universitaire : 2021/2022

A dissertation submitted for the degree of

DOCTORAT

Field: Electronics

Option: Electronics and Telecommunications

THEME

Contribution to the Analysis and Design of Millimeter Wave Microstrip Antennas for Wireless Communication Networks.

Djamel KHEZZAR

2022

Acknowledgments

First and foremost, I am thankful to ***ALLAH ALMIGHTY*** for blessing me with sound health, strength, and ability to perform and complete this thesis in the best manner. *Alhamdulillah.*

I would like to express my sincere gratitude to Pr. Djamel Khedrouche for his guidance and wisdom sharing during all these years. I especially appreciate that he gave me the freedom to do my own research while, at the same time, guiding me in the right direction with insightful comments and encouragement in all stages of this work.

My sincere thanks also goes to my co-supervisor Pr. Tayeb Ahmed Denidni. I deeply appreciate the welcoming gesture of my co-supervisor , and for providing access to the laboratory and research facilities when needed for all LASS research projects.

I would like to express my sincere gratitude and appreciation to Dr. Camilla Kärnfelt for all his continuous support, availability, guidance and her efforts in the manufacturing and the measurement of the LTCC prototypes in this research work.

I would like also to express my sincere gratitude and appreciation to Dr. Francois Gallee for his efforts in the measurement of the LTCC prototypes.

My gratitude also goes to the Microwave department-IMT Atlantique for providing the necessary materials and equipment in the design and the measurement of the antenna prototypes.

I am deeply grateful to all examiners Pr. MEZACHE Amar, Pr. HOCINI Abdesselam and Pr. LIDJICI Hamza for taking their time to read and evaluate my thesis.

I would like to thank my father for his generosity and care for my education despite his poverty. I would especially like to express my gratitude to my mother for selling her bracelet and buying me this computer, which was essential to complete my LMD degrees.

I would like to extend my warmest thanks to my brothers Omar and Aymen, to my dear Sister, my dear wife and my dear son, Ahmed Rissel. This work has sometimes prevented us from sharing important moments of life.

My gratitude also goes to Rissel, Taha Hocine, Imad and all my friends and colleagues without exception.

Abstract

The subject of the thesis concerns microstrip antennas, in particular those operating at millimeter waves. Millimetre-wave technology is being emphasized because of its capacity to transfer massive amounts of data. The antenna design challenges, as well as the benefits of the specified spectrum, are several, making this an extraordinarily rich and profound topic of research in recent and future years. This thesis aims to provide new structures of microstrip antennas operating at millimeter waves that meet the requirements of wide bandwidth and high gain while granting a degree of miniaturization and compatibility with the LTCC technology for integration and packaging solution. For this, very powerful commercial software such as the *CST Microwave Studio* and the *ANSYS HFSS* will be used. The ease of simulation on such software will allow us to better interpret and explain the results. Throughout the thesis, novel antennas are designed, manufactured, and characterized for optimal operation in terms of bandwidth, gain, efficiency, polarization, and their integration using advanced technologies and experience.

Keywords: Microstrip Antenna, Millimeter wave, 60 GHz, 0.3 THz, LTCC, SOT.

ملخص

يتعلق موضوع الأطروحة بهوائيات الميكروستريب، و التي تستعمل الموجات المليمترية على وجه الخصوص. ذلك لأن تقنية الموجات المليمترية لها قدرة هائلة على نقل كميات ضخمة من البيانات. تتعدد تحديات تصميم الهوائي ، مما جعل هذا المجال موضوعًا ثريًا وعميقًا بشكل غير عادي للبحث في السنوات الأخيرة وكذلك في السنوات المستقبلية. تهدف هذه الأطروحة إلى توفير هياكل جديدة من هوائيات الميكروستريب التي تستخدم الموجات المليمترية. والتي تلبي متطلبات النطاق الترددي العريض والكسب العالي مع منح درجة من التدقيق والتوافق مع تقنية LTCC من أجل سهولة دمجها مع الدارات الأخرى.

لهذا الغرض ، تم استخدام برامج تجارية قوية جدًا مثل CST Microwave Studio و ANSYS HFSS خلال هذا المشروع البحثي ، وتم تصميم هوائيات جديدة وتصنيعها وتحليل تجاوبها للتشغيل الأمثل من حيث النطاق الترددي والكسب والكفاءة والاستقطاب وسهولة دمجها باستخدام التقنيات والخبرات المتقدمة.

الكلمات المفتاحية: هوائي الميكروستريب ، موجات المليمترية ، 60 جيجاهرتز ، 0.3 THz ، LTCC، SOT.

Resumé

Le sujet de thèse concerne les antennes microruban, en particulier celles fonctionnant en ondes millimétriques. La technologie des ondes millimétriques est privilégiée en raison de sa capacité à transférer des quantités massives de données. Les défis de conception d'antenne, ainsi que les avantages du spectre spécifié, sont multiples, ce qui en fait un sujet de recherche extraordinairement riche et profond dans les années récentes et futures. Cette thèse vise à fournir de nouvelles structures d'antennes microruban fonctionnant aux ondes millimétriques qui répondent aux exigences de large bande passante et de gain élevé tout en accordant un degré de miniaturisation et de compatibilité avec la technologie LTCC pour l'intégration et la solution de packaging.

Pour cela, des logiciels commerciaux très puissants tels que le $ CST $ $ Microwave $ $ Studio $ et le $ ANSYS $ $ HFSS $ seront utilisés. La facilité de simulation sur un tel logiciel nous permettra de mieux interpréter et expliquer les résultats. Tout au long de la thèse, de nouvelles antennes sont conçues, fabriquées et caractérisées pour un fonctionnement optimal en termes de bande passante, de gain, d'efficacité, de polarisation et de leur intégration par des technologies et d'expérience avancées.

Mots clés : antenne microruban, ondes millimétriques, 60 GHz, 0,3 THz, LTCC, SOT.

Contents

Title page i

Acknowledgments iii

Abstract v

Table of Contents vii

List of Figures xi

List of Tables xiv

Nomenclature **xv**

Introduction **1**

1 Millimeter-Wave Communications and Microstrip Antennas: State of the Art and Research Challenges **5**

1.1 Introduction 5

1.2 Millimeter Wave 6

1.3 60 GHz Spectrum 6

1.4 60 GHz Standardization 8

1.5 Microstrip Antenna in Millimeter Wave 8

1.5.1 Conventional Microstrip Patch Antenna 9

1.5.2 Patch Antenna Modeling 10

1.5.3 Concept of Transmission Line Model 11

1.5.4 Micostrip Antenna Broadbanding Techniques 13
1.5.5 Micostrip Antenna: Reducing Size Techniques 13
1.6 Antenna Integration 14
1.6.1 Antenna on Chip (AoC) 14
1.6.2 Antenna in Package (AiP) 15
1.7 LTCC Technology 15
1.8 LTCC Antenna 16
1.9 Metamaterials 17
1.9.1 EBG Applications 18
1.9.2 Artificial Magnetic Conductors (AMC) 18
1.9.3 Photonic Band Gaps (PBG) 19
1.10 Terahertz Band 20
1.11 Background Literature Review 20
1.12 Research Objects 22
1.12.1 Motivations 22
1.12.2 Challenges 23
1.13 Methodology 23
1.13.1 Antenna Design Models 23
1.13.2 Antenna Design Tools 25
1.13.3 Antenna Optimization Methods 26
1.14 Conclusion 29

2 Design of LTCC Antenna for 60 GHz Applications 30

2.1 Introduction 30
2.2 Microstrip Antenna Design Challenges 31
2.3 Antenna Design 31
2.3.1 Antenna Geometry 31

2.3.2 Design Procedure and Optimization 32
2.4 Simulation and Results Discussion 36
2.4.1 Return Loss 36
2.4.2 Axial Ratio 37
2.4.3 VSWR 38
2.4.4 Impedance 39
2.4.5 Radiation 40
2.5 Results Comparison 43
2.6 Conclusion 43

3 Design of Ultra Wideband and Low Profile Microstrip Antenna for Millimeter Wave under 100GHz Using LTCC Technology 45
3.1 Introduction 45
3.2 Antenna Design 46
3.2.1 Geometry 46
3.2.2 Parametric Study 47
3.2.3 Geometry Discussion 50
3.3 Results and Discussion 51
3.3.1 Frequency Sweep Based Solutions 51
3.3.2 Radiation Pattern 55
3.4 Conclusion 56

4 Design of LTCC Based and CPW-Fed Broadband Microstrip Antenna for Millimeter-Wave Applications at 60GHz 59
4.1 Introduction 59
4.2 Literature Review 60
4.3 Antenna Design 60

4.3.1 Geometry 60
4.3.2 Optimization 61
4.4 Results and Discussion 63
4.4.1 Input Impedance 64
4.4.2 Return Loss 64
4.4.3 Parametrical Variation 67
4.4.4 Gain and Radiation 67
4.4.5 Manufacturing and Measurement 70
4.4.6 Results Comparison to Recent Similar Works 70
4.5 Conclusion 72

5 New *PBG* Microstrip Antenna for The Low *THz* spectrum 74
5.1 Introduction 74
5.2 PBG Based Substrate 75
5.3 Background of Study and Scope 76
5.4 Basic Antenna 76
5.5 SOT Method 80
5.6 GAs Optimisation and SOT Guiding Approach 83
5.6.1 Optimization criterion 83
5.6.2 Genetic algorithms 84
5.7 Space Optimisation 87
5.8 Parameters Optimisation 88
5.9 Conclusion 91

General Conclusion and Perspectives 98

Bibliography 119

List of Figures

1.1 ISM and other unlicensed bands allocation up to 100 GHz. 7

1.2 Conventional patch antenna. 10

1.3 Fringing Effects in patch antenna. 12

1.4 Essential fabrication steps of the LTCC process 16

1.5 High impedance surface representation. 19

1.6 The intersection of the millimeter waves and the THz band 21

2.1 Antenna geometry. 33

2.2 Optimization procedure. 35

2.3 Surface current distribution 36

2.4 Reflection coefficient. 37

2.5 AR curve. 38

2.6 $VSWR$. 39

2.7 Antenna resistance. 40

2.8 Antenna reactance. 41

2.9 Polar radiation pattern for E plan and H plan. 41

2.10 3D radiation pattern produced at 55, 60, and 65 GHz. 42

3.1 Antenna geometry. 48

3.2 Surface current distribution. 52

3.3 Reflection coefficient. 53
3.4 $VSWR$. 54
3.5 Antenna resistance. 54
3.6 Antenna reactance. 55
3.7 Antenna gain. 56
3.8 Polar radiation pattern for E plan and H plan. 57
3.9 66, 77, 85 and 93 GHz radiation pattern in 3D. 58

4.1 Antenna geometry. 62
4.2 Surface current distribution. 65
4.3 Antenna impedance. 66
4.4 Return Loss. 66
4.5 Return loss; parametric variation of REC1. 67
4.6 Gain at 60 GHz; in E-plane for Phi = 90 and H-plane for Phi = 0. . . 68
4.7 The antenna gain variation as a function of frequency. 69
4.8 3D radiation pattern at different frequencies. 69
4.9 Prototypes manufacturing and measurements. 71
4.10 Prototypes manufacturing and measurements. 71
4.11 Comparison of S_{11} simulation results and measurement of prototypes 1, 2 and 3. 72

5.1 (A) PBG structure of the reference antenna, (B) created antenna in $HFSS$. 78
5.2 Return loss curve. 79
5.3 Segmented and true surfaces cylinders 80
5.4 Air gap setup 82
5.5 Return loss plots of the PBG A, B, and C configurations. 82

5.6 Optimisation flow chart. 87

5.7 (A) The achieved configuration after space optimisation, (B) $HFSS$ created antenna. 89

5.8 Produced return loss plots after space optimisation. 90

5.9 (A) The new setup after parameters optimisation, (B) $HFSS$ created antenna. 92

5.10 Parameters optimisation's return loss. 93

5.11 The gain of the final optimised antenna 93

List of Tables

1.1 Classification of optimization techniques. 27

2.1 LTCC design criteria 32
2.2 Optimized dimensions 34
2.3 Results comparison 43

3.1 LTCC design criteria 47
3.2 The impact of design parameters on various antenna properties [1] . . 49
3.3 Antenna parameters 50

4.1 Design parameters 63
4.2 Comparison of the proposed antennas to the relevant reported antennas. 73

5.1 Obtained dimensions for the reference antenna. 79
5.2 Antennas Comparison to the most recent reported works. 94

Abbreviation

AiP: Antenna in Package

AMC: Artificial Magnetic Conductors

AoC: Antenna on Chip

BCB: Benzo Cyclo-Buten

CPW: Coplanar Waveguide

CST: Computer Simulation Technology

DE: Differential Evolution

DNG: Double Negative

EBG: Electromagnetic Band Gap

ECMA: European Computer Manufacturer Association

EM: Electromagnetic

FCC: Federal Communications Commission

FDTD: Finite Difference Time Domain

FEKO: Feldberechnung Für Körpermitbeliebiger Oberfläche

FEM: Finite Element Method

FETD: Finite Element Time Method

FIT: Method,Finite Integration Technique

Fr: Resonant Frequency

FSS: Frequency Selective Surfaces

GA: Algorithms

GSM: Global System for Mobile communications

HF: High Frequency

HFSS: High-Frequency Structure Simulator

ISM: Industrial, Scientic and Medical

LCP: Liquid Crystal Polymer

LH: Left-Handed

LOS: Line-Of-Sight

LP: Linearly polarized

LTCC: Low Temperature Co-Fired Ceramic

MLFMM: Multilevel Fast Multipole method

mmWave: Millimeter-Wave

MoM: Method of Moments

MRTD: Multi-Resolution Time Domain

NEC: Numerical Electromagnetics Code

NLOS: Non-Line-Of-Sight

NRI: Negative Refractive Index

PBG: Photonic Band Gaps

PCBs: Printed Circuit Boards

PMC: Perfect Magnetic Conductor

PO: Physical Optics

PSO: Particle Swarm Optimizers

PSTD: Method, Pseudospectral Time Domain

RF: Radio Frequency

SBR: Shooting and Bouncing Rays

SETD: Spectral Element Time Domain

SiP: System in Package

SoC: System on Chip

Thz: Terahertz

UWB: Ultra-Windelband

WiGig: Wireless Gigabit Alliance

WPANs: Wireless Personal-Area Network

Introduction

Since the advent of language, drawing, and writing, and more recently with the development of radio communication, the Internet, and the newly enabled technology such as IoT, man has never ceased to develop the communication tools at his disposal. Using wireless communications, billions of individuals have been able to connect to the Internet, allowing them to participate in today's digital economy. Consumers may use their phones everywhere in the globe thanks to agreed-upon mobile phone standards.

The huge demand for wireless data bandwidth shows no signs of slowing down in the near future. Consumers' mobile data experiences are growing and evolving at the same time, putting increasing demands on the network's utilization of the available wireless spectrum. Thus, the cellular industry has shifted its focus to other frequency bands that can be employed in the development of new wireless technologies, such as 5G and 6G, in anticipation of this projected growth. The millimeter-wave bands were chosen because they can handle large bandwidths and high data rates, making them ideal for enhancing wireless networks' capacity.

Previously, the use of such high-frequency bands was considered inappropriate for cellular systems due to the high propagation losses where signals are easily obstructed not just by building materials and plants but also by the human body. Nowadays, The usage of these bands is supported by improved antenna technology

and a better knowledge of channel characteristics and signal transmission. As a result, there are several problems and rewards, making this an extraordinarily rich and profound area of research in recent and future years. The antenna is crucial for using this spectrum, where many academics have been attempting to improve the antenna response under these conditions in order to enhance the radiating element design's performance. The work done for this thesis is intended to tackle these problems.

This research was conducted out by LASS laboratory at University of M'sila. Throughout the thesis, novel antennas are designed, manufactured, and characterized for optimal operation in terms of bandwidth, efficiency, gain, polarization, and their integration using advanced technologies and experience.

In the first chapter, we present a bibliographic study that will allow us to review the solutions that have been provided to address these issues. This first chapter will also be an opportunity to understand the interest in the millimeter-wave spectrum and the problems that come with it. In this regard, we present the millimeter wave spectrum and the 60 GHz band's features and the band's standards and prospective applications. The principles of microstrip antenna models in general, as well as the transmission line model in particular, will be covered. After that, a state-of-the-art will be produced based on research already completed for radio-frequency devices and subsystems at 60 GHz. The study's motivation, as well as its objectives and contributions, are discussed.

In the second chapter, Using Low-Temperature Co-fired Ceramic technology, numerical research was conducted in order to develop a wideband circularly polarized 60 GHz antenna. This antenna is focused on achieving an improved gain, size, circular polarization (CP), and wide bandwidth tradeoff so it can be employed in next wireless communication systems and 60 GHz unlicensed band applications.

The proposed multi-layer antenna design is simplified and enhanced to reduce manufacturing costs by eliminating the usage of vias, cavities, and metasurface, among other things.

In the third chapter, an ultra-wideband low-profile microstrip antenna for millimeter-wave applications below 100 GHz is presented to meet the demands of future wireless communication systems with high data rates. The suggested microstrip antenna is particularly helpful for current wireless communication systems because of its capacity to cover a wide bandwidth with good impedance matching. This antenna also has the advantage of being directly integrated with other RF devices that use LTCC multi-layer technology.

In the fourth chapter, another antenna based on LTCC technology will be presented to operate in the 60 GHz band. We will move on to prototyping this time, where three prototypes will be manufactured and measured with *Rohde & Schwarz ZVA67* Vector Network Analyzers. The antenna's achieved findings are compared to recent similar efforts. The antenna's performance makes it appealing for use in future wireless communications devices, and supports various additional 60 GHz applications. This project is carried out by a collaboration between University of Mohamed Boudiaf of M'sila and IMT Atlantique, Lab-STICC.

In the fifth Chapter, a novel photonic bandgap based antenna for broadband applications of low terahertz spectrum is suggested. First, a parametric analysis is used to design and optimize the reference antenna to operate at the resonance frequency of 300 GHz. The optimization is then carried out using a creative approach known as the Segmented Objects Technique (SOT), which is used by genetic algorithms to drive the optimization of the PBG-based substrate (GA).

This thesis will be finished with a general conclusion and perspectives.

Related Works

- **Articles:**
  - Khezzar, D., Khedrouche, D., Denidni, A. T., & Kärnfelt, C. (2020). A Low-profile Ultra-wideband LTCC Based Microstrip Antenna for Millimeter-wave Applications under 100 GHz.
  - Khezzar, D., Khedrouche, D., & Denidni, T. A. (2021). 60 GHz Broadband LTCC Antenna for 5G Mobile Communication Systems. Communications, 1, 5.
  - Khezzar, D., Khedrouche, D., & Denidni, T. A. (2021). New Design of a Broadband PBG-based Antenna for THz Band Applications. Photonics and Nanostructures-Fundamentals and Applications, 100947.
- **Conferences:**
  - Khezzar, D., Khedrouche, D., Denidni, TA., & Bencherif, H. (2018, December). 60 GHz Circular polarized patch antenna based on LTCC technology. In Second Int. Conf. Electr. Eng. ICEEB, no.
  - Khezzar, D., Khedrouche, D., Karnfelt, C., Denidni,TA., Gallee, F. LTCC Based Broadband Microstrip Antenna for Millimeter-Wave Applications at 60 GHz. 19th IEEE International Multi-Conference on Systems, Signals & Devices 2022 May 06-10, 2022. Faculty of Technology, University Ferhat Abbas Setif 1, Algeria.

Chapter 1

Millimeter-Wave Communications and Microstrip Antennas: State of the Art and Research Challenges

1.1 Introduction

This chapter presents an overview of the millimeter wave spectrum and its importance in antenna engineering. The main aspects, factors and techniques are introduced and discussed. We go through the basics of microstrip antenna models in general and the transmission line model in particular. This involves employing modern antenna technologies to integrate the antenna with the rest of the wireless module in millimeter waves, namely AoC and AiP solutions and their performance. The research's motivation, as well as the objectives and contributions, are outlined.

1.2 Millimeter Wave

The millimeter wave band is the electromagnetic spectrum where waves propagating in the frequency interval between 30 and 300 GHz. This is equivalent to wavelength of $10 - 1$ mm in the air [2, 3]. A narrow bandwidth is offered in previously employed technologies of low-gigahertz wireless communication bands, offering a data rate lower than 1 Gb/s. Nowadays, it is an important research topic to keep providing a high-speed wireless connection with acceptable QOS and range capabilities. The millimeter-wave frequency bands are less congested and have a larger unlicensed RF bandwidth compared to low-gigahertz wireless communication bands. Thus, the use of millimeter waves provide an essential advantage in ensuring that enough bandwidth for the transmission of a variety of multimedia material [2, 4].

The millimeter-wave spectrum has been used for many decades where the available millimeter-wave systems have primarily been employed in military domain [5]. This technology has begun to garner increasing attention in the industry, academia, and organizations of standardization because of the advance in processing technologies and low-cost integration solutions [3]. At 60 GHz, a bandwidth of $3 - 7$ GHz is available worldwide and changes depending on the region. The automobile sector is moving toward the 77 GHz band for car radar systems due to their various advantages specific to the field of automotive radar. Increased activity has also been seen in the 94, 120, and 194 GHz bands, which are used for home-land security applications like as radar, remote sensing, and imaging systems [6].

1.3 60 GHz Spectrum

For low operating costs, unlicensed or industrial, scientific, and medical (ISM) radio bands should be used instead of regulatory licensed bands [7]. One of the determin-

ing aspects that makes 60 GHz technology interesting and has sparked substantial attention recently is the availability of large unlicensed bandwidth (up to 7 GHz free to use around 60 GHz) that is available worldwide [8, 9]. 60 GHz spectrum is very favorable for wireless short-distance communications due to strong absorption by oxygen [10]. This could importantly offer various advantages over existing communication systems utilized in short range communications and indoor network where the frequency efficiency can be improved. The FCC's bandwidth distribution for the ISM and unlicensed bands below 100 GHz is shown for USA in Figure 1.1.

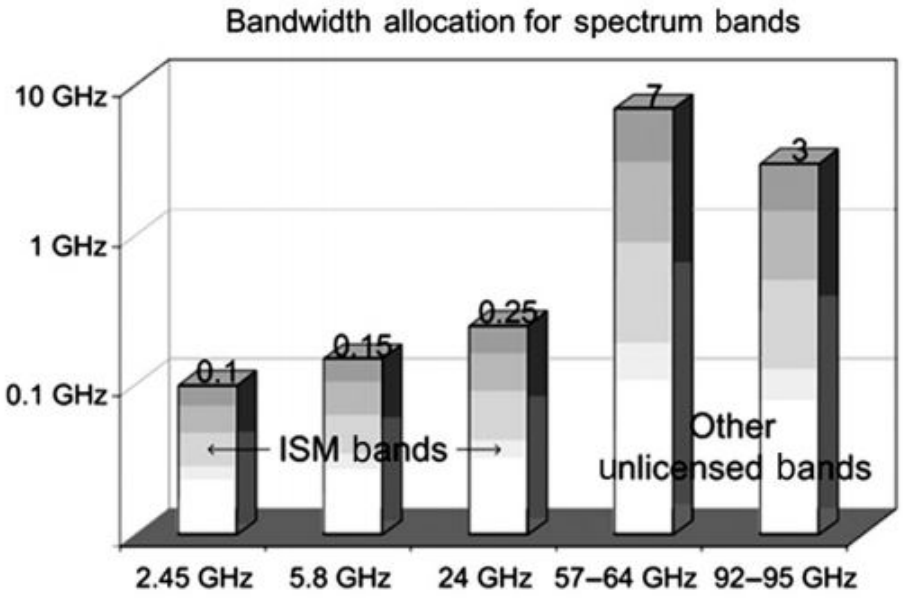

Figure 1.1: ISM and other unlicensed bands allocation up to 100 GHz [7].

Due to frequency slots designated for military, civilian, and personal communications services, the RF spectrum is crowded under 25 GHz. Without a doubt, most of conventional mobile data communications and commercial products are operating in the frequency spectrum below 10 GHz. By way of example, the Global System for Mobile Communication (GSM) is employed in Europe at 900, 1800 MHz and 850, 1900 MHz in the USA. Ultra Wideband (UWB) radios are permitted to

operate from 3.1 to 10.6 GHz [7]. The appropriate electromagnetic waves propagation environment and hardware capabilities are the basic reasons [11]. However, the bandwidth that is given for the unlicensed ISM bands is less than 1 GHz in total, at 2.45, 5.8, and 24 GHz. On the contrary, in the 60 GHz spectrum area 7 GHz of bandwidth is available for free exploitation.

1.4 60 GHz Standardization

The $IEEE$ 802.15.3c standard was established in [12] for wireless personal area networks (WPANs). The European Computer Manufacturer Association (ECMA version 2.0 in December 2010) [13] has established a 60 GHz technology standard for unlicensed short range communications with very high-data rates. The $IEEE$ 802.11ad [14] standard, for Wireless Gigabit Alliance (WiGig) was approved in 2013. It supports data speeds of up to 7 Gb/s, which is more than ten times faster than the previous maximum speed enabled by the $IEEE$ 802.11 standard [7].

1.5 Microstrip Antenna in Millimeter Wave

The antenna is one most indispensable elements in every wireless communications system [15]. In millimeter wave spectrum, this element suffers from various design problems such as complicated structures, higher order modes loss and, low gain. Because of its compactness, ease of production and integrability, the microstrip antenna is the preferable alternative for millimeter wave components [16]. 60 GHz band offers many opportunities, making this band an attractive solution for short-distance and wideband indoor wireless communications. However, many types of antenna structures are considered not suitable for 60 GHz WPAN/WLAN applications due to the requirements for high gain, low cost, lightweight, and small size [3].

Electromagnetic waves at 60 GHz are strongly attenuated because of free space losses, atmosphere, and solid obstacles. Due to these signal propagation problems at this range of frequency, certain additional requirements are necessary for the design of the antenna to compensate for these significant losses. A high gain directional radiation pattern is one of the most desired features due to the high attenuation at 60 GHz, where various studies show that achieving gigabit per second data rate requires high antenna gain, especially in relatively long ranges. For example, to achieve a data rate of 5 Gbps in a distance of 20 m, a combined antenna gain of 25 and 37 dBi is required for LOS (Line Of Sight) and NLOS (Non Line Of Sight) links, respectively [17]. Note that a single antenna element is not sufficient in many applications. Thus, either external devices like as horn or lense or antenna arrays must be used to produce the beam [18]. Moreover, the narrow bandwidth is a critical drawback in high data rate systems. With the classical microstrip antennas, it is challenging to acquire a bandwidth of more than 8 %. Thus, several researchers have performed significant works in designing multi-band and wideband antennas for millimeter waves spectrum over the last decades because of their ability to support multiple bands.

1.5.1 Conventional Microstrip Patch Antenna

At microwave frequencies, microstrip patch antennas have been widely investigated and are now well known. They're simple to make, work with integrated microstrip circuits, and inexpensive. As shown in Figure 5.1, a microstrip patch antenna consists of a ground plane on one side of a dielectric material and a metallic radiator on the other. The patch is constructed of a conducting material like gold or copper. The patch shape can be square, rectangular, circular, triangular, elliptical, or some other common shape [19, 20]. The patch shape, the ground, and the feed lines are

photo-etched on the dielectric substrate. A variety of feeding configurations are possible for the microstrip patch antenna, such as microstrip line feed, probe feeds, aperture feed, inset feeds, and proximity feed. Each method has advantages depending on the application. Despite their benefits, microstrip antennas pose significant design issues related to their naturally restricted bandwidth. At millimeter-wave frequencies, this type of antenna suffers from the low radiation efficiency, the surface wave, the losses in the feed lines, and the mutual coupling in antenna array [21, 22].

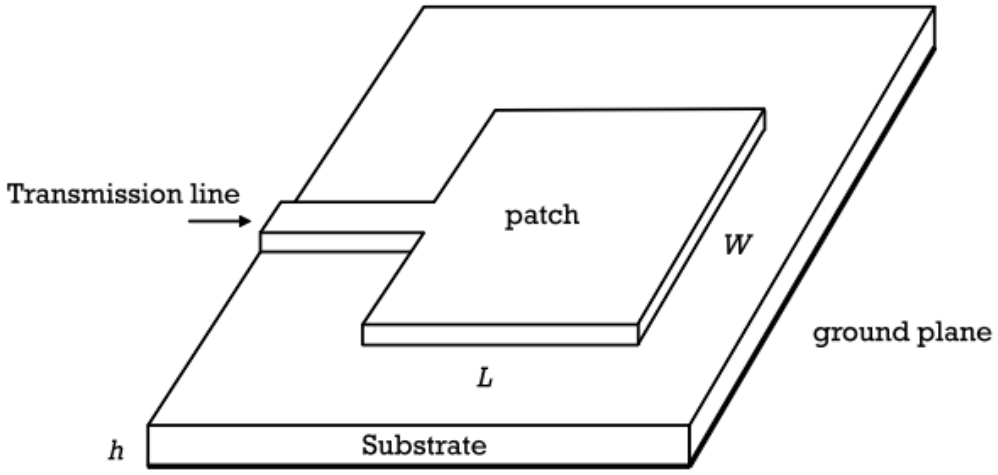

Figure 1.2: Conventional patch antenna.

1.5.2 Patch Antenna Modeling

Several models are known that can be used to analyze printed antennas. The most popular are the transmission line model, the cavity model, and the full-wave model (which mainly includes the integral / moment equation method) [23]. The transmission line model gives a good physical insight, and it is the simplest of all models, but it is the least accurate result [24]. On the other hand, the cavity model is more

precise in terms of results, but it is complex. These two techniques make many simplifying assumptions on the geometry of a problem to apply closed solutions. Full-wave approaches examine the full geometry without making assumptions about which field interactions are the most important a priori. Since a result, the full-wave analysis approach is extremely precise and adaptable, as it can handle single component, shaped element, multilayer element, finite and infinite arrays, and coupling [25–27].

The transmission line model, despite its inaccuracy, is nevertheless a helpful tool were it is very practical to begin the design of the microstrip element by using this model due to its simplicity. After that, further optimization and modeling are carried out in a full wave based solvers of any electromagnetic software [23].

1.5.3 Concept of Transmission Line Model

The intention of this subsection is to discuss basic concepts of the transmission line model according to Balanis [25]. In the transmission-line model, the patch are represented by two slots separated by a low impedance Zc transmission line of length L. Since the patch's length and width are limited, some field are contained within the dielectric, while some is in the air. As the dielectric constant of the substrate is much greater than the air permittivity ($\epsilon_r >> 1$), a new effective permittivity value ϵ_{reff} has to be calculated.

$$\epsilon_{\text{reff}} = \frac{\epsilon_r + 1}{2} + \frac{\epsilon_r - 1}{2}\left[1 + 12\frac{h}{W}\right]^{-1/2} ; W/h > 1 \tag{1.1}$$

Because of the fringing effects, electrically the patch of the microstrip antenna looks greater than its physical dimensions, see Figure 5.2.

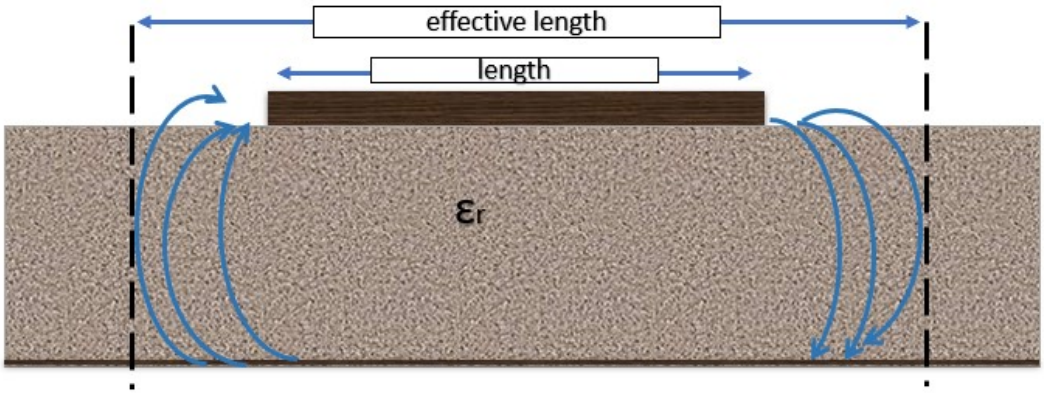

Figure 1.3: Fringing Effects in patch antenna.

$$\frac{\Delta L}{h} = 0.412 \frac{(\epsilon_{\text{reff}} + 0.3)\left(\frac{W}{h} + 0.264\right)}{(\epsilon_{\text{reff}} - 0.258)\left(\frac{W}{h} + 0.8\right)} \tag{1.2}$$

As the length is extended by ΔL per side, the effective length is :

$$L_{\text{eff}} = L + 2\Delta L \tag{1.3}$$

The resonant frequency in the dominant TM_{010} mode, is a function of length :

$$(f_r)_{010} = \frac{1}{2L\sqrt{\epsilon_r}\sqrt{\mu_0\epsilon_0}} = \frac{v_0}{2L\sqrt{\epsilon_r}} \tag{1.4}$$

The patch length can then be known by evaluating :

$$L = \frac{1}{2f_r\sqrt{\epsilon_{\text{reff}}}\sqrt{\mu_0\epsilon_0}} - 2\Delta L \tag{1.5}$$

The width that permits an acceptable radiation efficiency of the radiator is :

$$W = \frac{1}{2f_r\sqrt{\mu_0\epsilon_0}}\sqrt{\frac{2}{\epsilon_r + 1}} = \frac{v_0}{2f_r}\sqrt{\frac{2}{\epsilon_r + 1}} \tag{1.6}$$

1.5.4 Micostrip Antenna Broadbanding Techniques

The bandwidth of the microstrip antenna can be increased by using lossy substrates, but this is usually not desirable as the radiation efficiency will be reduced. A number of techniques have been developed in microwaves to broaden the bandwidths without compromising the efficiency of microstrip patch antennas. These techniques can be extended to millimeter-wave for designing an efficient wideband patch antenna. In this way, it is possible to use one or a combination of the following techniques [26, 28]:

- Increasing the substrate thickness.
- Decreasing the dielectric constant.
- Adding parasitic elements or slots.

In this last method for increasing the microstrip patch antenna bandwidth, parasitic elements permit the creation of dual or multiple resonances. Exciting these additional resonances in conjunction with the main resonance resulting in a broader overall band response. Designs based on one or a combination of the above principles can be used in the millimeter-wave spectrum. Note that a wide band microstrip antenna may cover more than the interest frequencies, making the antenna receive non-desired frequencies. In order to reject such frequencies, a filtering network is used.

1.5.5 Micostrip Antenna: Reducing Size Techniques

The microstrip patch antenna's resonant length is nearly $lambda/2$, where $lambda$ is the wavelength in the dielectric medium. However, it is advantageous that the dimensions of the patch be a small fraction of the free-space wavelength. By employing a substrate material with a high dielectric constant, the patch's size may be

lowered. However, this method results in a patch antenna with a narrow fractional bandwidth. The following techniques have been developed for size reduction [26] :

- By constructing a shorting wall along the null in the electric field across the middle of the patch, the resonant length may be lowered by a factor of two.
- By placing a shorting pin near the feed, the resonant length and surface of a circular patch can be reduced by a factor of three and nine, respectively.
- Small size patch antenna can also be achieved by applying previous broad-banding methods such as layered patches, sloted patch [29].

1.6 Antenna Integration

The method of integrating the radiator with the rest of the wireless modules is one of the most notable difference of millimeter waves and microwave technologies under 10 GHz [30]. In general, there are two mainly hardware solutions for consumer electronic devices in millimeter-wave antenna packaging, the Antenna on Chip (AoC) and the Antenna in Package (AiP). System on Chip (SoC) technology integrates digital, analog, and radio frequency (RF) circuits on a chip by a semiconductor process. In SiP technology, the functional blocks are separately manufactured and assembled in a package by a packaging process [31].

1.6.1 Antenna on Chip (AoC)

Miniaturization is a crucial factor in RF System on Chip design. Its principle consists of the integration of the RF component with the rest of the digital and analog circuits in one chip using advanced CMOS technology [32]. To minimize the transmitter size, the antenna has to be miniaturized as it is the largest part of a typical transceiver

module. This technology yields improved system reliability and functionality at a much lower system cost and size with a low power consumption [31, 32].

1.6.2 Antenna in Package (AiP)

System in package (SiP) is another efficient method that enhances system performance and reduces system power consumption. AiP is an antenna that is built into the driving circuit package. This technology permits the realization of multilayer antennas that minimize the system's total size with no additional printed circuit boards (PCBs) for antennas manufacturing or external antenna board connections. At millimeter-wave bands, this packaging technology increases compactness and cost savings, low-loss and more efficient antennas can be realized [31].

1.7 LTCC Technology

In terms of design freedom, antenna performance, and cost effectiveness, the substrate material for millimeter-wave antenna modules is a significant design element [30]. The industry standard for PCBs based on FR-4 has become inappropriate due to impractically massive losses, so that it is not suited for SoP in high speed wireless applications. The Low temperature cofired ceramic (LTCC) is an attractive integration solution. It has excellent packaging hermeticity and can allow dense multilayer circuit integration [3]. Because of its process maturity / stability and relatively high dielectric constant, LTCC has been widely employed as a packaging material, allowing for a substantial decrease in module / function size [4].

The LTCC manufacturing is a multi-step process comprised of simple series of manufacturing steps that are summarized in Figure 5.5. The main fabrication steps of the LTCC process consist of forming via hole, via filling, conductor printing,

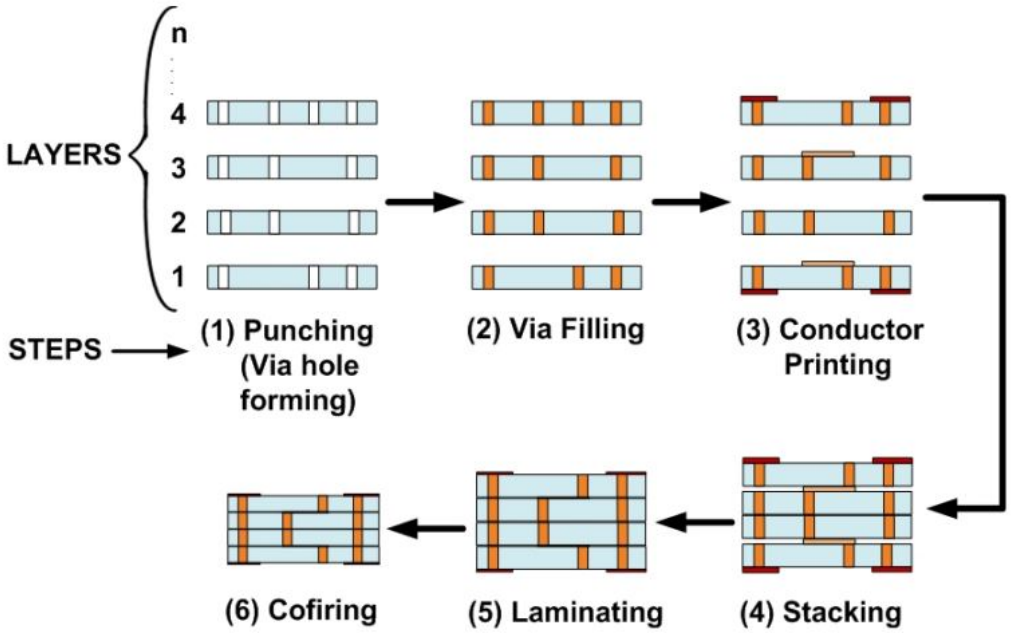

Figure 1.4: Essential fabrication steps of the LTCC process [34].

stacking, laminating, and co-firing. This process is terminated by measurement and validation of the design quality. Gold and silver are generally used for metallization, which reduces the conductor losses [33].

1.8 LTCC Antenna

Due to the rapidly expanding need for multifunctionality, high performance, and miniaturization of modern mobile terminals, researchers have begun to focus on antennas in LTCC technology since the turn of the century [35]. The LTCC technology is actively studied for millimeter wave antennas and packaging solution because it guarantees low dielectric and conductor losses. Besides, LTCC technology permits high design freedom in antenna manufacturing throughout the high possible number of layers, ease of integration, flexibility in via holes distribution, and mechanically robust, which make it the promising technology for excellent high-frequency perfor-

mance [36–38].

1.9 Metamaterials

Metamaterials have gained a great interest in microwave, millimeter wave and THz spectrum as they offer new functionalities and enhanced performance compared to conventional antennas [39]. Meta-surfaces have been proposed for the development of many other devices such as filters [40], phase shifters [41], polarization converters [42], absorbers [43], etc.

Various terminologies are used in respect to the application domain, such as photonic band gaps (PBG), photonic crystals, and frequency selective surface (FSS). All these are classified under the broad terminology of "Electromagnetic Band Gap (EBG)" structures [44, 45]. Different names have also been used in terms of the exhibited electromagnetic properties, such as [45, 46]:

- **Double negative (DNG)** both negative permittivity and permeability;
- **Negative refractive index (NRI)**;
- **Left-handed (LH)** when a left-hand relation is ensured;
- **Magneto materials** high permeability controlled artificially;
- **Soft and hard surfaces** Prevent or assist the propagation of wave;
- **Artificial magnetic conductors (AMC)** provide same properties as PEC;
- **High impedance surfaces**.

1.9.1 EBG Applications

These unique electromagnetic properties of EBG structures have led to a wide range of applications in antenna engineering [45].

- **Surface wave suppression:** To boost the antenna gain, eliminate the back lobe, and lower the mutual coupling level in the antenna array, EBG structure is employed.
- **Efficient low profile antenna designs:** The EBG surface has a lot of promise for low-profile wire antenna applications such dipole antennas, monopole antennas, and spiral antennas.
- **High gain antenna:** Antennas with a high gain are also designed using EBG structures.

EBG structures offer a wide range of applications in microwave circuit design, in addition to antennas [47].

1.9.2 Artificial Magnetic Conductors (AMC)

According to research on EBG structures, they can achieve the PMC condition in a specific frequency range. AMC is a metamaterial configuration. At its resonance frequency, it can offer zero-degree reflection phases, simulating the properties of a perfect magnetic conductor (PMC) [48]. AMC's reflected wave is in phase to the source wave. The additional reflected waves interfere with the original wave in a positive way. The antenna's radiation gain and efficiency are improved by combining reflected and source waves. The AMC structures are often made up of dielectric materials and metallic conductors arranged in a regular pattern, see Figure 5.4. The surface impedance consists of real and imaginary parts. Note that AMC

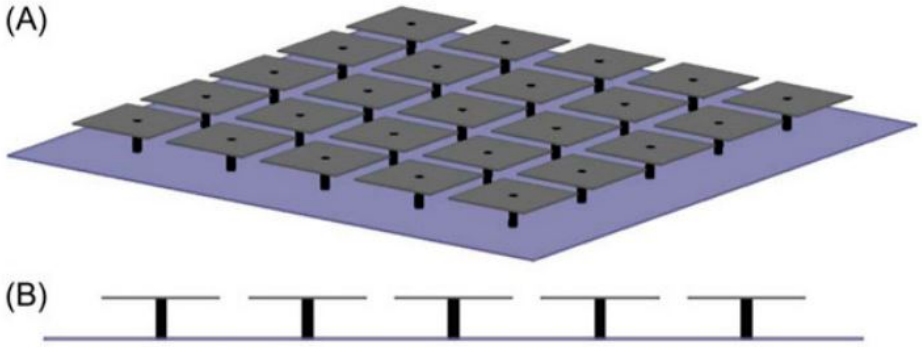

Figure 1.5: High impedance surface representation. (A) bird's eye view; (B) cross-sectional view [49].

unit cells can be constructed with and without shorting pin from the metallic patch of AMC unit cell to the ground. [48].

1.9.3 Photonic Band Gaps (PBG)

The use of thicker substrates in microstrip antenna generates surface-wave losses as the substrate traps the majority of the emitted power. Such losses can be compensated for by the use of PBG substrate, which is obtained by periodically implanting air gap cylinders on a substrate [50]. The bandwidth of a microstrip patch antenna using PBG substrate can be greater than 35% of that of a simple patch antenna. [51]. Moreover, as antennas applications move to higher frequencies, resulting in microstrip patch antennas with reduced efficiency and gain as well as an unacceptably high level of mutual coupling and cross-polarization within an array environment. PBG technology has been applied as a new promising solution to these problems [27].

1.10 Terahertz Band

As the demand for unoccupied and unregulated bandwidth for wireless communication networks increases, operation frequencies will eventually switch to the lower THz frequency range. The portion of the electromagnetic spectrum between the microwave band (100 GHz) and the far-infrared band ($>$ 10 THz) is known as terahertz (THz). Due to its unique properties and diverse application sectors, this spectrum is a particularly active study topic [52]. Terahertz technology has attracted increased research attention due to its wide variety of applications, which include material characterization, spectroscopy, sensing, earth and space science, defense, telecommunication, THz imaging, medical applications, and space science astronomy [53–55]. Furthermore, it is envisaged that it will be employed in the next generations of mobile communications system as higher carrier frequency will enable the rapid transmission of massive volumes of data, which will be required for new emergent applications [56, 57].

Figure 1.6 shows the intersection of the millimeter waves and the THz band [58]. Since atmospheric-transmission windows are available in the lower THz frequencies spectrum, carrier frequency of 300 GHz and beyond are likely to be employed for communication once the high-bitrate data transmission technologies are available[57].

1.11 Background Literature Review

In literature, extensive research efforts have been devoted, and various methods are proposed for the millimeter waves spectrum. In [59], a bandwidth of 13.3 % is obtained using an antenna implemented on a silicon membrane with an upper BCB (Benzo Cyclo-Buten dielectric material) thin film. This antenna is deposited

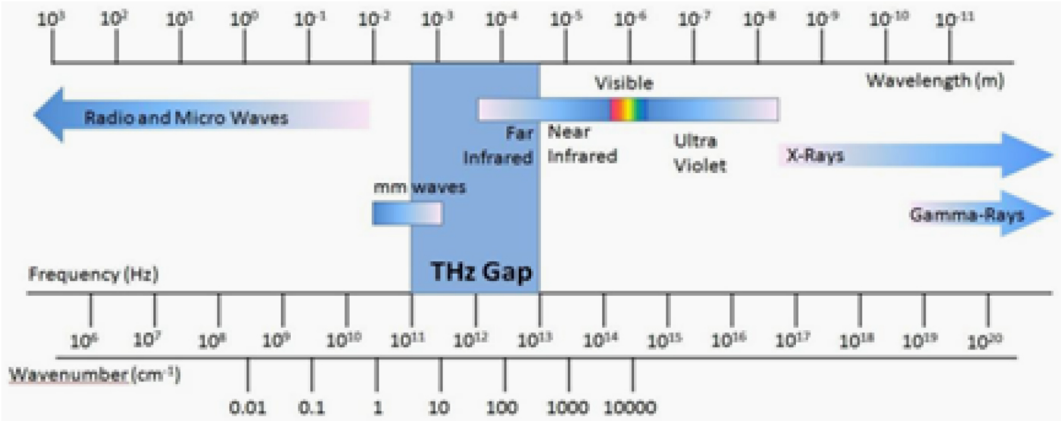

Figure 1.6: The intersection of the millimeter waves and the THz band [58].

and excited with a U-shape and T-shape microstrip feeder via a dielectric gap. In [60], a 60GHz coplanar waveguide (CPW) fed patch antenna implemented on a high dielectric constant substrate ($\epsilon_r = 9.9$). This proposed antenna has an operational bandwidth of 4.7 GHz or 7.75 % ranging from 58.3 GHz to 63 GHz. Note that the employed substrate is close to the dielectric constant of commercial GaAs and mimics the CMOS process. In [61], the artificial magnetic conductors (AMCs) with in-phase reflection characteristics have been investigated, where a 60 GHz CPW-fed patch antenna on multilayer LTCC- and LCP-based achieved a bandwidth of about 16 % and a peak gain of 5.1 dBi using the LCP (Liquid Crystal Polymer) substrate.

In [62], an antenna of two stacked dielectric layers of Roger Duroid, the grounded coplanar waveguide is located on the bottom layer and the microstrip ring on the top layer. The radiator part consists of a vertical ring patch in the middle position with a microstrip ring attached to its base. The antenna is fed by the special grounded CPW/microstrip/printed ring combination. An air cavity is employed to enhance the antenna gain. In terms of results, it has an impedance bandwidth of 26 % (28.4 GHz to 37 GHz) with an average gain of 7.9 dBi and stable radiation patterns across the operating bandwidth.

A multitude of configurations of printed antennas have been proposed and eval-

uated by several authors. Recent studies have shown that using millimeter-wave antennas with a restricted coverage area of 200 m or less can reduce meteorological attenuations while still allowing for frequency reuse. The necessity to deploy a high number of antennas is crucial in terms of cost as we move towards a short-range wireless communication architecture [63]. Thus, it is important to note that the use of a complex antenna structure may lead to overpriced systems. That's why much of the effort has to be focused on techniques for enhancing antennas within simple structures.

1.12 Research Objects

1.12.1 Motivations

The key benefits of the millimeter-wave spectrum are the microwave spectrum's needs such as wideband capability, small size and excellent performance. Millimeter-wave technology has received a lot of attention because of its potential to transfer very big data with low transmission power in short range outdoor and indoor wireless communication. [61, 64–67]. The considerable bandwidth within this frequency range allows for extremely high data throughput transmission. Moreover, millimeter waves at 60 GHz are more sensitive to outdoor environmental conditions like rain, gas, dust, vegetation, etc. The oxygen absorption introduces typical free-space propagation losses of 10-15 dB/km. Thus, the propagation of signals at 60 GHz is inherently limited to a short-range and, consequently, frequency reuse becomes naturally available across distances of a few tens of meters where more near co-sited systems operating on the same frequency can be established [13]. Thus, the challenges and benefits are many, making this an incredibly rich and deep area of research in the recent and coming years. Antennas play an essential role in taking

advantage of this band, and many researchers have been working on enhancing the antenna response under these conditions to offer higher performance of the radiating element design.

1.12.2 Challenges

To meet nowadays needs, the designed antenna should simultaneously provide multiple functionalities such as multi-band, broadband, and reduction in the power emitted in the direction of the user. It has been noted that as the frequency increases into the millimeter waves, the difficulties in antenna design move away from structural challenges to the fabrication process in order to avoid significant tolerances so as to decrease the manufacturing cost. To meet these requirements of fabrication, much attention has been directed to the antenna integration and packaging solution. Researchers have recently attempted to the development of new antenna design approaches that offer low conductor and dielectric losses and high design freedom. These additional features complicate the task of antenna designers, who must ensure good performance of the antenna system regardless of the above-mentioned environmental conditions and manufacturing difficulties.

1.13 Methodology

1.13.1 Antenna Design Models

Whether it is obvious or not, designing and optimization of passive components rely on solving Maxwell's equations. It is well known that manually solving complicated differential equations is very difficult and limited. These methods can only be applied for structures with basic shapes [68]. Computational electromagnetics is a crucial field that provides efficient numerical solutions to Maxwell's equations

for antennas construction and improvement. These numerical methods are based on empirical models where appropriate solutions can be found more easily, even in complex systems that can not be solved by analytical methods. To solve Maxwell's equations, all numerical methods divide space into subdomains in order to find solutions more easily [69]. The time domain solvers and frequency domain solvers are the two most often used computational approaches for antenna modeling [68]:

- **Frequency domain**
  - Integral Equation Solvers: surface integral equation solvers based on the MOM are the most commonly used
  - Partial differential equation solvers: include finite element method (FEM), spectral element method, finite difference frequency domain method, and pseudospectral frequency-domain method. Note that the FEM is the most commonly used frequency-domain technique in a commercial tool
- **Time domain methods**
  - Partial differential equation solvers: include finite difference time domain (FDTD) method, finite element time method (FETD), spectral element time domain (SETD) method, pseudospectral time domain (PSTD) method,finite integration technique (FIT), and multi-resolution time domain (MRTD) method. the FDTD is the mostly commonly used time domain technique in commercial tools.
  - Integral equation solvers : Solve the surface or volume integral equations derived from Maxwell's equations and Green's function for the background medium in time domain.

For wideband applications, time domain techniques are favored because they can offer all frequency domain data in a single simulation. Frequency-domain solvers,

are favored when a narrow band solution is required. The employment of various numerical approaches is imposed by the necessity for sensible results; nevertheless, every method has advantages and weaknesses, and therefore no solver is ideal for all situations.

1.13.2 Antenna Design Tools

Multiple numerical methods are generally integrated into a single commercialized simulation program to fully provide the benefits of each method. Thus, the use of commercial antenna design software to study how the antenna structure interacts with electromagnetic waves so that the structure and materials can be optimized to achieve the design goals. Many academics and engineers employ a number of tools that have been proved to be effective for antenna analysis and design. The following is a list of commonly used commercial tools [26, 68, 70, 71].

- **Numerical Electromagnetics Code (NEC):** a very popular open-source and noncommercial antenna simulation tool for wire and surface antennas based on the MoM technique.
- **High-frequency structure simulator (HFSS):** employs various electromagnetic solvers, including its highly accurate FEM, the large scale MoM technique, the ultra-large scale asymptotic methods of physical optics (PO) and shooting and bouncing rays (SBR) to simulate high-frequency EM fields and structures.
- **Computer Simulation Technology (CST):** CST Microwave Studio (CST-MWS) is used for simulation of high-frequency components and structures using a variety of solver modules based on different time-domain and frequency-domain methods such as FEM, MoM, Multilevel Fast Multipole method (MLFMM),

and SBR with distinct advantages in their own domains.

- **Feldberechnung für Körpermitbeliebiger Oberfläche (FEKO):** a computational software product for analyzing EM structures based on the method of moments (MoM) and asymptotic high-frequency techniques. It permits to analyze a broad spectrum of electromagnetic problems related to antenna design and placement, radar cross-section, and electromagnetic compatibility.

Note that this is a non-exhaustive list as there are certainly many other software and packages capable of doing antenna design simulations.

1.13.3 Antenna Optimization Methods

The initial design based on electromagnetic equations is often not the optimum. Most of the determining parameters are a function of the antenna's geometry, operating frequency as well as comprising materials. The basic antenna design can be improved via a parametric sweep. The change of design and materials parameters may assist in ensuring that the antenna response meets mandated performance standards for particular features such as antenna efficiency, radiation pattern, input impedance, and so on. However, this method becomes very difficult when the number of parameters increases. In many situations, an optimization procedure has to be applied in order to find near-optimal values of all of the design parameters. In other words, the numerical optimization permits to find of a suitable set of geometric and material properties for antenna design. Various optimization techniques have been employed in the literature for designing high-performance antennas. These techniques can be classified as indicated in Table 1.1 [70].

To minimize the design effort and shorten the development time, automation of the antenna design process can be realized by formulating the antenna parameter

Table 1.1: Classification of optimization techniques [70].

TYPE	e.g.,
local optimization with limited exploration ability	the classic Powell (CP) and grid search (GS) approaches
classical derivative-free standard local search	the Nelder–Mead simplex algorithm (N-M) and pattern search method (PS)
standard derivative-based local search	the quasiNewton (QN), sequential quadratic programming (SQP), sequential nonlinear programming (SNLP), and integeronly SNLP (ISNLP) techniques
surrogate-assisted local optimization with enhanced exploration ability	the trust region framework (TRF) and interpolated QN (IQN) methods
surrogate-assisted global optimization	The surrogatemodel-assisted differential evolution for antenna optimization approach (SADEA)
standard evolutionary algorithms	particle swarm optimization (PSO) and differential evolution (DE), covariance matrix adaptation evolution strategy (CMA-ES), and genetic algorithms (GAs) and simulated annealing (SA)

adjustment task as an iterative optimization problem with the objective function supplied by an EM solver. The cost function is used to apply a local or external evaluation process based on statistical analysis that compares the performance characteristics of the device generated using the associated set of input parameters. The cost function can return one or more values for single-objective or multi-objective optimization [72]. The simulations are usually very time-consuming processes and the evaluation time per design takes many hours. Thus, to reach the desired cost function goal, it is very desirable to utilize an optimization method that needs the fewest cost function calls. There are many various sorts of optimization algorithms, and some are unquestionably more suited to specific types of antenna design over others. In recent years, population-based search methods (also referred to as meta-heuristics) have gained considerable popularity [72, 73]. Here are three of the most commonly used algorithms :

- Particle Swarm Optimizers (PSO) [74].
- Genetic Algorithms (GAs) [75].
- Differential Evolution (DE) [76].

The GA can be implemented in a binary scheme or by using binary strings to represent discretized real values according to the number of bits chosen to represent each value. The remaining algorithms are naturally real-coded and lend themselves to optimisations with continuously variable parameters [76]. There exist many other types of optimization strategies, while some are more suitable for specific types of antenna design over others.

1.14 Conclusion

This chapter provided an overview of the background, motivation, and challenges of millimeter wave antennas in different wireless sectors. We've also gone over the various feeding strategies for microstrip antenna, as well as their analysis methodologies and the most popular commercial simulators in the field. The particular characteristics of the millimeter-wave spectrum and significant variables to consider during antenna design are also highlighted.

Chapter 2

Design of LTCC Antenna for 60 GHz Applications

2.1 Introduction

In this chapter, we suggest a broadband antenna for 5G cellular mobile networks to satisfy the need for high-speed data. This antenna is circularly polarized, allowing linearly polarized (LP) waves to be received in any direction. As a result, the transmission mistakes caused by polarization inconsistency are significantly reduced [36, 77]. The suggested multi-layer antenna design is simplified and improved to reduce manufacturing costs by eliminating the usage of vias, cavities, and metamaterial surfaces, among other things. To attain these goals, a parametrical study is used to conduct the numerical optimisation of the antenna response, with the vision of attaining better accuracy in terms of resonance frequency, wider bandwidth, adequate gain, and good impedance matching achieving higher resonance frequency accuracy, best impedance matching, broader bandwidth, and appropriate gain when compared to previously published antennas.

2.2 Microstrip Antenna Design Challenges

The antenna at millimetre waves, as an essential component of any wireless communication system, it has many design difficulties, including low gain, complicated construction, higher-order mode losses, and so on. Due to its compactness, conformity, integrability, and simplicity of manufacturing, the microstrip antenna is the preferable option for millimetre-wave devices [16]. This antenna is used in a variety of wireless communication systems, notably in mobile communications [78]. Nevertheless, a basic disadvantage of conventional microstrip antenna is the limited BW which is typically about 5 % [79]. A vast body of studies has been devoted to increase the BW of this type of planar antennas, resulting in a variety of enhancement options, including the use of metamaterials, cavities, and multilayer geometries [80–82]. However, the circuit's complexity and manufacturing cost rise as a result of the additional production procedure. Furthermore, the antenna construction displays substantial tolerances in this frequency band. As a result, antenna design challenges shift away from structural restrictions and toward the manufacturing process in order to reduce production and assembly tolerances.

2.3 Antenna Design

2.3.1 Antenna Geometry

Figure 2.1 illustrates the cross section and the top view of the proposed geometry. Using an irregular hexagon form, the antenna is meant to provide broad BW and CP features. On the sixth layer, a strip-line feeding method is used to feed the patch element which is located on the top layer. These two parts are connected by a vertical via throughout the established slot in the top ground on the seventh

layer. To obtain a broad band, this feeding mechanism is employed by allowing the use a thicker substrate. By lowering the number of vias, the total module size and without using cavities, this simplified construction permits to save manufacturing costs. The antenna geometry was created in accordance with the LTCC technology design guidelines. After fire, each tape has a layer thickness of 100 μm. Gold is used in each metal layer with a thickness of 9 μm. Table 2.1 shows the design criteria of the LTCC technology.

Table 2.1: LTCC design criteria

Dielectric permittivity	$\epsilon_r = 5.9$	*Number of layers for top substrate*	$NL = 4$
Loss Tangent	$tan\delta$= 0.002	*Conductor type*	*Gold*
Layer thickness	100 μm	*The metal layer thickness*	9 μm
Number of layers for down substrate	$NL = 7$		

2.3.2 Design Procedure and Optimization

We consider that the radiator is a rectangle patch and using the design criteria values as constants. The operating frequency is determined by the length of the typical patch, while the antenna's impedance is controlled by its width. The antenna length should be calculated by taking into account the fringe coupling effect for higher accuracy in terms of resonant frequency. A MATLAB code is used to calculate the width and effective length of the radiator element. The obtained length of the antenna has to be further adjusted using parametric study in order to achieve more accuracy in terms of the desired center frequency. To offer a better impedance matching response, the width is calculated and adjusted in the same way. The

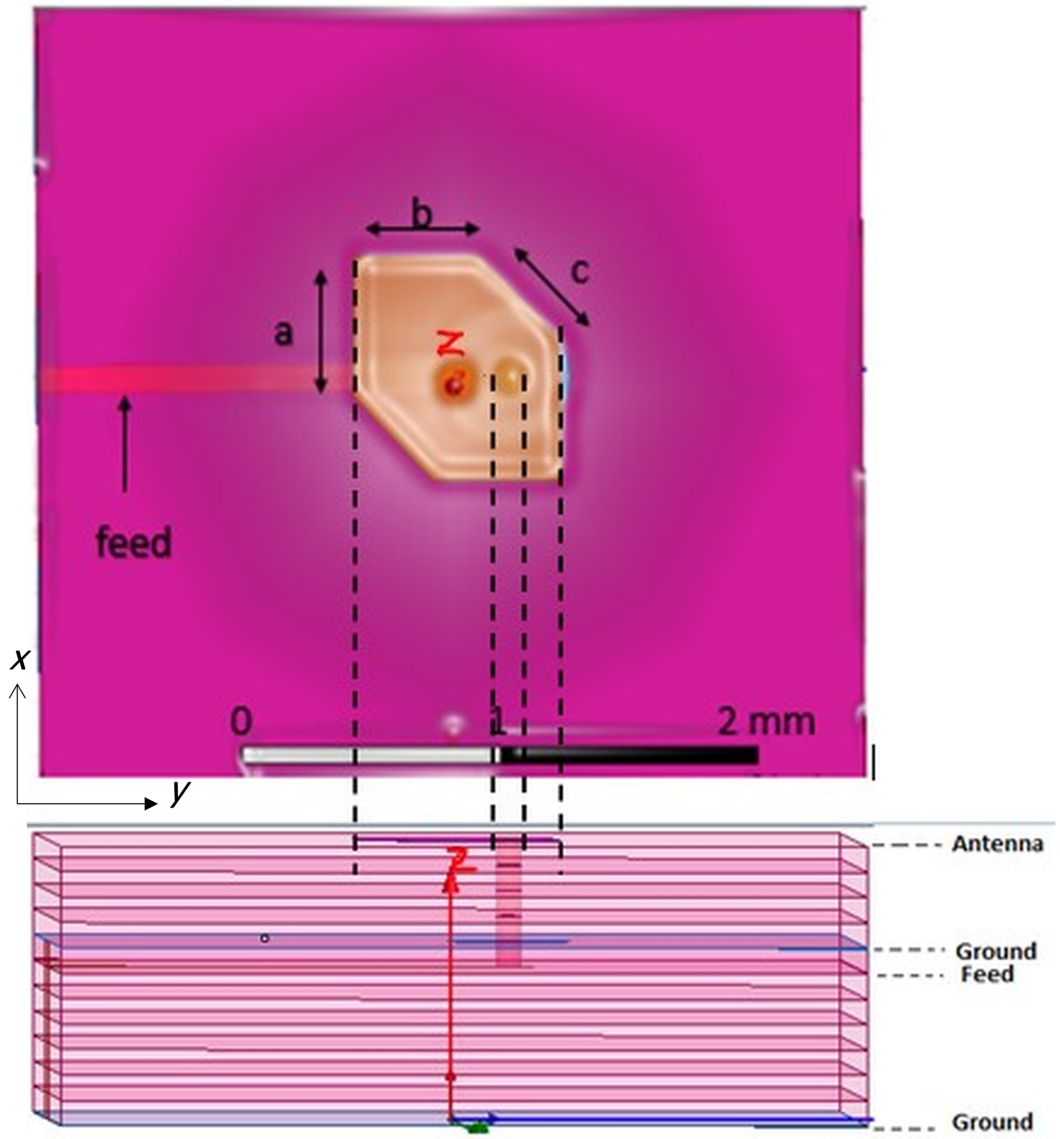

Figure 2.1: Antenna geometry.

parametric analysis seeks to achieve a better compromise between the two variables at the given center frequency by increasing or decreasing the length and width of the antenna.

After setting the rectangle patch width and length, the corners of the radiator element are trimmed to form an irregular hexagon shape. All hexagon dimensions have been changed in addition to the feed width and length, the probe diameter and location for a better compromise between several desirable but incompatible characteristics of the antenna such as resonant frequency, bandwidth, impedance, axial ratio, etc. Thus, another parametric examination which covers all dimensions parameters of the antenna has been applied. The parametrical study allows more than three-dimensional parameters to be changed, whereas the other parameters are fixed in a fixed value. Figure 2.2 depicts a flow chart of the technique based on parametric research. This design process is repeated until the reach of a configuration that fulfils the design expectations in terms of antenna performances and the intended optimizations. The optimal dimensions of the antenna that offers circularly polarized and broad impedance bandwidth are listed in Table 2.2. The radiating element is placed on an LTCC substrate with a thickness of $h_0 = 0.4\ mm$ from the top ground to the radiating element, $h_1 = 0.1\ mm$ from the integrated stripline to the top ground, and $h_2 = 0.7\ \ mm$ from the down ground to the stripline. The overall antenna height is $h_0 + h_1 + h_2$.

Table 2.2: Optimized dimensions

Parameter	Length (mm)	
a	0.52	0.104 λ_0
b	0.49	$0.098\lambda_0$
c	0.438	$0.0876\lambda_0$
Feed length	1.743	$0.3486\lambda_0$
Probe radius	0.05	$0.01\lambda_0$
Probe height	0.50	$0.1\lambda_0$
Slot radius	0.24	$0.048\lambda_0$

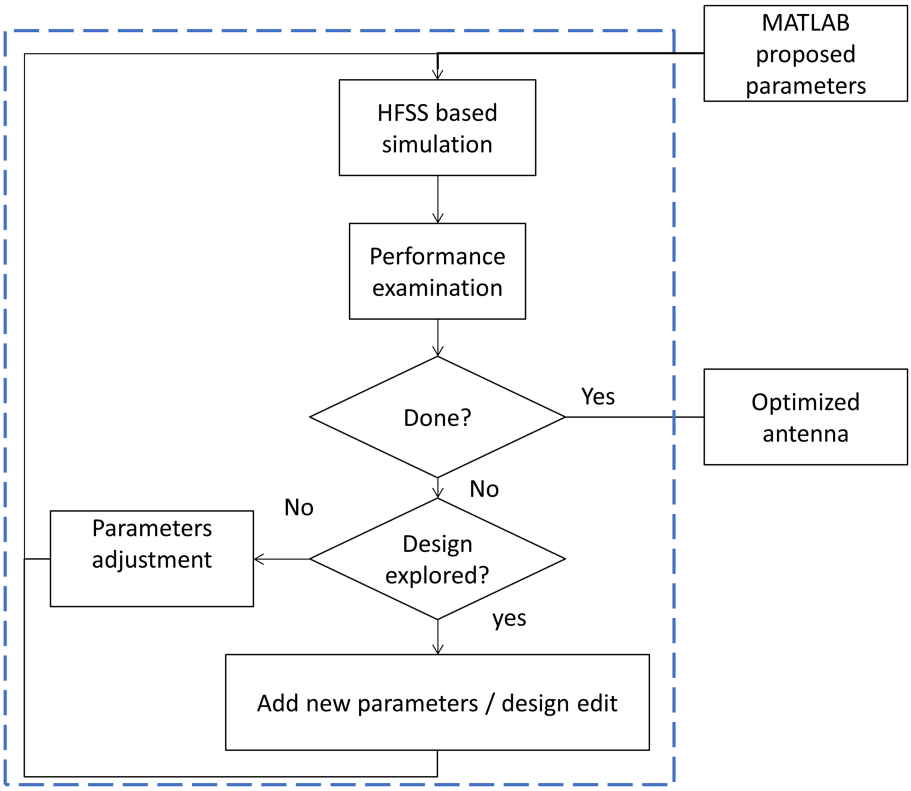

Figure 2.2: Optimization procedure.

2.4 Simulation and Results Discussion

The High-Frequency Structure Simulator (HFSS) was used to model the outcomes of this LTCC-based antenna. The surface current distribution for the proposed antenna is shown in Figure 2.3. The surface current is minimum in radiating slots and maximal in non-radiating slots, according to this diagram. This aids in the identification of radiating corners and their related effective lengths, which have a direct impact on the resonant frequencies.

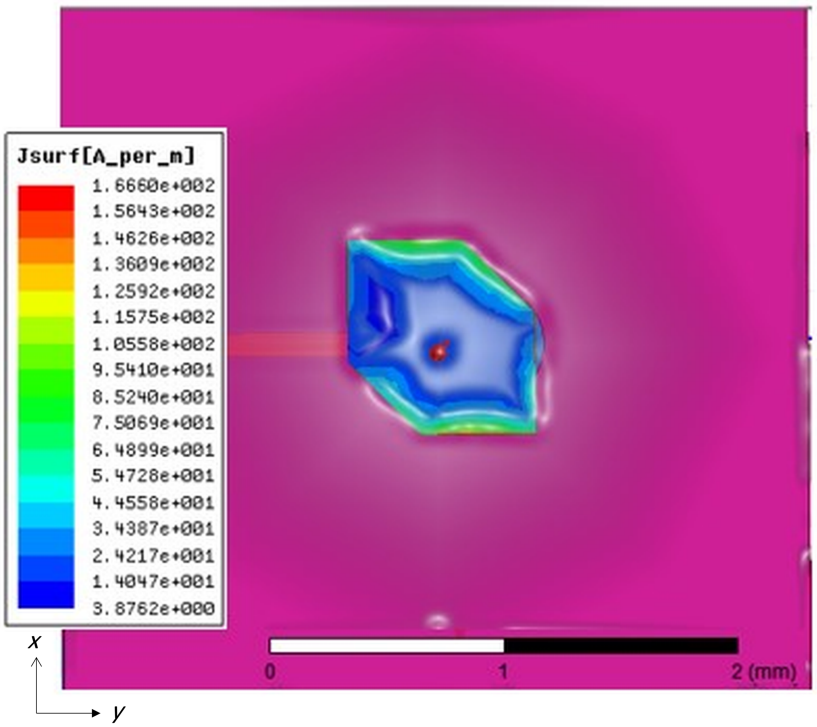

Figure 2.3: Surface current distribution .

2.4.1 Return Loss

The graph of refletion coefficient as a function of frequency is shown in Figure 2.4. The frequency range where the return loss is less than 10 dB is referred to as the relevant bandwidth. The solution demonstrates a 33 % impedance bandwidth,

which covers the unlicensed frequency range surrounding 60 GHz. According to this graph, there are two resonant frequencies. The good choice of via location to feed the radiator part results in good impedance matching. This feeding method with thicker substrates permits the achievement of a broader bandwidth. The thickness of the substrate, on the other hand, should be carefully selected to prevent surface wave propagation.

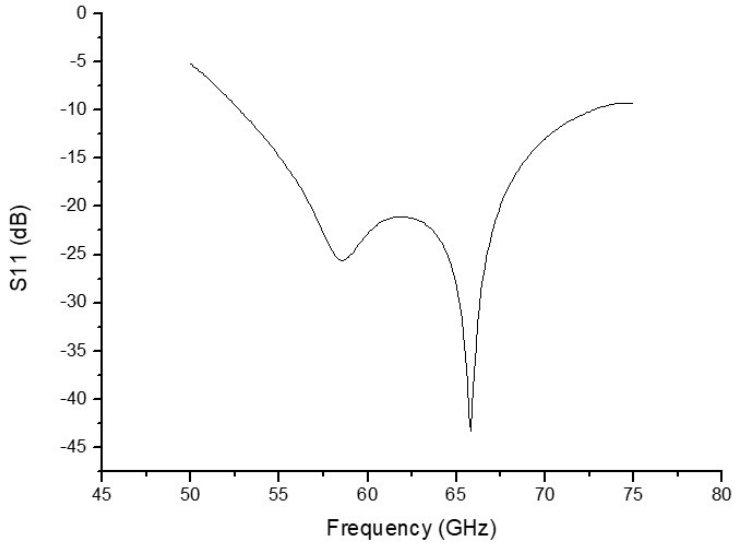

Figure 2.4: Reflection coefficient.

2.4.2 Axial Ratio

The Axial Ratio (AR) is the ratio between the major and minor axis of a circularly polarized antenna pattern. Two orthogonal modes must be activated to create the antenna circularly polarized, and the electric field vector must match all of the following criteria [27]:

- Two orthogonal and linear components are required in the field;
- The magnitudes of the two components must be equal;

- The time-phase difference between the two components must be odd multiples of 90 deg.

The utilization of an irregular hexagonal form of the radiating element ensures this. The resultant curve for this feature by this suggested antenna is shown in Figure 2.5. At frequencies where the axial ratio is less than 3 dB, the antenna has a circularly polarization. The resonance frequency of this design is 59 GHz, with a bandwidth of 2.383 GHz spanning from 57.94 GHz to 60.33 GHz.

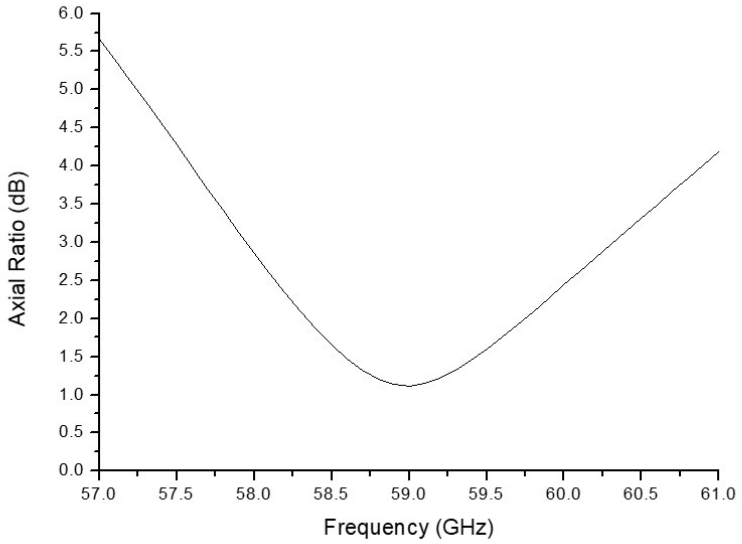

Figure 2.5: AR curve.

2.4.3 VSWR

Figure 2.6 shows the VSWR of the proposed antenna, which indicates how well the antenna input impedance is matched to the transmission line's characteristic impedance. The VSWR should be 1.0 in the ideal scenario, which implies no power is reflected from the antenna. When the VSWR is less than 2, however, there is still adequate impedance matching between the antenna and the feed. According to the

VSWR curves, there is a reasonable impedance match to the bandwidth frequency range, with less than 2. The closer the VSWR is to 1, the better the antenna is matched to the transmission line and the more power it receives. The developed antenna has a wide bandwidth spanning from 52.7 GHz to 72.8 GHz, according to the return loss and VSWR curves.

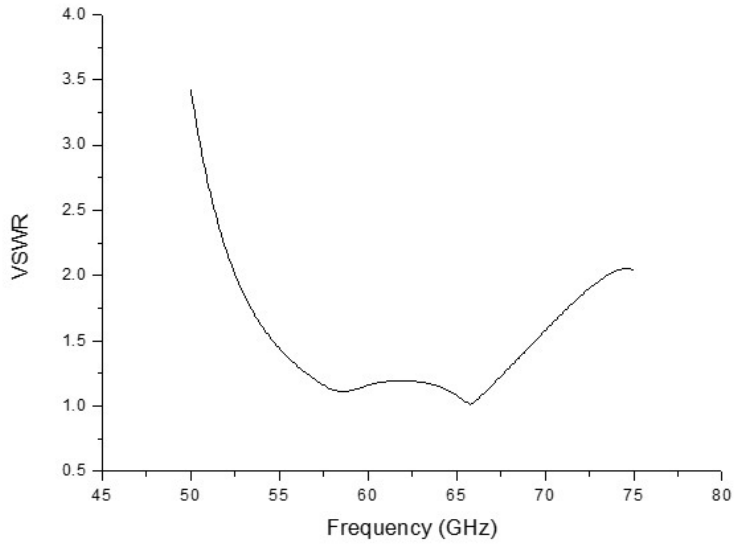

Figure 2.6: $VSWR$.

2.4.4 Impedance

Figure 2.7 represents the real component of the antenna impedance. The antenna input resistance is nearly 50 ohms in the area under consideration. This input impedance should be equal to 50 ohms in an ideal circumstance, implying that the power received by the antenna is radiated out. The antenna would absorb the incoming power otherwise. The antenna resistance curve that results shows that the impedance matching is appropriate for the frequency spectrum under consideration.

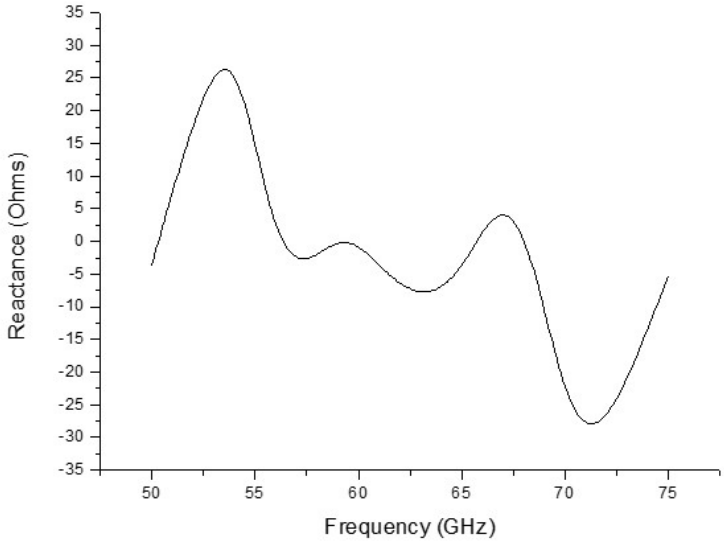

Figure 2.7: Antenna resistance.

The power stored in the near field of the radiator is represented by the imaginary side of the input impedance in Figure 2.8. This power isn't thought to be radiated. At the relevant frequency, an antenna with a real input impedance and a zero reactance is termed resonant. The antenna reactance findings demonstrate good impedance matching across the operating frequency range.

2.4.5 Radiation

The 2D radiation pattern of the proposed antenna is shown in Figure 2.9 in the E-plane and H-plane. The Radiation pattern represents the energy emitted by an antenna. This diagram form displays the dispersion of radiated energy into space and specifies the variation of the power emitted by an antenna as a function of the direction away from the emitter.

The 3D radiation pattern of this developed antenna is represented in Figure 2.10, to check the stability of the radiation pattern over the required frequency spectrum.

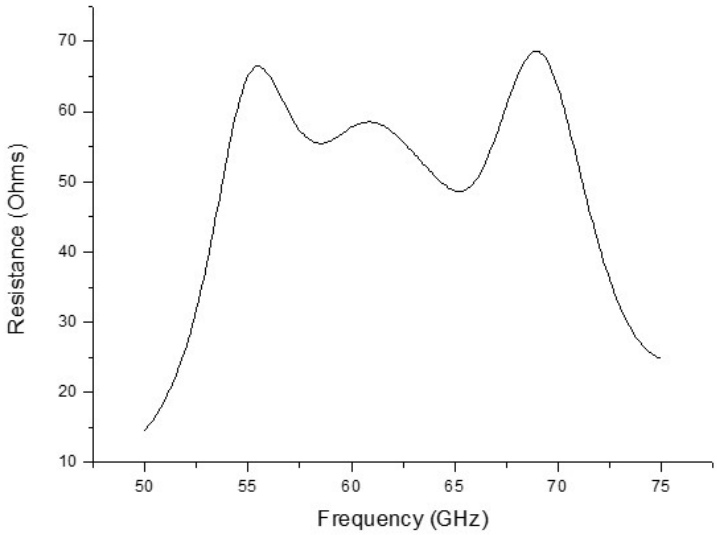

Figure 2.8: Antenna reactance.

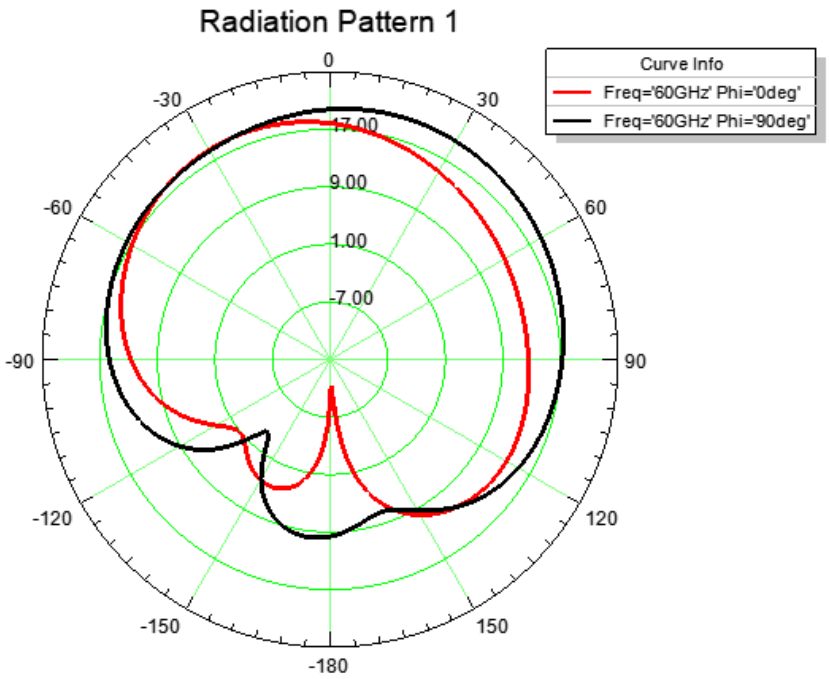

Figure 2.9: Polar radiation pattern for E plan and H plan.

This antenna has another critical performance feature in terms of the stability of the generated radiation pattern for specified frequencies of 55 GHz, 60 GHz, and 65 GHz, according to this figure. The antenna emits the most radiation in the Z-axis, regardless of frequency, throughout the whole bandwidth. In terms of gain, this antenna has a gain of around 4,9 dBi. At this region of the spectrum, the achieved gain is suitable for a single radiator element, where the radiator gets too small as its dimensions must be scaled with the operating wavelength.

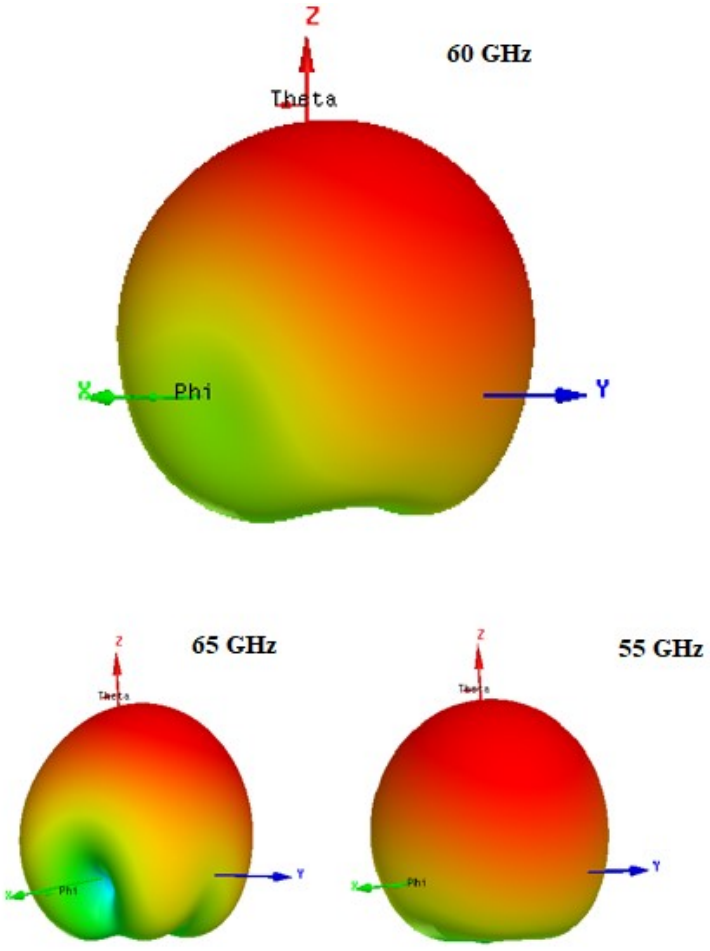

Figure 2.10: 3D radiation pattern produced at 55, 60, and 65 GHz.

2.5 Results Comparison

In Table 2.3, the suggested antenna's acquired findings are compared to previous efforts in this research area. A 60 GHz antenna using LTCC technology has been proposed in [61], presents a gain of 4.9 dBi and a bandwidth of 16.16 %. The found S11 parameter is -27dB. Three antennas based on LTCC technology are proposed in [82]. These antennas have a peak bandwidth of 22.7 percent and a peak gain of 4.8 dBi, respectively. The lower S11 parameter is -36 dB. As a result, the 60 GHz radiator we recommend has a higher gain, a wider bandwidth, and a deeper S11. Furthermore, the proposed design is simple and enhanced without the need of sophisticated features like metamaterial surfaces or cavities.

Table 2.3: Results comparison

Antenna	Technology	*Center Frequency* (GHz)	*S*11 (dB)	*BW* (GHz)	*BW*	*GAIN* (dBi) at 60 GHz	*Year*
Proposed antenna	*LTCC*	60	-43	19.8	33%	4.9	-
[61]	*LTCC*	60	-27	10	16.6%	4.9	2016
[82]	LTCC *AMC*1	60	-29	13.3	22.1%	4.8	2019
	*LTCC AMC*2	60	-36	13.7	22.7%	4.4	
	*LTCC AMC*3	60	-23	8.6	13.7%	4.8	

2.6 Conclusion

This paper provides a design for a 60 GHz antenna that uses LTCC technology to improve gain and bandwidth. HFSS software was used to design and simulate the proposed antenna. The design has good impedance matching and a good radiation pattern response with a gain of about 4.9 dBi, and a bandwidth of more than 33 %

centered at 60 GHz. As a consequence, the obtained findings indicate a preferable size, gain, CP, and bandwidth trade-off. Wide bandwidth, appropriate gain, planar shape, and the possibility to integrate utilizing LTCC multilayer technology are all advantages of the suggested antenna. This antenna's capabilities make it a promising option for future wireless modules as well as other millimetre-wave technologies.

Chapter 3

Design of Ultra Wideband and Low Profile Microstrip Antenna for Millimeter Wave under 100GHz Using LTCC Technology

3.1 Introduction

After the growing need for larger BW, the attention toward the millimetre wave band at 30 to 300 GHz has notably risen in the last several years [83, 84]. The interest in ultra wideband technology is related to the capabilities of this technology of delivering a huge quantity of data with minimal transmissions power in the short range outdoor and indoor wireless communications network [85]. Antennas are essential parts of wireless systems. It plays a vital role in taking advantage of this band where today's researches in this area are focusing on enhancing the antenna response to improve the radiating element design's performance, and efficiency [86].

The limited BW is a major limitation in high data rate system; an antenna having ultra wide BW allow to overcome this drawback because it supports several frequency-bands. Over the past two decades, many academics have made important contributions to the design of UWB-antennas [87, 88].

UWB technology is the wireless link that occupies a BW higher than 20% [89]. In the literature, a broad range of antenna designs for diverse uses have been presented. Unfortunately, the development and deployment of an UWB-antenna face several obstacles. To enable the features of UWB technology, an antenna must maintain acceptable impedance match and radiation pattern across a wide range of frequencies [90]. Microstrip antennas are particularly appealing due to their light weight, small size, and inexpensive cost and so on [89, 91, 92]. Based on PCBs technology, this kind of antenna has a wide variety of applications in wireless communications such as mobile cellular terminals [93]. Balanis developed a set of design principles and guidelines for microstrip patch antennas in order to create this antenna, which can be adjusted and optimized depending on the intended purpose [25, 94]. Various approaches have been studied to enhance BW and gain performance of the microstrip antenna, such as using patch slot modification, metamaterial structure, and defected GND structures (DGS) [90, 95].

3.2 Antenna Design

3.2.1 Geometry

Figure 3.1 shows the geometry of the suggested ultra-large band antenna. This antenna consists of a non-uniform hexagon patch laid on top of the 13^{th} layer of ceramic, and is considered as the main radiating element. This antenna is developed based on LTCC multilayer technology for vertical integration. The 50 Ohm strip line

Table 3.1: LTCC design criteria

Dielectric permittivity	$\epsilon_r = 4.11$	Conductor type	Gold
Loss Tangent	tand = 0.008	Number of layers above the strip line ground to the antenna radiating element	NL = 4
Layer thickness	75 μm	Number of layers Between the strip line and the top ground layer	NL = 1
Metal layer thickness	9 μm	Number of layers below the strip line	NL = 8

in the 8^{th} layer feeds this multilayer microstrip antenna. A vertical probe connects the stripline to the radiating element, allowing the antenna BW to be increased by utilizing a thicker substrate. The top slotted ground in the 9th layer separates the strip line from the radiating element. The proposed Ultra wide band antenna is printed on LTCC dielectric substrate with relative permittivity of 4.11 and loss tangent of 0.008, has dimensions of $3.16 \times 3.2 \ mm^2$. This antenna's geometry was created in accordance with the LTCC technology design standards. After fire, each tape's layer thickness is 0.75 μm, and the metal layer is 6 μm thick. Table 3.1 lists further LTCC design characteristics.

3.2.2 Parametric Study

The dimensions of the radiating element are calculated using a MATLAB algorithm based on the transmission line model, see section 1.5.3. Due to the inaccurate results in terms of antenna dimensions using the transmission line model, a massive parametric study is applied in order to fix the desired frequency range of operation and to optimize the other antenna characteristics where the obtained outputs of the algorithm are used as initial values of parametric study [96]. Note that the parametric study permits certain parameters to be varied while the other parameters are

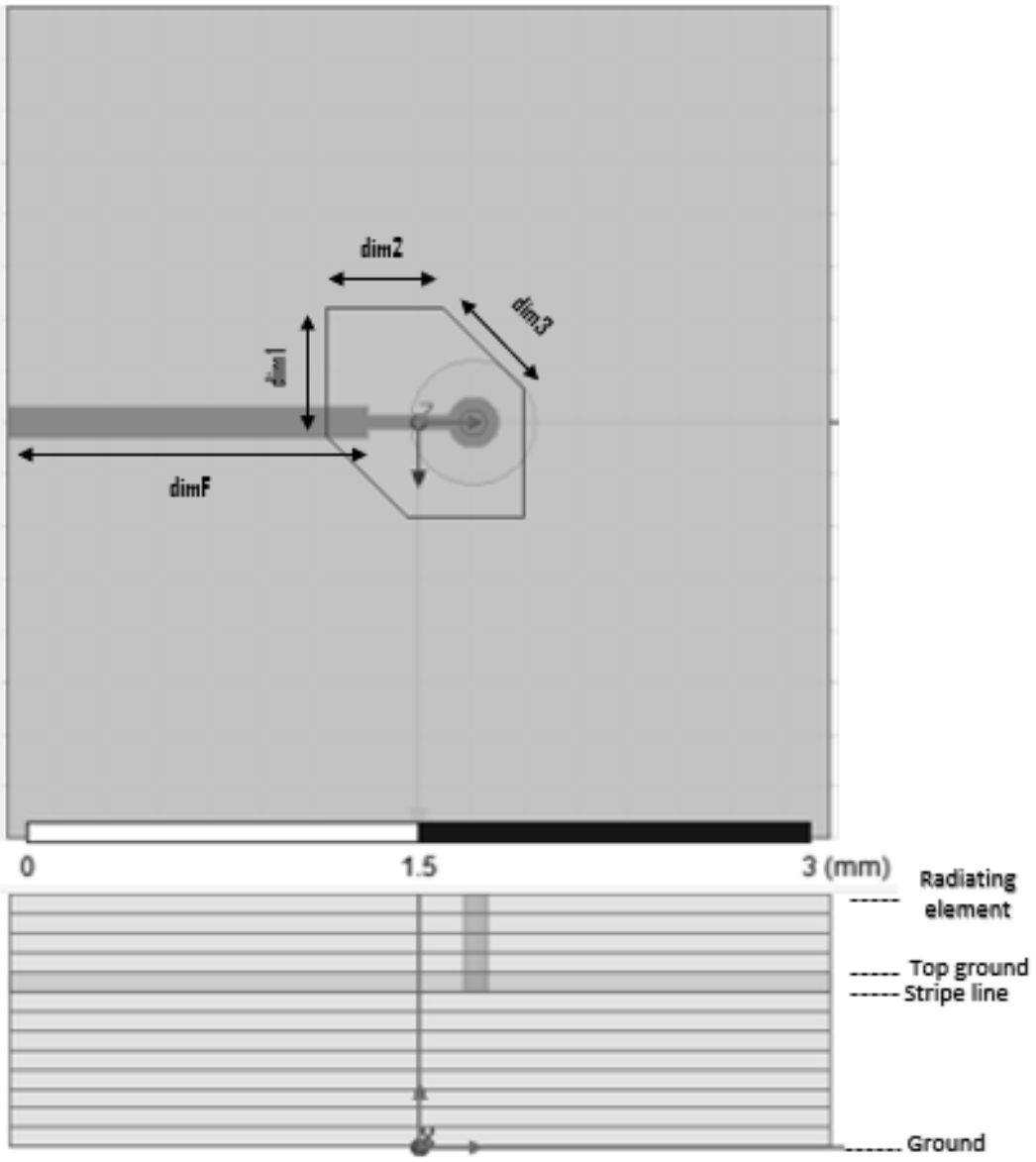

Figure 3.1: Antenna geometry.

Table 3.2: The impact of design parameters on various antenna properties [1]

Parameter	Influence
Length	• Mainly controls the resonant frequency • $F_c \cong \frac{C}{2\ L\sqrt{\varepsilon_s}}$
Width	• Controls the input impedance (in general, the wider the patch, the lower the input impedance)
h	• Influences the BW (higher the height, the broader the BW
ϵ_r	• It controls the fringing of the fields and thereby the radiation pattern. Lower the dielectric constant, wider the fringing and broader the radiation pattern. • The input impedance increases with higher permittivity • Higher the permittivity constant, the smaller the patch size

fixed in a constant value. The parametric study was guided based on the influences of the design structural parameters on various antenna characteristics, see Table 3.2. The corners of the radiating components are then truncated, and a new parametric study was conducted to improve the response of this UWB antenna by looking for broader BW, greater gain, and optimum impedance matching. Thus, the applied parametric study includes all dimensional parameters of the antenna. Note that this parametric optimization is repeated until reaching an optimal solution that meets the design requirements in terms of the antenna performance previously indicated. The final optimized dimensions are presented in Table 3.3.

3.2.3 Geometry Discussion

The antenna corners have been truncated in order to provide the parametric study further design freedom by increasing the number of parameters to be optimized. The objective of this design as an UWB-antenna is to increase the fractional BW of the antenna so that it can receive all frequencies at the same time instant. Furthermore, antennas made using LTCC technology may be directly and easily connected with RF circuits on LTCC substrates. The suggested antenna has been reduced in order to minimize fabrication costs and make the production process easier.

Table 3.3: Antenna parameters

Parameter	Length(mm)	
$dim1$	0.49	$0.129\lambda_0$
$dim2$	0.45	$0.119\lambda_0$
$dim3$	0.438	$0.115\lambda_0$
$dimF$	1.39	$0.366\lambda_0$
Probe radius	0.05	$0.013\lambda_0$
Probe height	0.5009	$0.132\lambda_0$
Slot *radius*	0.24	$0.063\lambda_0$

3.3 Results and Discussion

This UWB microstrip antenna is simulated using two software products: HFSS and CST Studio. The two software employed allow for quick and precise simulation of high frequency (HF) components such as antennas, couplers, filters, planar and multilayer structures. The surface current distributions of the proposed UWB-antenna at various frequencies of $66GHz$, $75GHz$, $85GHz$, and $93GHz$ are shown in Figure 3.2. The higher amplitude of this parameter is shown in this image to be at the feeding probe position and to be small at the radiating element's borders. Because the voltage is inversely proportional to the current, the low level of the current at the radiation edges indicates that the voltage has reached its maximum value, and the related edges are regarded as the radiating sides of this proposed UWB-antenna.

3.3.1 Frequency Sweep Based Solutions

The obtained return loss curves of the designed antenna are illustrated in Figure 3.3. According to the observed curve, this designed antenna has a BW of more than $33.5GHz$, ranging from $62.5GHz$ to more than $96GHz$ in the two employed software. In the millimetre wave spectrum below $100GHz$, this antenna has an extremely wide BW. Since the impedance matching varies between $\breve{}12dB$ and $\breve{}28dB$, this return loss result points that there is adequate impedance match at the considered BW.

Two main resonance frequencies are observed at $65.7GHz$ and $83.4GHz$. The microstrip antenna's low BW characteristics were one of its major drawbacks when compared to the requirements of UWB technology. By raising the matching impedance BW to more than 40%, the limitation is successfully overcome. Note that due to the usage of two distinct simulation solvers, a slight difference may be seen between

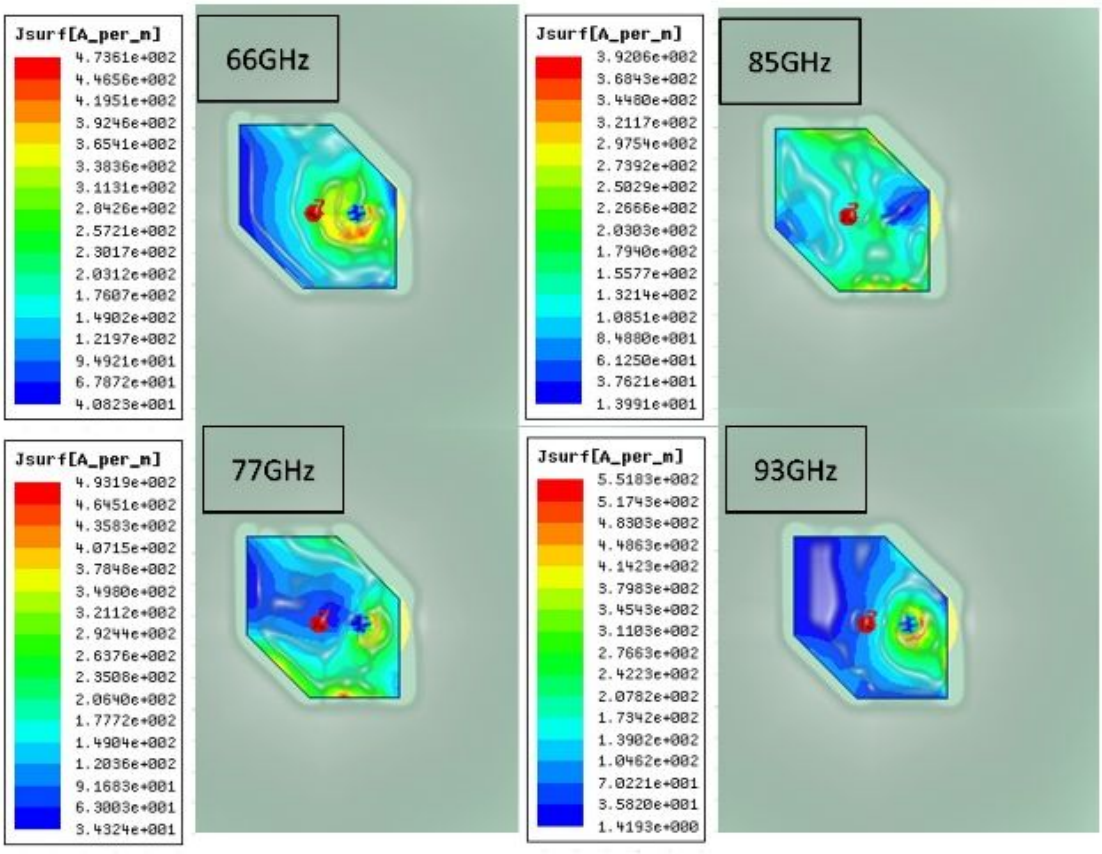

Figure 3.2: Surface current distribution.

the two graphs.

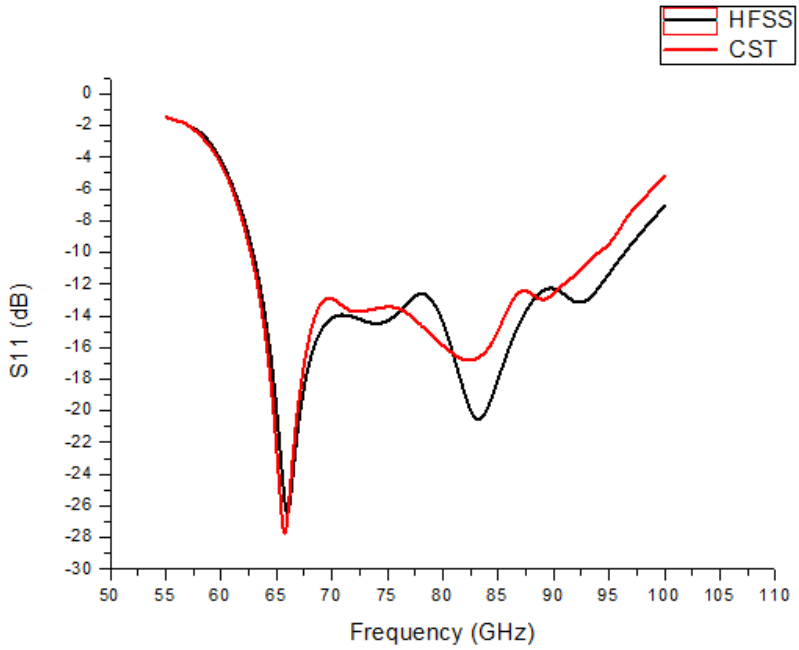

Figure 3.3: Reflection coefficient.

In the VSWR characteristics of this antenna, as shown in Figure 3.4, the difference between the two solvers is less noticeable. According to the curves found in this figure, there is acceptable impedance matching throughout the whole frequency BW, as it is indicated less than 2. The closer the VSWR curve gets to 1.0, the less power is reflected by the antenna. This indicates how well the antenna terminal input impedance is matched to the transmission line's characteristic impedance.

In Figures 3.5 and 3.6, the imaginary and real parts of the antenna impedance are shown, respectively. The antenna input resistance is equal to or near to 50 Ohms at the frequency range of interest, indicating that the power sent to the antenna is radiated away. Otherwise, the received power is absorbed by the antenna. The obtained results of the antenna reactance and resistance show good impedance matching at the considered frequency band.

The graphs of gain as a function of frequency in the two software programs are

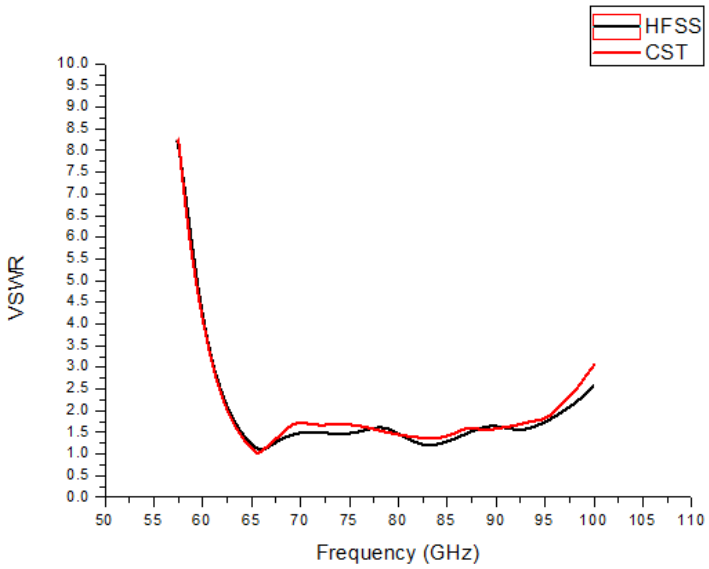

Figure 3.4: $VSWR$.

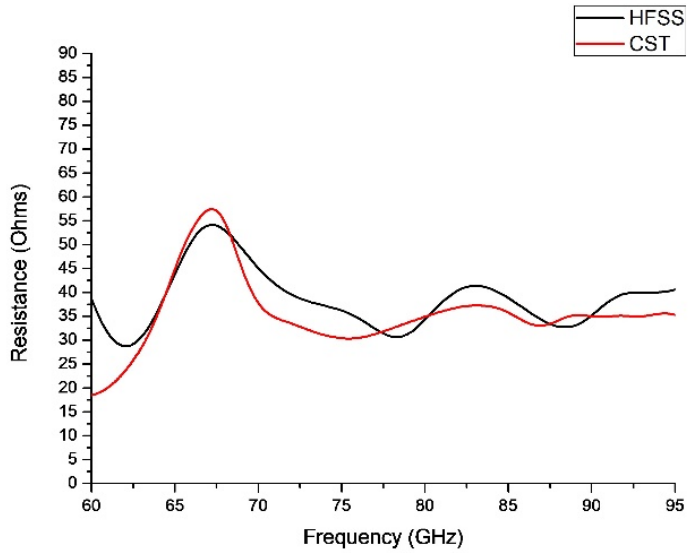

Figure 3.5: Antenna resistance.

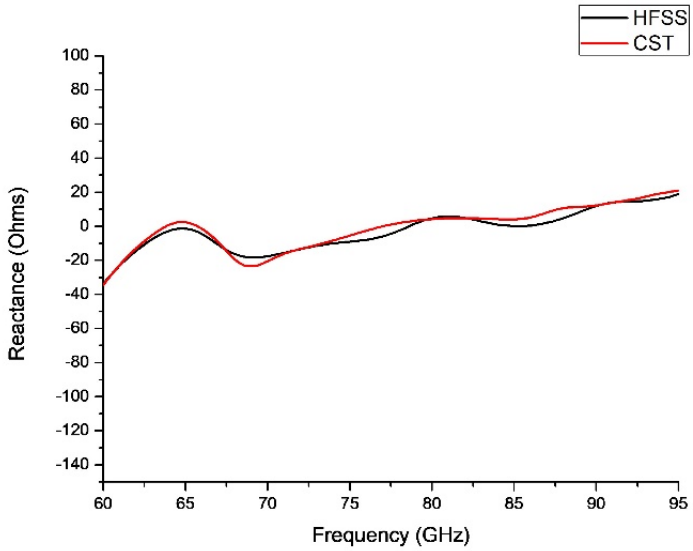

Figure 3.6: Antenna reactance.

shown in Figure 3.7. The antenna gain is a measurement of how effectively an antenna transforms input power into radio waves. The resulting gain is acceptable for a single antenna since the radiating element gets too small when its size is scaled to the wavelength. This UWB-antenna presents a peak gain of $5.7dBi$.

3.3.2 Radiation Pattern

In order to evaluate the stability of the radiation pattern of this constructed UWB-antenna in the considered frequency BW, figure 3.8 displays the computed polar radiation pattern of this proposed antenna. Figure 3.9 shows 3D radiation patterns at 66, 75, 85, and 93 GHz. According to this figure, the antenna presents another important factor of performance in terms of the stability of the radiation pattern all over the BW. The proposed UWB-antenna radiates omnidirectionally, having the most radiation on the Z-axis. Such achieved results make this antenna very

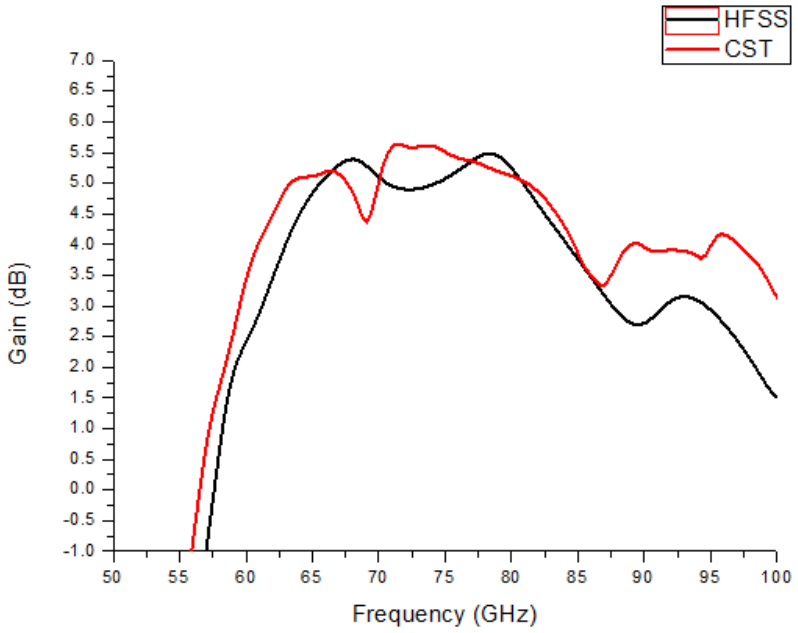

Figure 3.7: Antenna gain.

interesting for use in practical devices.

3.4 Conclusion

A low profile ultra wideband microstrip antenna using LTCC technology is suggested in this chapter. HFSS and CST Studio were used to confirm the obtained results. In both utilized software, this antenna offers a very wide BW in the millimetre wave spectrum below $100GHz$, ranging from $62.5GHz$ to more than $96GHz$. The founds indicate that there is a adequate impedance match and a max gain of 5.7 dBi. At the considered spectrum, satisfactory antenna behavior is seen in terms of response stability and the antenna radiation pattern. Another benefit of this antenna as it can directly integrated with other RF chips utilizing LTCC multi-layer technology. These factors make this proposed antenna a suitable candidate to support the UWB technology needs.

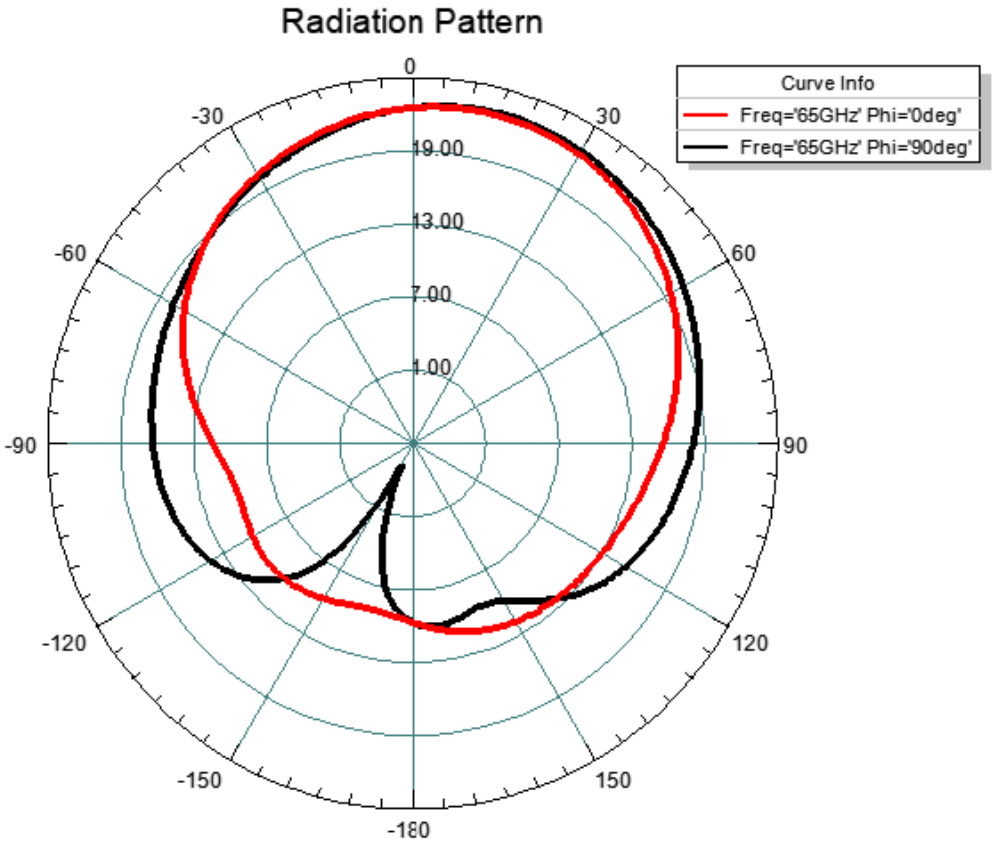

Figure 3.8: Polar radiation pattern for E plan and H plan.

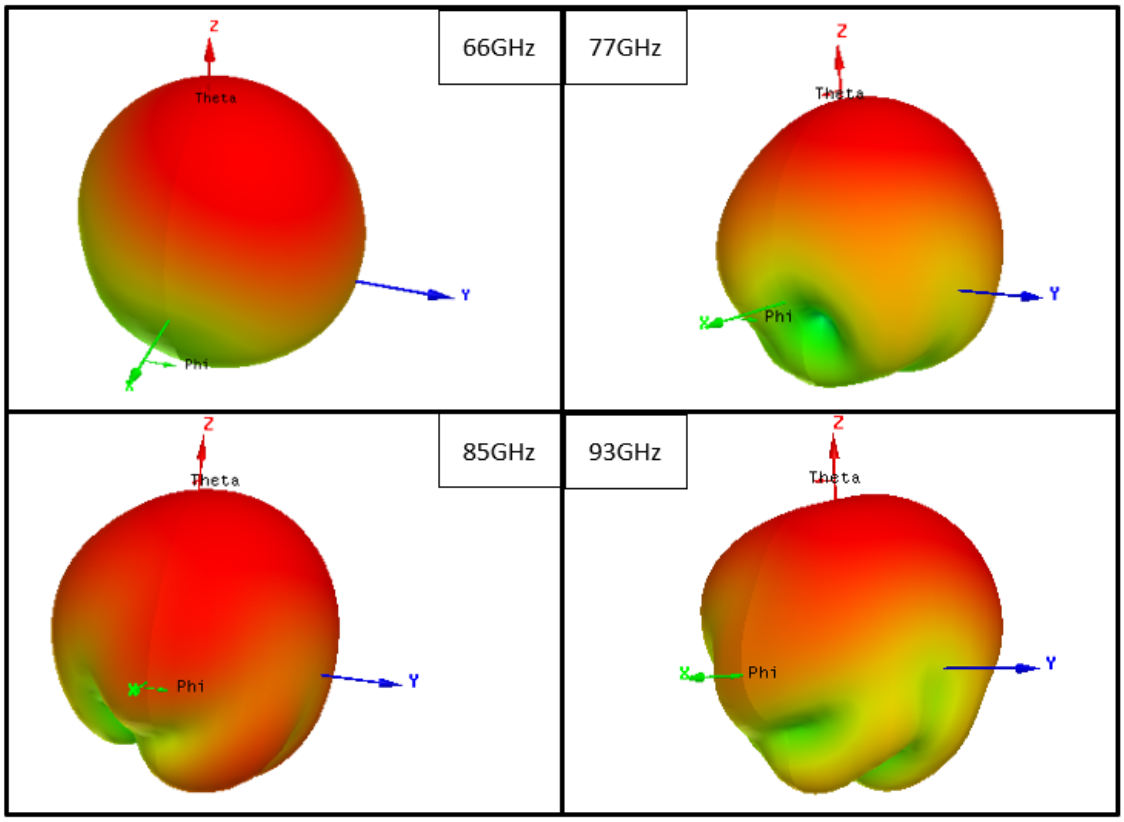

Figure 3.9: 66, 77, 85 and 93 GHz radiation pattern in 3D.

Chapter 4

Design of LTCC Based and CPW-Fed Broadband Microstrip Antenna for Millimeter-Wave Applications at 60GHz

4.1 Introduction

Rain, gas, dust, plants, and other outside environmental factors influence millimeter waves at 60 GHz. Due to these hard propagation characteristics, this band requires a unique hardware circuitry where more system design complexities are needed to benefit from it [97–99]. The antenna's performance enhancement and design considerations are becoming more significant challenges for facing many stringent requirements of this spectrum. The operation at such frequencies will allow wideband communication and consequently much higher data rates compared to the current microwave-based communication systems [100].

4.2 Literature Review

Due to its attractive characteristics and advantages, microstrip antennas are widely employed in today's radio communication equipment. Microstrip patch antennas, on the other hand, have a low gain and a very narrow operating bandwidth (usually less than 5%). [79, 101, 102]. Various approaches and considerable study efforts have been devoted to this subject in the literature. In [103] a 9.5 % of bandwidth is obtained using an aperture-coupled microstrip line-fed patch antennas (ACMPAs) in which air cavities processed inside the substrate have been used to enhance the bandwidth and gain of the antennas. In [104] a low-profile metamaterial-mushroom antenna array consists of a single-layer mushroom radiating structure and a single-layer substrate integrated waveguide (SIW) feeding network exhibiting an impedance bandwidth of 56.3 – 65.7 GHz. In [105] the artificial magnetic conductors (AMCs) with in-phase reflection characteristics have been investigated, where a 60 GHz CPW-fed patch antenna on multilayer LTCC- and LCP-based achieved a bandwidth of about 16% and a peak gain of 5.1 dBi using the LCP (Liquid Crystal Polymer) substrate. However, the additional fabrication process for the air cavity, SIW cavity, slotted AMC cells and EBG surfaces with metallic vias in each unit cell increases circuit complexity and fabrication cost.

4.3 Antenna Design

4.3.1 Geometry

The proposed antenna's geometry is represented in Figure 4.1. This design was created with the goal of achieving a broad bandwidth. The first stage in achieving LTCC-based wideband geometry is to build a traditional microstrip patch antenna

that can function in the desired bandwidth. The radiator element's corners are then shortened to create a non-uniform octagon shape. The antenna, which has a relative permittivity of 4.11 and a loss tangent of 0.008, is mounted on top of six LTCC layers. A coplanar waveguide (CPW) arrangement is used to feed the antenna. This antenna is composed of two grounds; the first ground is printed on the top of the second LTCC layer. This top ground is composed of metallic square patches etched on the top of the bottom substrate. The second ground is found at the bottom of the first layer. Between the patch and the second ground plane, there is no via, which helps to decrease fabrication costs and simplify the manufacturing process. Note that these periodically integrated patches are a metamaterial inspired surface [106], [107]. However, it is not considered as a metasurface because it not studied as a function of phase reflection where a zero-phase of the unit cell must be at the same resonating frequency of the antenna. The unit cell in our case has a zero-phase degree at around 0.1 THz [108].

4.3.2 Optimization

The antenna is designed by the same procedure in section 3.2.2. To give more freedom to the optimization process, the radiator was preferred to be octagonal to add another parameter (corner) to the optimization. With the insertion of the periodic square patches' matrix in the antenna substrate, another parametrical study was carried out to keep the desired resonance frequency, which includes the new parameters of this structure, namely the lattice constant, the patch radius, the dimensions and the position of the patches array in Y-axis.

Typically, the parametrical study permits to explore the structure more effectively and permits to better analyze the antenna behavior. When a large number of parameters have to be explored, a sensitivity analysis of the parameters is applied

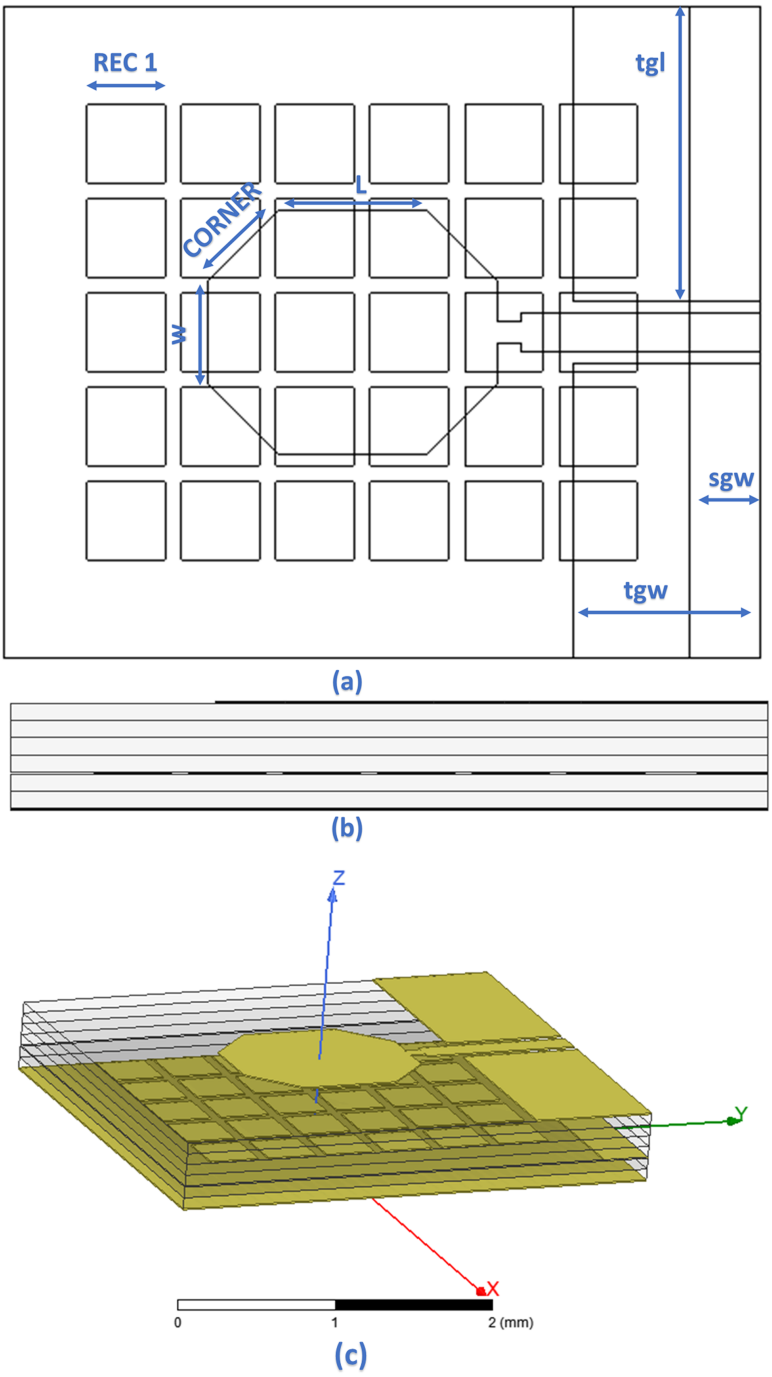

Figure 4.1: Antenna geometry.

Table 4.1: Design parameters

Parameter		Value (μm)
Radiating element layer	L	630
	w	441
	tgl	1246
	tgw	792
	corner	420
Periodic structure layer	sgw	300
	REC 1	330
	Lattice constant	400

to effectively guide the optimization by moving form parameters with a significant effect to those with a weaker effect. This study is repeated until achievement of a configuration that satisfies the design needs in terms of antenna performance such as impedance matching, gain, etc.

As per usual, The proposed structure is simplified to minimize the fabrication cost, by reducing of the total module size without the use of integrated cavities, vias, and other complex structures such as EBG Structures. The antenna geometry has been developed respecting the LTCC technology design rules [109]. The single LTCC layer thickness is 75 μm for each tape after firing. The used conductor for the metal layers is gold having a thickness of 6 μm . Four layers are used to compose the top substrate and two LTCC layers in the bottom substrate, giving a height of 300 μm for the top substrate and 150 μm for the bottom substrate. Table 4.1 shows the values of the rest parameters.

4.4 Results and Discussion

The proposed antenna is designed and simulated using High-Frequency Structure Simulator (HFSS), which is based on finite element modeling (FEM). Figure 4.2 shows the surface current distribution in logarithmic scale at the top and the mid-

dle metal layers. The current distribution is maximum at the edges of the antenna and minimum at the center of the antenna. The current distribution on the periodic square patches is maximum at the bottom of the antenna and minimum outside this region. Therefore, the number of these periodic patches is chosen to be 5×6 elements to provide an adequate space for current distributions. Note that a relatively large number of elements only slightly improves antenna performance where the manufacturing of the antenna becomes more complex.

4.4.1 Input Impedance

The antenna input impedance is examined to ensure that the maximum power is transferred from the RF circuity to the antenna with negligible amount being reflected back. Figure 4.3 shows the curves of the real and the imaginary parts of the input impedance of this proposed antenna structure. According to the reactance curve, a zero imaginary part is obtained at 60 GHz. The antenna input resistance is around 50 Ohms, which means the power that arrives at the antenna is radiated away. These simulation results of the input impedance show a good impedance matching at the considered frequency spectrum.

4.4.2 Return Loss

Figure 4.4 shows the obtained return loss of the proposed antenna as a result of simulation. As it is observed in this figure, the obtained S_{11} is -51 dB with a single resonance frequency at 60 GHz. The obtained bandwidth based on the -10 dB criterion of the reflection coefficient is 14.5 GHz ranging from 55.5 GHz to 70 GHz. According to these results, the antenna offers a good impedance matching with a wide bandwidth. This wide bandwidth, equivalent to 24.16 %, allows this multilayer antenna to largely surpass the requirement of 11.66 % of the bandwidth of 60

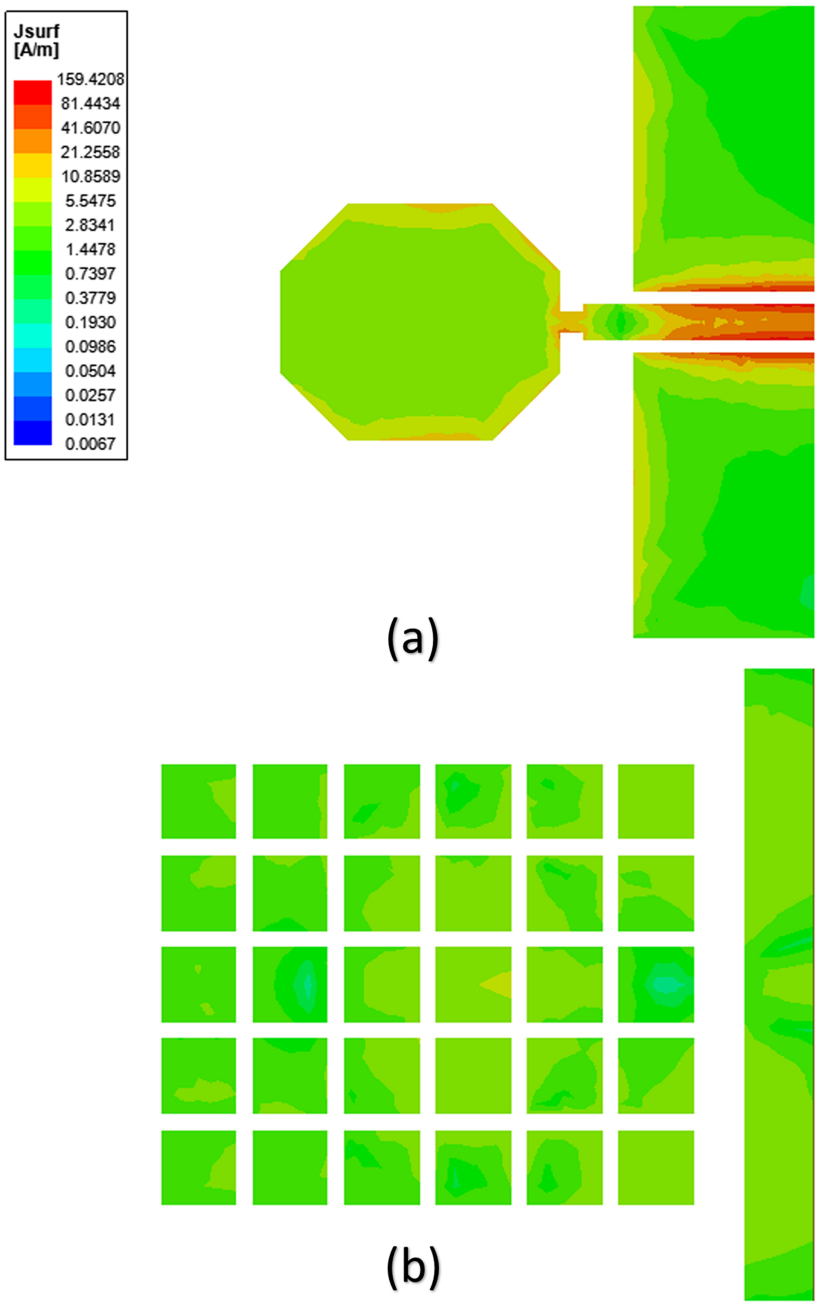

Figure 4.2: Surface current distribution.

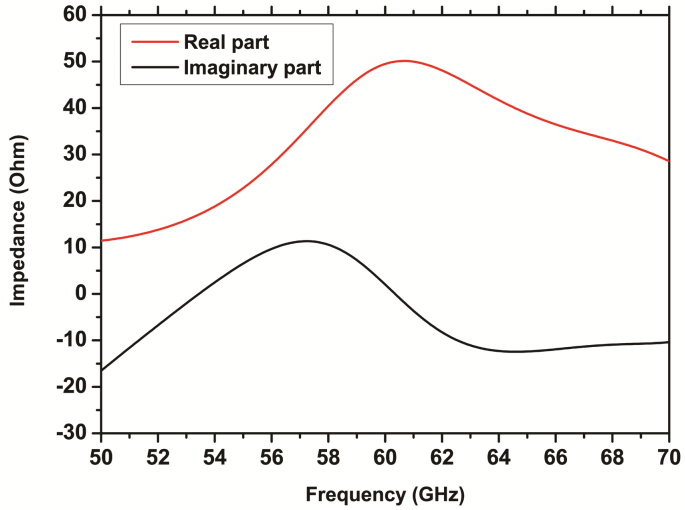

Figure 4.3: Antenna impedance.

GHz spectrum and to cover the entire unlicensed spectrum [110].

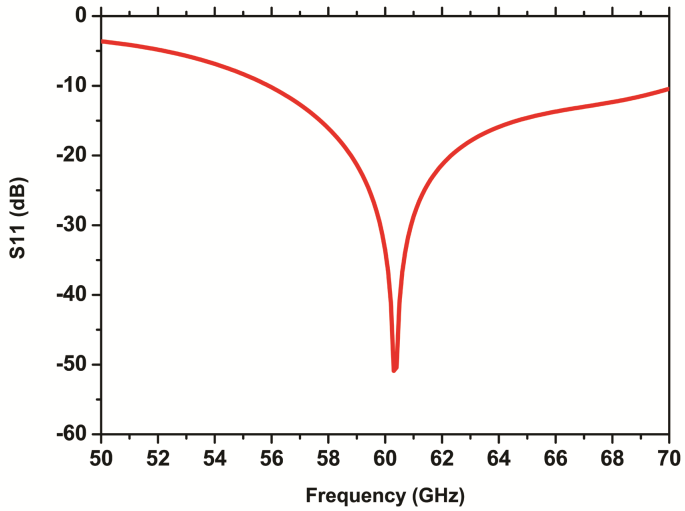

Figure 4.4: Return Loss.

4.4.3 Parametrical Variation

Figure 4.5 shows a parametrical variation of $RECT1$ parameter. According to these curves, the change in the dimensions of the patches has an influence in terms of resonant frequency and S_{11} magnitude. Decreasing the dimensions of the patch results in a transition to a higher resonant frequency. It is also observed that a good precision in terms of resonance frequency can be obtained by choosing $RECT1 = 170$ μm . However, this dimension reduces the space between the patches to less than 65 μm , which may not be achieved in practical designs due to manufacturing tolerances. Note that the larger the space between two patch elements, the more precision can be obtained. According to these graphs, the dimension of the integrated patches is chosen in order to have deeper S_{11} at the resonance frequency.

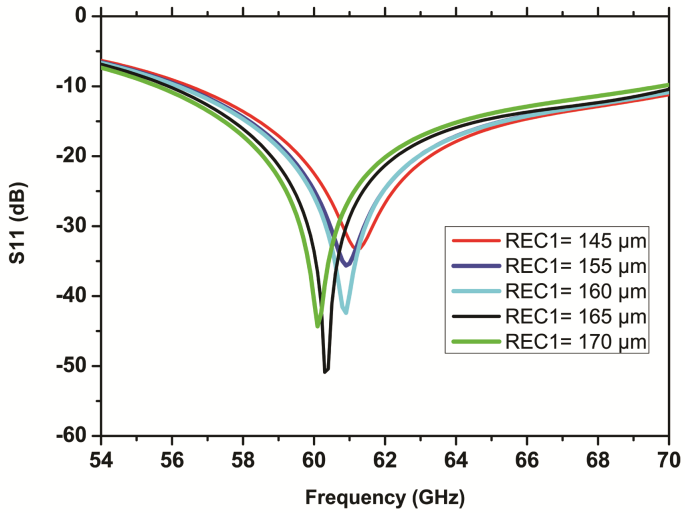

Figure 4.5: Return loss; parametric variation of REC1.

4.4.4 Gain and Radiation

Figure 4.6 shows the plots of gain at 60 GHz in E-plane for Phi = 90 and H-plane for Phi = 0. According to these curves, the maximum radiation is obtained at Theta

= 0 in both E plane and H plane having a peak gain of 5.1 dBi. Figure 4.7 shows the obtained simulation plots of gain as a function of frequency in the used software program. The antenna has a gain of 5.10 dBi at 60 GHz. It is also observed that the antenna exhibits a gain reduction as the frequency increases. This obtained gain is acceptable for a single antenna at this range of spectrum where the size must be scaled to the wavelength, which leads to a reduction in the radiating element dimensions.

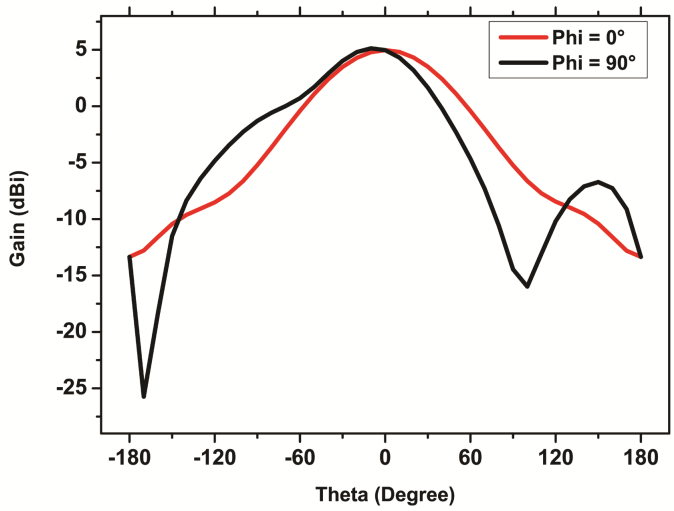

Figure 4.6: Gain at 60 GHz; in E-plane for Phi = 90 and H-plane for Phi = 0.

The 3D radiation pattern is illustrated in Figure 4.8 in order to verify the stability of the radiation at the considered frequency bandwidth. The shown figure illustrates the produced radiations pattern at 56 GHz, 60 GHz and 66 GHz. According to this figure, this antenna has another important factor of performance in terms of stability of the radiation pattern.

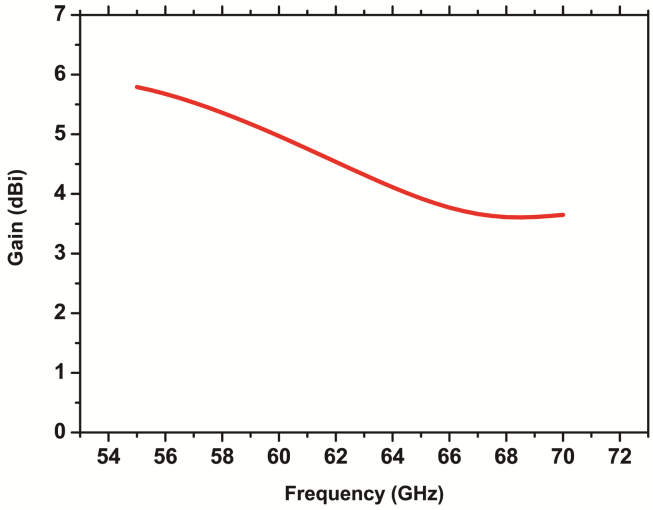

Figure 4.7: The antenna gain variation as a function of frequency.

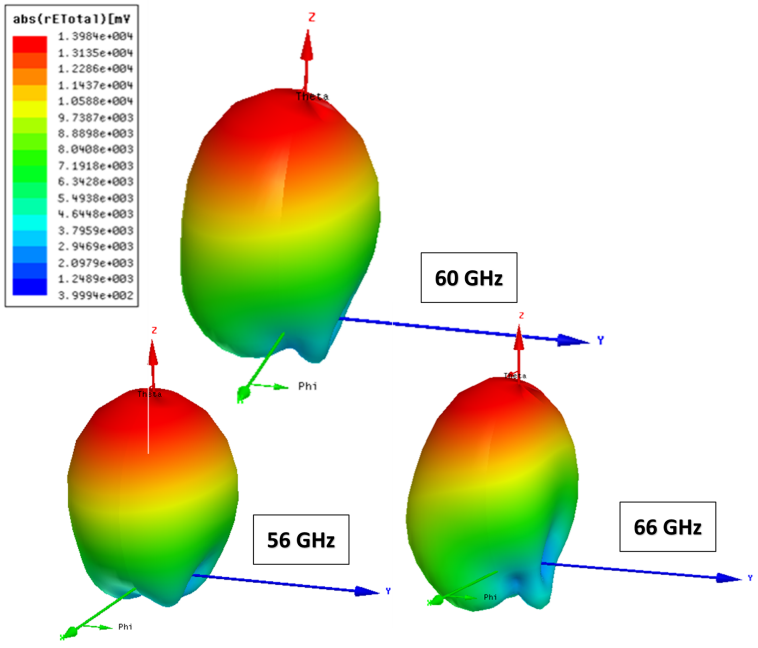

Figure 4.8: 3D radiation pattern at different frequencies.

4.4.5 Manufacturing and Measurement

Figure 4.9 shows the antennas manufacturing and measurement. Figure 4.10 shows three manufactured prototypes. The prototypes of the proposed antenna are manufactured based on LTCC multilayer technology which consists of assembling many individual ceramic layers, the manufacturing is performed using ESL41111-G tape with a dielectric permittivity of 4.11 and a layer thickness of 75 ± 5 after firing, fired shrinkage of 15 ± 1% in X and Y directions and 16 ± 2% in the Z direction. After preparing the individual ceramic layers and printing the conductive tracks, the ceramic layers are stacked onto each other to form the circuit. The laminating pressure is 21 MPa at 70 °C and the firing temperature is 850 °C. The S-parameters are measured with *Rohde & Schwarz ZVA*67 Vector Network Analyzers. The obtained results of the three prototypes are illustrated in Figure 11. These realized prototypes show a very small shift in terms of the resonance frequency. A good impedance matching is obtained in all tested prototypes where the obtained S_{11} is close to -50 dB in the first prototype, close to -30 dB in the second prototype and close to -40 dB in the third prototype. In terms of bandwidth, the manufactured prototypes show a wide bandwidth that looks larger in comparison to the simulation result. This can be justified by the previously indicated tolerances, and the tolerances in the printed metal layers, see Figure 4.10 *zoom*, and the tolerances of layer misalignment in LTCC manufacturing. The influences of these process tolerances become more important at high frequencies as more as the dimensions of the antenna are reduced.

4.4.6 Results Comparison to Recent Similar Works

These obtained results of our antenna are compared to recent similar works in Table 4.2. The proposed antenna has a higher gain at 60 GHz and a second lower gain

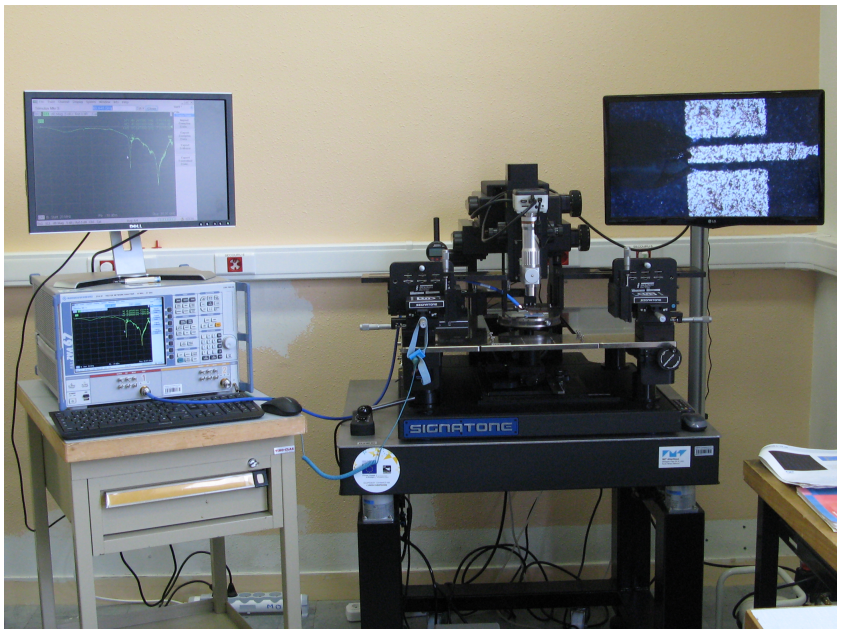

Figure 4.9: Prototypes manufacturing and measurements.

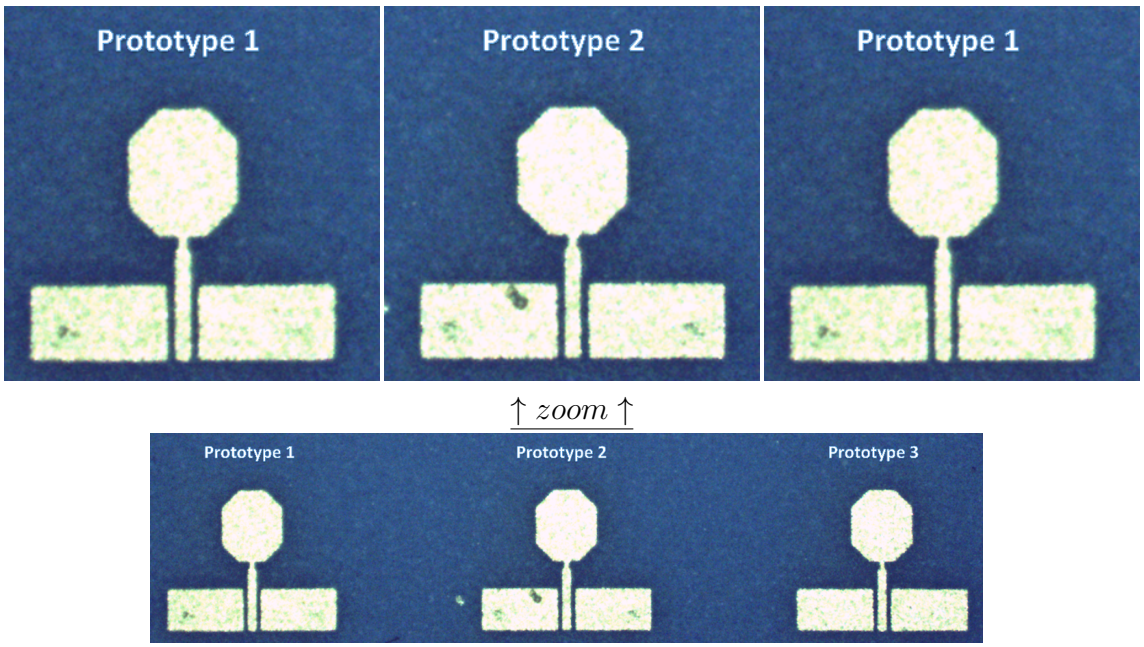

Figure 4.10: Prototypes manufacturing and measurements.

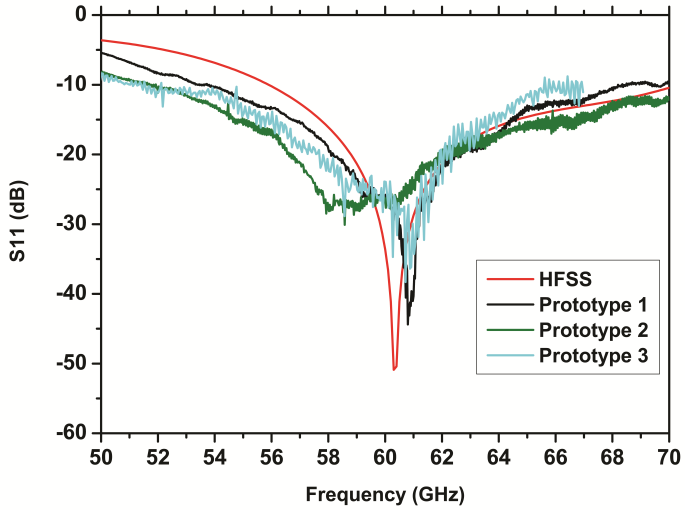

Figure 4.11: Comparison of S_{11} simulation results and measurement of prototypes 1, 2 and 3.

variation over the considered bandwidth. Moreover, the antenna has a higher bandwidth compared to other antennas. In terms of return loss, the proposed antenna has a deeper value of S_{11}. In [25], three AMC based antennas are proposed, our antenna can be compared to this antenna when we consider the periodic structure as an artificial magnetic conductor with a zero phase of the unit cell at around 0.1 THz, showing that the use of zero-phase reflection at a higher frequency leads to better performance than a zero-phase reflection at the resonant frequency.

4.5 Conclusion

This chapter presents a design of 60 GHz band antenna based on LTCC technology, with a bandwidth of more than 26% centered at 60 GHz and stable radiation over the considered bandwidth. The proposed antenna offers a good impedance matching with an adequate gain. The obtained results have been verified using HFSS software and three prototypes are manufactured for measurement purposes. A good

Table 4.2: Comparison of the proposed antennas to the relevant reported antennas.

Antenna	Technology	Center Fr (GHz)	S_{11} (dB)	BW (GHZ)	BW	GAIN (dBi) at 60 GHz	Gain variation	Year
Proposed	LTCC	60	-51.70	14.5	24.16%	5.10	2.15	-
Proposed in [111]	LTCC	60	-43	19.8	33%	4.9	-	2021
[105]	LCP	60	-31	10	16.6%	5.10	1.9	2016
	LTCC	60	27	10	16.6%	4.9	2.6	
[82]	LTCC AMC1	60	-29	13.3	22.1%	4.8	2.6	2019
	LTCC AMC2	60	-36	13.7	22.7%	4.4	-	
	LTCC AMC3	60	-23	8.6	13.7%	4.8	-	

agreement between simulation and measurement results was obtained. These antenna performances make it attractive for use in practical devices in future wireless communications and to support many other 60 GHz applications needs.

Chapter 5

New PBG Microstrip Antenna for The Low THz spectrum

5.1 Introduction

The terahertz band encompasses the frequency range 0.1 THz to 10 THz. [112]. The specified spectrum is regarded as a promising solution to meet the increasing demand for higher speed in future wireless communications. The non-ionizing nature of THz technology, as well as its low attenuation and great penetration, high-resolution image capabilities, and reduced diffraction compared to microwave spectrum, have sparked a lot of interest. [113]. The antenna is a vital component in enabling wireless communication and in meeting the needs of high data rates [114]. In the literature, several THz antennas have been reported, including dipole and spiral antennas, graphene antennas, leaky-wave antennas, and many other on-chip antennas. [115, 116]. Microstrip antennas have a number of desirable properties, such as low cost, small size, lightweight, etc [101]. This form of antenna has been used in several applications of wireless devices such as mobiles and wireless routing devices [78].

Microstrip patch antenna, on the other hand, presents a low gain and an extremely narrow operational bandwidth that is often less than 5 % [79]. At terahertz frequency band, electrically thick substrate generates undesired resonances response in the substrate. These undesired resonances may be avoided by reducing the thickness of the substrate by $\lambda_0/20$, where λ_0 is the wavelength in free-space [117].

5.2 PBG Based Substrate

Metamaterials provide unique properties including frequency pass bands, stop bands, and band gaps that aren't typically found in nature. These metamaterial structures are actually realised by arranging dielectric materials and metallic conductors in a periodic pattern. Artificial periodic objects, depending on the application area, may prevent or facilitate the transmission of electromagnetic waves in a certain frequency range, regardless of polarization state or incident angles. Metamaterial characteristics, namely crystal photonic and PBG based, which that are grouped under the wide term Electromagnetic Band Gap (EBG), are utilized to minimize antenna size and enhance performance According to [118], the bandwidth of a microstrip patch antenna utilizing PBG based substrate might be increased by 35% compared to a conventional microstrip patch antenna. By implanting periodic air gap cylinders into the antenna substrate, the effective dielectric permittivity of the dielectric can be reduced [119]. PBG based substrate minimizes surface wave loss, which importantly improves the antenna response in terms of bandwidth, gain, and directivity [120]. Furthermore, the periodic arrangement of airspace within PBG based designs improves the radiation efficiency without changing radiator size [118].

5.3 Background of Study and Scope

According to the literature, cylindrical holes in the PBG based substrate are commonly used to improve performance of the antenna. In [121], This is accomplished by distributing cylindrical air holes in a hexagonal pattern. In [122], the influence of different symmetries on the return loss of photonic bandgap devices is examined, including rectangular, hexagonal, and quasiperiodic symmetries. However, there have been few studies in terms of the variation of the distribution and the form of the air holes in the PBG based substrates. In [123], by employing quadratic holes in the PBG based substrate, the antenna gain is increased from 4.5 dBi for the structure with cylindrical holes to 5 dBi for the substrate containing quadratic holes. In [124], the air cylinders were split into multiple groups of air holes, each with a distinct radius. In [125] a numerical optimisation of the air cylinder form is applied by discretizing every unit cell using a binary map.

In our contribution, the features of patch antenna are improved for THz wireless applications by employing PBG based structures. A novel PBG based structure with greater bandwidth and higher gain is presented based on these earlier achievements. Initially, segmented air cylinders are used to improve the reference antenna. Next, genetic algorithms and segmented objects approach is employed to assist the optimisation of the PBG based structures. Segmented objects method with genetic algorithms approaches are used to efficiently identify an optimum solution of the best air gap design and their arrangement in the antenna substrate.

5.4 Basic Antenna

The goal of this initial design is to create a high-gain structure with an irregular octagonal form. For this objective, an extensive parametric study is applied. A 50

Ohms microstrip feed line is used to excite the radiator element, which is mounted on top of the inhomogeneous grounded substrate. The octagonal radiator was chosen in order to introduce another parameter (Corner) to the optimisation process via a parametric analysis, allowing for additional flexibility in the optimisation process. The length of the radiator is set to be a half-wavelength at the desired operating frequency as an initial point for the design process. The length of the antenna is better matched to the other parameters of the antenna by means of a parametric research in order to deliver higher accuracy in terms of resonant frequency. With the addition of PBG based to the antenna substrate, a parametrical research was conducted to maintain the required resonance frequency, which included just the parameters of the PBG based configuration, namely the cylinders radius, lattice constant, location and dimensions of the air cylinders matrix. Figure 5.1 (a) shows the final antenna geometry, whereas Table 5.4 contains the final antenna parameters.

All of the suggested antenna designs are made on a Polyamide substrate with a height of $h = 100\mu m$, a dielectric permittivity of $\epsilon_r = 3.5$, and a loss tangent of 0.008. The greater gain and radiation efficiency values of polyimide in the dielectric section of the antenna, as studied in [126], are the reasons for choosing it over FR-4. The photonic bandgap configuration of this first antenna is made up of 7×7 air cylinders embedded in the substrate with the same radius, height, and lattice constant. Note that all conductors are modeled as two-dimensional perfect electrical conductors (PEC) [127].

Ansoft High-Frequency Structure Simulator ($HFSS$) is used to design and model this antenna, which allows for quick and accurate analysis of high-frequency components such as couplers, filters, antennas, planar and multilayer components. The developed PBG based antenna is shown in Figure 5.1 (b) as a 3D view. Figure 5.2 shows the S11 curve derived for this reference antenna. The frequency interval

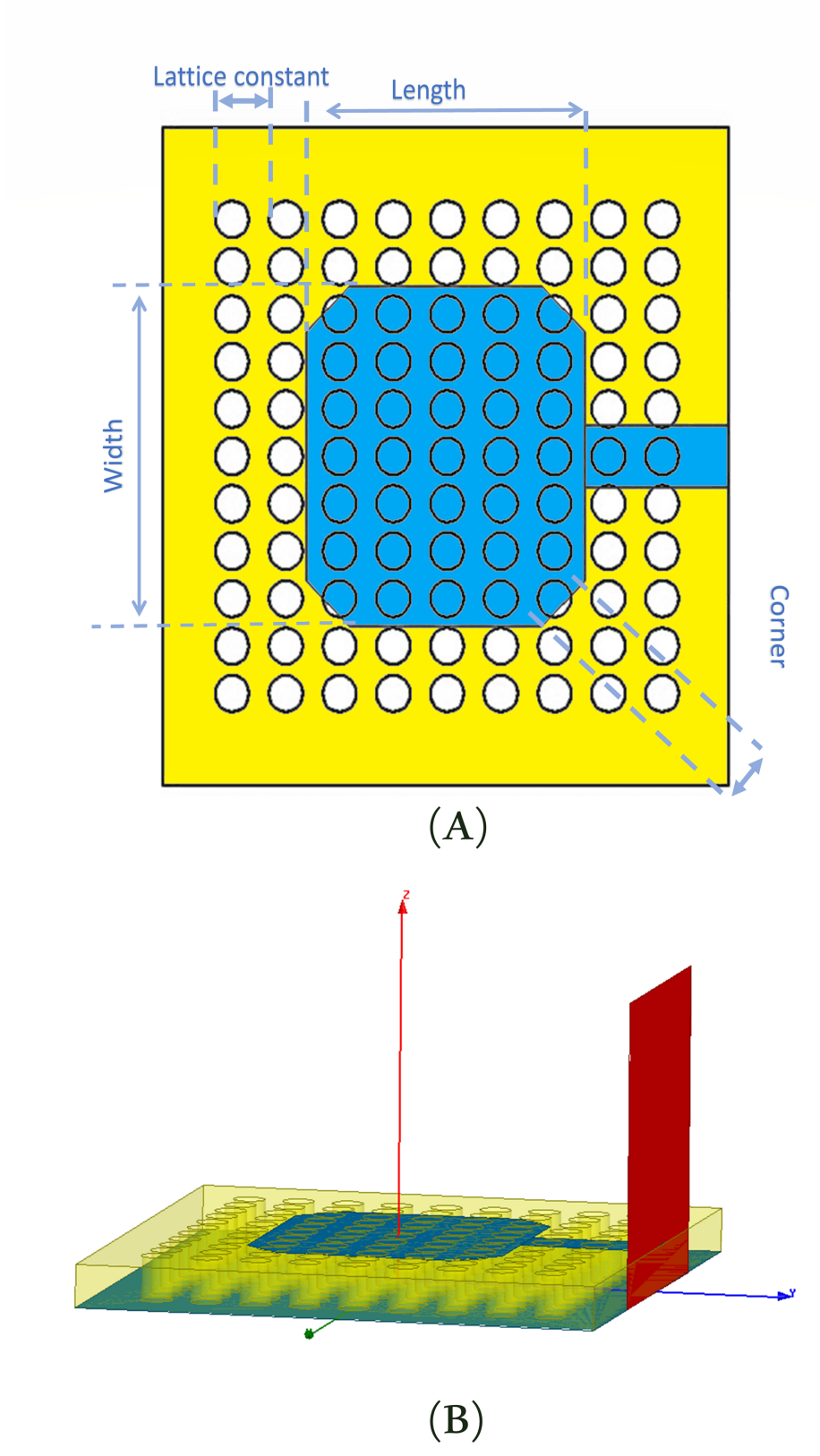

Figure 5.1: (*A*) *PBG* structure of the reference antenna, (B) created antenna in *HFSS*.

Table 5.1: Obtained dimensions for the reference antenna.

Parameter		*Value* (μm)
Antenna	*Length*	470.8
	Width	404
	Corner	124.4
Substrate	*Hight*	100
	Width	118
	Length	118
	Cylinder radius	035
	Lattice constant	
	$Y - axis$	100
	$X - axis$	100

where the return loss is below 10 dB is known to as the corresponding bandwidth. Accordingly, the antenna has a 65 GHz impedance bandwidth spanning 0.255 THz to 0.32 THz. This outcome is due to the usage of PBG based, which allows for the decrease of the surface wave's influence along the grounded dielectric substrate, hence improving the antenna's return loss and increasing the antenna bandwidth and gain [128]. The attained gain and radiation efficiencies are 9.09 dBi and 93 %, respectively, overcoming the primary shortcoming of printed antennas in terms of low gain and efficiency.

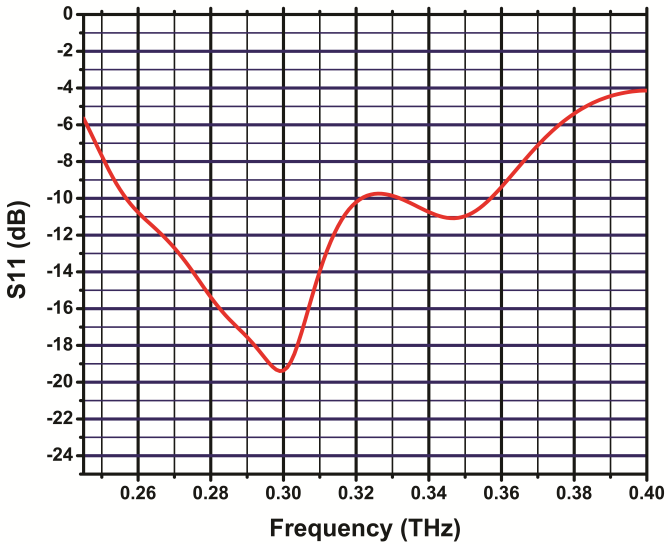

Figure 5.2: Return loss curve.

5.5 SOT Method

In most cases, based on design space optimisation using bio-inspired techniques, microstrip antenna optimisation entails creating a binary map by extracting the object to optimize into a 2D matrix of sub-objects and encoding this object into a binary string where a "1" indicates the existence of the generated sub-object and a "0" indicates the absence of the generated sub-object [129, 130]. To attain a decent map resolution, this optimisation approach necessitates a significant number of data processing steps, which dramatically increases simulation time because of the increased mesh size, and a huge number of iterations are necessary to explore the entire object space. In our case, the optimisation of the reference antenna will be guided by an efficient design optimisation approach based on design space optimisation that is reasonably affordable in terms of processing time. The Ansoft $HFSS$ design environment's cylinder feature allows to construct segmented shapes like circles, ellipses, and cylinders. By changing the parameter S_g, the number of segments may be changed automatically. This aids in the creation of a large number of segmented cylinders of various shapes with the same radius and a variable integer value for S_g parameter. The cylinder object is termed true surfaces cylinder in the initial value, $Sg = 0$, and the integer values 1 and 2 are not acceptable values. Figure 5.3 displays a top section view comparison of a cylinder generated with true and segmented surfaces giving a parameter S_g values of three or more which will be employed in the optimisation procedure. Figure 5.4 illustrates a basic three-type

Figure 5.3: Segmented and true surfaces cylinders

antenna layout generated using this optimisation approach. The difference between these three setups is in the S_g parameter when using the same antenna settings and modifying the PBG substrate configuration. The values of S_g in configurations "A," "B," and "C" are 3, 4, and 0 respectively. Figure 5.5 provides the obtained S11 curves for different combinations. In configuration “A”, the related bandwidth is 93 GHz ranging from 0.26 THz to 0.353 THz. In configuration “B”, 88 GHz of bandwidth is obtained, ranging from 0.265 THz to 0.353 THz. In configuration “C”, 85 GHz of bandwidth ranging from 0.268 THz to 0.453 THz. The minimum reflection coefficient is -27.15 dB, -23.50 dB and -23.69 dB for configuration “A”, “B”, and “C” respectively. These findings show a bandwidth improvement from 20 to 28 GHz, as well as a deeper S11 at the resonance frequency of 0.3 THz. For configurations "A," "B," and "C," the resulting gain is 9.18 dBi, 9.3 dBi, and 9.06 dBi, respectively.

Since there is an observed diminution in gain of th configuration "C," an optimal solution between antenna bandwidth, gain, and frequency invariance must be found. It’s worth noting that there isn’t much of a change between such settings. Once we utilize a much more intricate arrangement and give varied radius and S_g values to each air cylinder, the difference is more obvious.

The PBG based substrate is created using this segmented object idea by including an $X \times Y$ array of true surface cylinders onto the substrate and assigning a separate value of Sg_{xy} and radius to each air cylinder. The optimisation method looks for the optimal antenna substrate design in terms of air-gap distribution, shape, and size. The optimisation method can automatically modify the surface of the substrate and explore the antenna space using the SOT guiding approach. In order to adjust the substrate structure throughout the optimisation process and identify the optimum air gap configuration for the given ideal solutions, genetic

algorithms will be used with the *SOT* guiding approach.

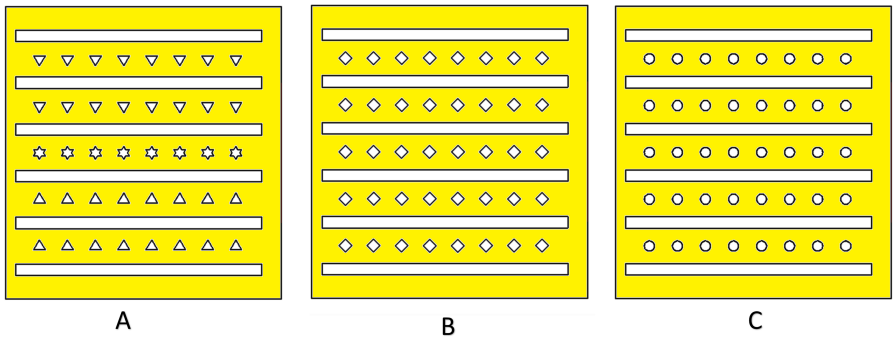

Figure 5.4: Air gap setup

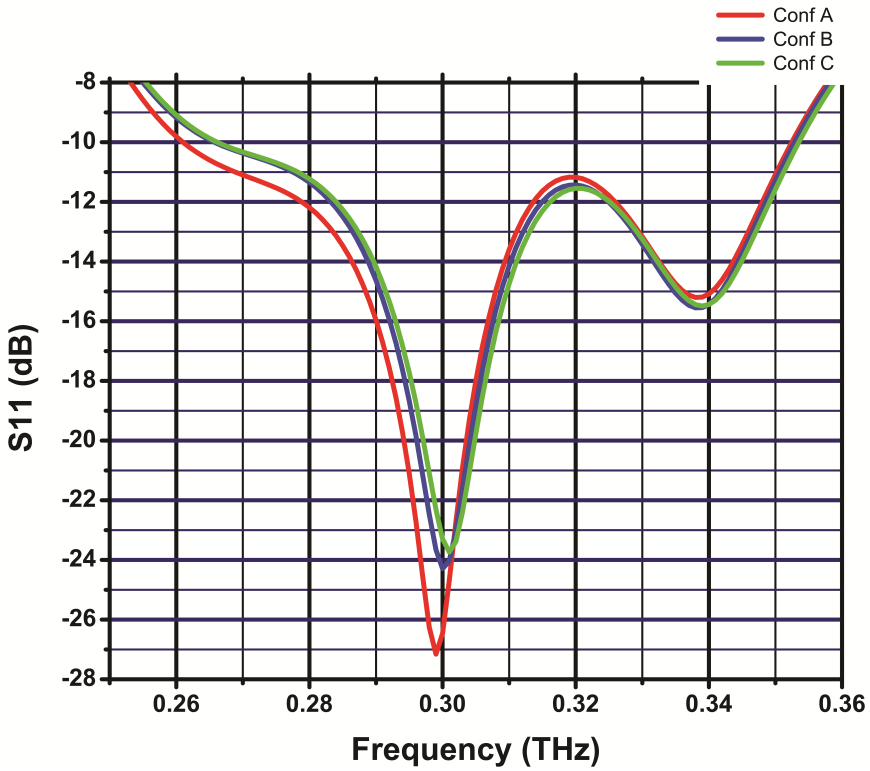

Figure 5.5: Return loss plots of the *PBG* A, B, and C configurations.

5.6 GAs Optimisation and SOT Guiding Approach

5.6.1 Optimization criterion

To determine the optimal PBG based substrate design, the segmented objects approach is employed to guide the optimisation utilizing genetic algorithms. The PBG based substrate is first created by including an X $\times$ Y matrix of real surface cylinders into the substrate. The optimisation process is then given additional design freedom by using vertical rectangular boxes. The four rectangular boxes are constructed utilizing the rotation feature in the $HFSS$ design environment to allow the algorithm to automatically modify the angle of the rectangular boxes from 0° to 360°. To avoid the junction of rectangles and cylinders and to maintain the periodic distribution of the PBG based structure, only two states are permitted: 0° for a horizontal rectangle and 90° for a vertical rectangle. Then, within a certain range, we describe a set of variables to solve, each of which is linked to a design parameter such as the width, length, angle, cylinder radius, number of segments, placements, and distances between these air objects. Finally, the optimisation is carried out by applying a variety of configurations utilizing GAs to apply a completely automated design space optimisation.

$HFSS$ includes modeling and statistical analysis interfaces that may be used to assess the response of the optimized structure locally. This type of optimisation usually needs dozens or hundreds of rounds and may not yield satisfactory results. To address this issue, we include antennas 1, 2, and 3 in the first generation with the other randomly produced people in order to improve the optimisation efficiency by employing a better beginning generation. The processing data when a large number of variables to be optimized will be quite huge, and the system may become sluggish owing to the high I/O needs. The optimisation is separated into two parts

to solve this problem. The geometry is adjusted in the first stage to determine the optimal air gap arrangement. In the second stage, the optimum configuration's characteristics are tweaked in order to find ways to improve antenna performance. When no geometry modifications are necessary, such as when optimizing a material attribute or port excitation, the algorithm may choose a copy of geometrically comparable meshes to reuse the mesh. The total optimisation process will be sped up as a result of this. Small modifications to some design items may be ignored by the algorithm, allowing the mesh refinement to continue without having to restart the entire process. To acquire an accurate simulation result, the mesh convergence must be validated at the end of optimisation.

5.6.2 Genetic algorithms

After the main features of design space optimisation have been presented using the segmented object approach, genetic algorithms are introduced in this section. In the field of electromagnetics, genetic algorithms (GAs) are a powerful optimisation approach. GAs belong to a category of optimisation techniques known as stochastic optimizers. In general, GAs has been utilized to improve the performance of microstrip patch antennas by improving bandwidth, resonant frequency accuracy, gain, directivity, and compactness, among other things [131, 132]. The cost function is used to evaluate a group of persons termed generation. After then, a new generation is formed by mating these individuals depending on their assessed fitness. Under the pressure of the cost function, the trial solutions are meant to converge toward an optimal solution. GAs create numerous generations using stochastic operators such as selection, crossover, and mutation in order to find the best solution. The information from the analyzed solution or the fitness function is not used by genetic algorithms to select where to explore the design space further. Instead, they

employ a systematic approach to random selection in order to arrive at an optimal solution that fulfills a minimal cost value in relation to the cost function. It's worth noting that this iterative process generates consecutive generations until a specified minimum cost value is attained.

The *GAs* optimisation's convergence is determined by two main factors: the automated design (or parameter) modification method and the applied cost function. The first factor allows the optimisation method to efficiently lead the algorithm and explore the antenna space, while the second factor allows the space discovery to evaluate a wide range of design configurations. The GA handles the optimisation variables that are supplied as an n-dimensional vector x after they have been specified. Finite element analysis may be used to analyze each design instance and provide a cost value. *GAs* generate the first generation of individuals at random and tweaks the variable values with each successive generation until an optimum solution is found with acceptable precision. The flow chart of the genetic algorithm-based optimisation is shown in Figure 5.6.

The goal of *GAs* is to reduce return loss, increase bandwidth, and increase gain. As a result, a multi-goal cost function that covers all of these factors is required. Equation 1 compares the calculated return loss at the resonant frequency ($S_{11}(f_r)$ to the desired return loss $d_1S_{11}$and quantifies the error. Subtracting these two parameters permits the evaluation of the design in terms of the obtained return loss. The closer the value of $dcost_1$ is to 0, the deeper S_{11} is obtained and the closer to the desired one. This equation is squared in order to increase the exploration interval to better discover the design space. Similarly, equation 2 compares the calculated gain with the desired gain ($dGain$) and quantifies the error. Equation 3 is a multipoint search where the algorithm looks for the largest possible bandwidth according to the d_2S_{11} criterion.

νolt

$$cost_1 = \left(S_{11}\left(f_r\right) - d_1 S_{11}\right)^2 \tag{5.1}$$

Where

f_r : the resonance frequency.

$d_1 S_{11}$: the desired return loss.

$$cost_2 = \left(G\left(f_r\right) - dGain\right)^2 \tag{5.2}$$

Where $dGain$: the desired return loss.

$$cost_3 = \left(S_{11}\left(f_i\right) - d_2 S_{11}\right)^2 \tag{5.3}$$

Where

f_i : the sampling frequency.

$d_2 S11$: the desired bandwidth criterion.

Equation 4 allows for the overall cost of all earlier parameters to be calculated. This cost function includes numerous objectives, and the parameter w_i allows to assign a higher or lower weight to each of them. The objective with the highest weight is the one that gets the most attention.

$$COST = \sum_{i=1}^{3} w_i \cos t_i \tag{5.4}$$

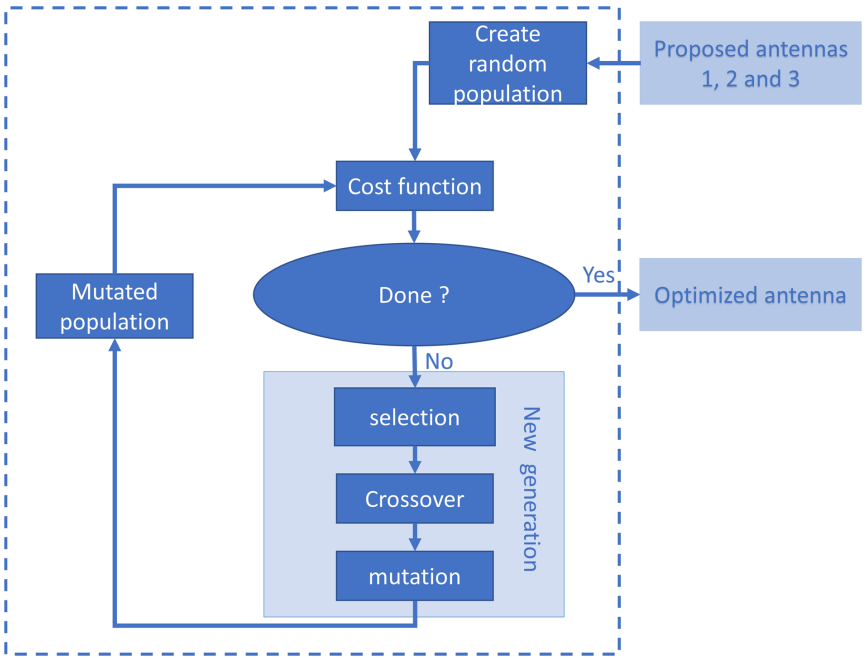

Figure 5.6: Optimisation flow chart.

5.7 Space Optimisation

The use of high-fidelity EM analysis in the design of modern antennas structures provides precise performance evaluation, but it is CPU expensive, notably if the number of geometrical parameters to be changed is large. As a result, the antenna optimisation is divided into two steps. The first step is to optimize the design space. The derived configuration's parameters are then optimized. The optimisation method looks for the optimal substrate arrangement in the first stage. To put it another way, the method is utilized to find the ideal air gap geometry and distribute it throughout the antenna substrate. The following parameters entered into the optimisation analysis: the number of segments S_g for each air cylinder, the matrix dimensions, the width and angle of rectangle boxes, and the number of segments S_g for each air cylinder, lattice constants L_x and L_y in x and y directions respectively. The desired return loss, gain and bandwidth criterion in this first optimisation are

$d_1S_{11} = -35$ dB, $dGain = 9\ dBi$, $d_2S_{11} = -10\ dB$ respectively. The weights for each sub-goal are as follows : $w_1 = 0.2$, $w_2 = 0.4$, $w_3 = 0.4$. It was observed during this optimisation that the segmented cylinders could be classified into three groups based on their distribution in the substrate. As a result, the number of segments for each type of segmented cylinder is allocated to a distinct parameter; such as S_{g1} for the first type, S_{g2} for the second type, S_{g3} for the third type. In order to produce a uniform distribution for the PBG based structure, these parameters are given to another optimisation using GAs. The obtained PBG based configuration is shown in Figure 5.7 shows the PBG based setup that was developed. When it comes to the first sort of cylinders, $S_{g1} = 4$, the unit function is used to link rectangular air boxes to segmented cylinders of this type so that they do not collide. The segmented air holes in the second type of cylinder with $S_{g2} = 8$, are centered and form a 3×6 matrix. For the third kind of segmented cylinders with $S_{g3} = 3$, the same matrix dimension is achieved, which is replicated in the two areas alongside the first matrix.

Figure 5.8 shows the antenna return loss utilizing the resulting substrate structure with GAs. The indicating bandwidth is 110 GHz, starting from 261 GHz to 371 GHz. The resultant gain for this optimised antenna is 9.08 dBi. When compared to the findings of the reference antenna, this antenna offers a bandwidth improvement of more than 69.23 %. The antenna gain and return loss, on the other hand, can be improved further. Another optimization is made in the next section for this reason.

5.8 Parameters Optimisation

The remainder of the parameters are optimized using the acquired arrangement from the previous step. The parameter Sg, the position of the air holes, and the dimension of the air holes matrix are not included in this second GAs-based optimisation study. This allows us to keep the same PBG based distribution and geometry and continue

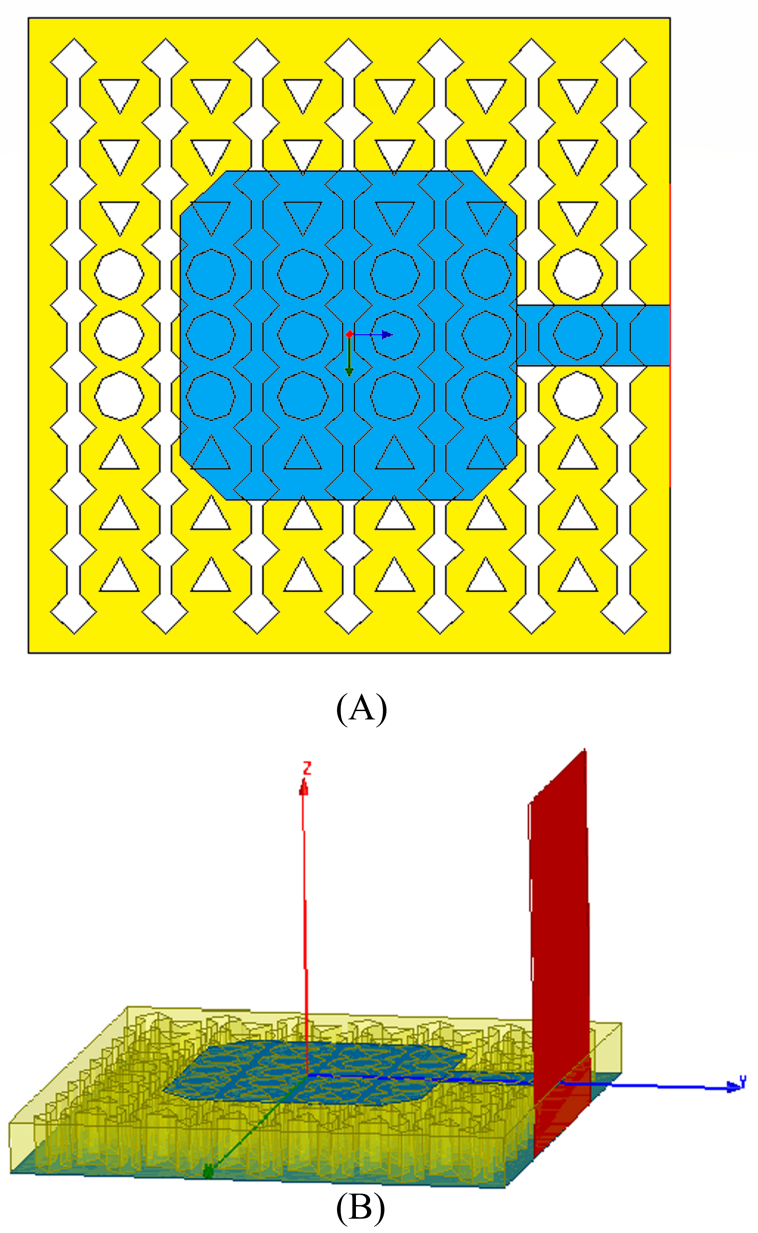

Figure 5.7: (A) The achieved configuration after space optimisation, (B) *HFSS* created antenna.

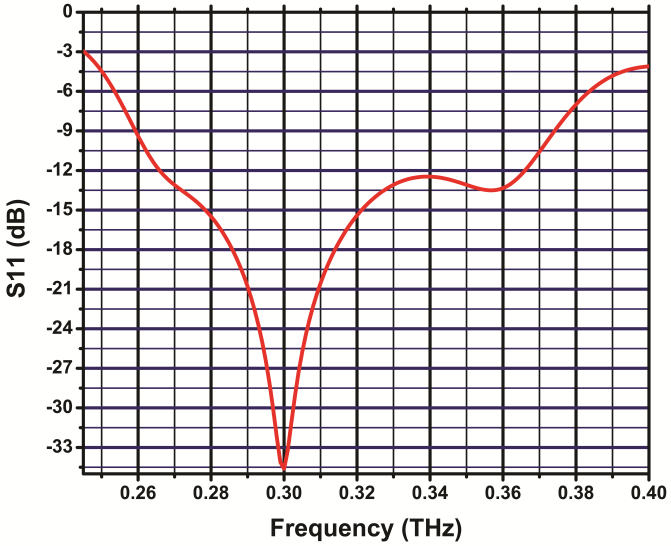

Figure 5.8: Produced return loss plots after space optimisation.

the simulation by optimizing the dimensions of the PBG based configuration we've acquired. As a result, the width and length of the rectangular air boxes, as well as the radius of the three types of segmented cylinders, are all optimized. The same GAs are used to optimise these PBG based structure parameters based on the folowing stop criterion: $d_1S_{11} = -70$ dB, $dGain = 10$ dBi, $d_2S_{11} = -10$ dB. It's interesting to note that the better these numbers are, the less probable it is to achieve the stop condition. Thus, a maximum number of generations must be set, during which the algorithm selects the best solution from among all those considered. Figure 5.9 presents the finalized substrate configuration. For segmented cylinders with Sg = 3, the radius is significantly reduced, and the other parameters are just adjusted to this new radius with a minimal change. The resulting graph of the return loss for this final optimization are shown in Figure 5.10. As it can be seen, adjusting the air gap dimension of the generated configuration from the first GAs-based optimisation results in a significant improvement. With a return loss of -58.70 dB and a gain of 9.43 dBi, the achieved bandwidth is 133 GHz, range from 255 GHz to 388 GHz.The

plot of the total gain radiation pattern is shown in Figure 5.11. Accordingly, a positive gain is obtained in H-plane from $-90°$ to $90°$, and a peak gain in E-plane close to 10 dBi in the broadside direction.

In Table 5.2, the achieved results are compared to some of the most recent similar research. The suggested antenna, which was optimized using SOT and GAs, has a greater gain. The antenna gain in the optimized antenna has increased by 3.74%, from 9.09 dBi in the reference antenna to 9.43 dBi in the optimized antenna. note that at this range of frequency, the antenna element becomes too small as its size must be scaled with the wavelength, and the acquired gain is fairly acceptable for a single radiator element. The BW/Fr factor is used to measure the performance in terms of bandwidth since these comparable antennas resonate at various frequencies and the bandwidth grows at the same time as the resonant frequency Fr. accordingly, the enhanced antenna has a higher bandwidth factor compared to other published antennas. Note that the SOT guiding approach and GAs optimization led in a 104.62 % increase in bandwidth. The improved antenna has a second deeper value of S_{11}. How ever, When this value is less than or equal to -10 dB, it is less important than the other stated parameters, hence it was given a lower attention (reduced weight) in the cost function. Nonetheless, when compared to the reference antenna, there was a 208.94 % increase in return loss.

5.9 Conclusion

This chapter describes a novel PBG based THz band antenna having a bandwidth of 44% and a center frequency of 0.3 THz. GAs and SOT guiding methods were used in the optimization. The segmented objects approach was utilized to assist the optimisation of the PBG based substrate, to explore the design space, and to automatically adjust the shape and dimensions. After the optimization, the gains,

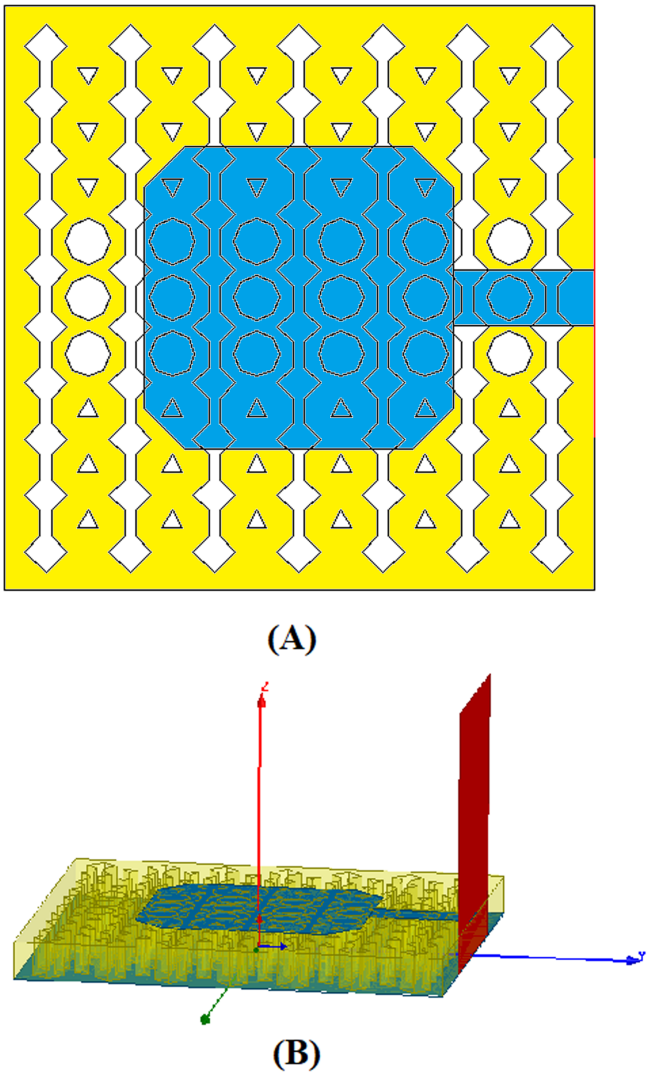

Figure 5.9: (A) The new setup after parameters optimisation, (B) *HFSS* created antenna.

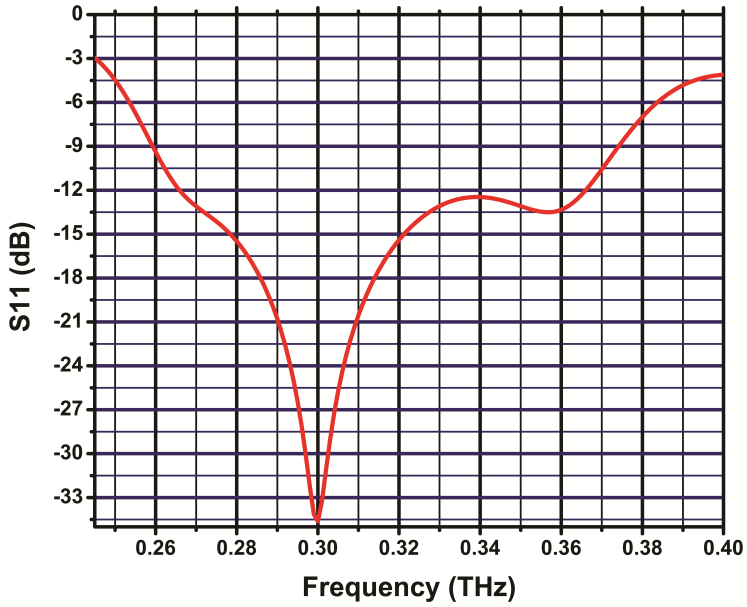

Figure 5.10: Parameters optimisation's return loss.

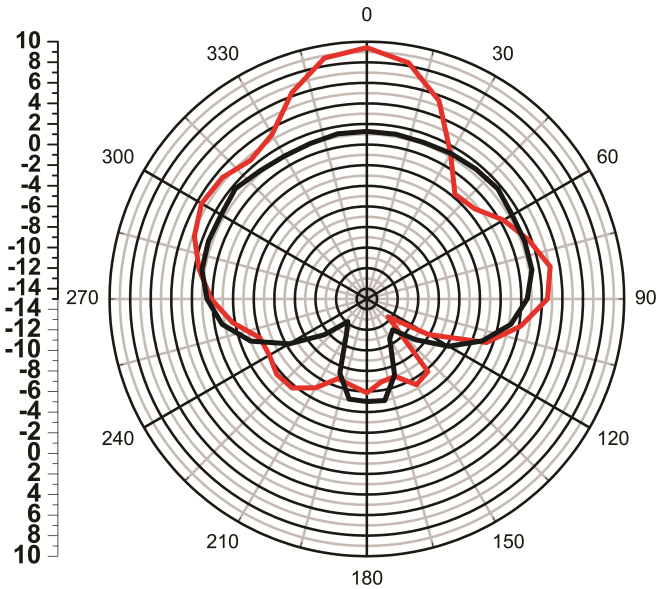

Figure 5.11: The gain of the final optimised antenna

Table 5.2: Antennas Comparison to the most recent reported works.

	$Fr\ (THz)$	$S11\ (dB)$	$BW\ (GHZ)$	BW/Fr	$GAIN\ (dBi)$	$Year$
Reference antenna	0.3	−19	63	21%	9.09	2021
Antenna A	0.3	−27.15	93	31%	9.18	2021
Antenna B	0.3	−23.50	88	29.33%	9.3	2021
Antenna C	0.3	−23.69	85	28.33%	9.06	2021
Optimized Antenna	0.3	−58.70	133	44.33%	9.43	2021
[133]	0.96	−13.05	310	32.29%	3.8	2017
[134]	0.75	−35	50	6.66%	5.09	2018
[125]	0.62	−28.42	128	20.64%	9.17	2019
[135]	0.312	−51.24	22.68	7.269%	5.6	2018
[124]	0.61	−83.73	280	37.70%	9.19	2019
[136]	0.1	26	6	6%	7.56	2016

bandwidth, and return loss increased by 3.74 percent, 104.62 percent, and 208.94 percent, respectively. In comparison to the relevant reported antennas, the suggested antenna has a larger bandwidth, acceptable gain, and excellent impedance matching. $HFSS$ software was used to verify the acquired results. These antenna characteristics make it a better contender for future wireless communications modules as well as other THz and millimeter wave technologies.

General Conclusion and Perspectives

The goal of this thesis is to design new millimeter-wave microstrip antenna structures that meet the requirements of wide BW and high gain. In the first chapter, the research's motivation, as well as the objectives and contributions, are outlined. This chapter shows the literature research efforts that have been devoted and various methods that are proposed for the millimeter waves spectrum. The specific properties of the millimeter-wave spectrum, as well as major factors to consider during antenna design, are also described. During this chapter, it was demenstrated that complex antenna structure may lead to overpriced systems. That's why much of the effort has to be focused on techniques for enhancing antennas within simple structures. This chapter also discusses several analytical approaches as well as the most prominent commercial simulators in the area. The remaining chapters construct and describe innovative antennas for optimal functioning in terms of BW, gain, and other features.

The first contribution includes a design for a 60-GHz circularly polarized antenna that makes use of LTCC technology. This proposed multilayer antenna was designed and simulated using HFSS software. The design exhibits a good radiation pattern response and a BW of more than 33 % at 60 GHz.

In the second contribution, a design of ultra-wideband microstrip antenna is presented for millimeter-wave applications below 100 GHz. This design has the capacity to cover a wide BW with good impedance matching. In the two utilized software, CST Studio and HFSS, this antenna offers a large BW in the millimetre wave spectrum below 100 GHz, ranging from 62.5 GHz to more than 96 GHz with a peak gain of 5.7 dBi. Another advantage of this antenna is that it may be directly integrated with other RF circuits using LTCC multilayer technology.

In the third contribution, another proposed antenna based on LTCC technology is presented to operate in the 60 GHz band.The proposed antenna offers a good impedance matching with an adequate gain. The obtained results have been verified using HFSS software and three prototypes are manufactured for measurement. A good agreement between simulation and measurement results was obtained.

In the fifth contribution, For broadband applications in the terahertz band, a novel optimised PBG-based antenna is presented. First, a parametric analysis is used to design and optimize the reference antenna to run at the resonance frequency of 0.3 THz. The optimisation is then carried out using a revolutionary approach known as segmented objects technique, which guides the optimisation of the PBG-based substrate using GAs. SOT enables you to alter the shape of the design space automatically and lead the optimisation using evolutionary algorithms in a simple and efficient manner. To identify the ideal PBG configuration, GAs are employed for optimisation and to determine an optimal solution for better trade-off of gain, BW and frequency invariance. Various PBG configurations are developed and examined throughout this optimisation using HFSS. The antenna has a 133 GHz of BW, a gain of 9.43 dB, and an extremely deep reflection coefficient of -58.70 dB. After optimisation, the gains, BW, and return loss improved by 3.74 %, 104.62 %, and 208.94 %, respectively. The electrical properties of these enhanced antennas were

compared to previous studies. The improved PBG structure's findings make the suggested antenna a feasible contender for meeting the requirement for high speed data in the future generation of wireless mobile networks.

There are several avenues for continuing this work. Some already mentioned in the manuscript concern the improvement of the structures proposed here or their integration into a more complete system, while others can be considered:

- Extending these proposed antennas to arrays for higher gain.
- Inroducing extra metasurfaces for higher efficiency and wider BW.
- Apply the SOT technique on the radiator surface (metallic part) for further enhancement.
- Increasing the capacity of the proposed antennas using other antenna technologies such as MIMO, Reconfigurability, Beamforming ...etc.

Bibliography

[1] Gijo Augustin, Qinjiang Rao, and Tayeb A. Denidni. Low-profile antennas. pages 1–29. Springer Singapore, 2015. doi: 10.1007/978-981-4560-75-7_55-1. URL https://doi.org/10.1007/978-981-4560-75-7_55-1.

[2] Michael Marcus and Bruno Pattan. Millimeter wave propagation: spectrum management implications. *IEEE Microwave Magazine*, 6(2):54–62, 2005.

[3] Kao-Cheng Huang and David J Edwards. *Millimetre wave antennas for gigabit wireless communications: a practical guide to design and analysis in a system context*. John Wiley & Sons, 2008.

[4] Shao-Qiu Xiao and Ming-Tuo Zhou. *Millimeter wave technology in wireless PAN, LAN, and MAN*. CRC Press, 2008.

[5] Mohamed Himdi. Tutorial 1: Mm-wave antenna design and technologies. In *2014 IEEE Asia-Pacific Conference on Applied Electromagnetics (APACE)*, pages xiv–xiv. IEEE, 2014.

[6] Duixian Liu, Ulrich Pfeiffer, Janusz Grzyb, and Brian Gaucher. *Advanced millimeter-wave technologies: antennas, packaging and circuits*. John Wiley & Sons, 2009.

[7] Wanghua Wu, Robert Bogdan Staszewski, and John R Long. *Millimeter-wave digitally intensive frequency generation in CMOS*. Academic Press, 2015.

[8] Seong Ki Yoo, Simon L Cotton, and Lei Zhang. Measurement based path loss study for indoor device-to-device communications at 60 ghz. In *2019 8th Asia-Pacific Conference on Antennas and Propagation (APCAP)*, pages 239–240. IEEE, 2019.

[9] Thomas Deckmyn, Sam Agneessens, Ad CF Reniers, A Bart Smolders, Maarten Cauwe, Dries Vande Ginste, and Hendrik Rogier. A novel 60 ghz wideband coupled half-mode/quarter-mode substrate integrated waveguide antenna. *IEEE Transactions on Antennas and Propagation*, 65(12):6915–6926, 2017.

[10] Dmitriy S Makarov, Mikhail Yu Tretyakov, and Philip W Rosenkranz. Revision of the 60-ghz atmospheric oxygen absorption band models for practical use. *Journal of Quantitative Spectroscopy and Radiative Transfer*, 243:106798, 2020.

[11] Turker Yilmaz, Etimad Fadel, and Ozgur B. Akan. Employing 60 ghz ism band for 5g wireless communications. In *2014 IEEE International Black Sea Conference on Communications and Networking (BlackSeaCom)*, pages 77–82, 2014. doi: 10.1109/BlackSeaCom.2014.6849009.

[12] Ieee standard for information technology– local and metropolitan area networks– specific requirements– part 15.3: Amendment 2: Millimeter-wave-based alternative physical layer extension. *IEEE Std 802.15.3c-2009 (Amendment to IEEE Std 802.15.3-2003)*, pages 1–200, 2009. doi: 10.1109/IEEESTD.2009.5284444.

[13] Jian Zhang, Mury Thian, Guochi Huang, George Goussetis, and Vincent F Fusco. Mm-wave broadband wireless systems and enabling mmic technologies. *Microwave and Millimeter Wave Circuits and Systems: Emerging Design, Technologies, and Applications*, pages 295–324, 2012.

[14] Ieee standard for information technology–telecommunications and information exchange between systems–local and metropolitan area networks–specific requirements-part 11: Wireless lan medium access control (mac) and physical layer (phy) specifications amendment 3: Enhancements for very high throughput in the 60 ghz band. *IEEE Std 802.11ad-2012 (Amendment to IEEE Std 802.11-2012, as amended by IEEE Std 802.11ae-2012 and IEEE Std 802.11aa-2012)*, pages 1–628, 2012. doi: 10.1109/IEEESTD.2012.6392842.

[15] KV Rop, DBO Konditi, HA Ouma, and S Musyoki. Application of adaptive neuro-fuzzy inference system technique in design of rectangular microstrip patch antennas. *Journal of Agriculture, Science and Technology*, 15(1), 2014.

[16] Smriti Agarwal and Dharmendra Singh. Cpw-fed concurrent, dual band planar antenna for millimeter wave applications. *International Journal of Microwave and Wireless Technologies*, 10(9):1088–1095, 2018.

[17] Djamel Abbou. *Conception des antennes à haut gain pour la communication sans fil millimétrique à 60 GHz*. PhD thesis, 2019.

[18] Johann-Friedrich Luy, Peter Russer, et al. *Silicon-based millimeter-wave devices*. Springer Berlin Heidelberg, 1994.

[19] Indrasen Singh and VS Tripathi. Micro strip patch antenna and its applications: a survey. *Int. J. Comp. Tech. Appl*, 2(5):1595–1599, 2011.

[20] Gurdeep Singh and Jaget Singh. Comparative analysis of microstrip patch antenna with different feeding techniques. In *International Conference on Recent Advances and Future Trends in Information Technology (iRAFIT2012) Proceedings published in International Journal of Computer Applications®(IJCA)*, 2012.

[21] Bilal T Malik, Viktor Doychinov, Syed Ali R Zaidi, Nutapong Somjit, Ian D Robertson, and Charles W Turner. Higher-order mode substrate integrated waveguide cavity excitation for microstrip patch antenna arrays at 30-ghz. *Journal of Physics Communications*, 3(1):015017, 2019.

[22] Zhi Ning Chen and Xianming Qing. Gain enhancement of ltcc microstrip patch antenna by suppressing surface waves. *Substrate-Integrated Millimeter-Wave Antennas for Next-Generation Communication and Radar Systems*, pages 197–209, 2021.

[23] Jaco Du Preez and Saurabh Sinha. *Millimeter-wave antennas: configurations and applications*. Springer, 2016.

[24] Zhouyue Pi and Farooq Khan. An introduction to millimeter-wave mobile broadband systems. *IEEE communications magazine*, 49(6):101–107, 2011.

[25] Constantine A Balanis. Antenna theory, 4th editio, 2016.

[26] Kai Fong Lee and Kin-Fai Tong. *Microstrip Patch Antennas*, pages 787–852. Springer Singapore, Singapore, 2016. ISBN 978-981-4560-44-3. doi: 10.1007/978-981-4560-44-3_29. URL https://doi.org/10.1007/978-981-4560-44-3_29.

[27] Anil Pandey. *Practical microstrip and printed antenna design*. Artech House, 2019.

[28] Seyed Ali Razavi Parizi. Bandwidth enhancement techniques. In *Microstrip Antennas: Trends in Research on*, volume 1. BoD–Books on Demand, 2017.

[29] Aaron K Shackelford, Kai-Fong Lee, and Kwai Man Luk. Design of small-size wide-bandwidth microstrip-patch antennas. *IEEE antennas and propagation magazine*, 45(1):75–83, 2003.

[30] Wonbin Hong and Z Chen. Millimeter-wave antennas and arrays. *Handbook of antenna technologies*, pages 1787–1850, 2015.

[31] Duixian Liu and Yueping Zhang. *Antenna-in-package Technology and Applications*. John Wiley & Sons, 2020.

[32] Jin-Koo Rhee, Dan An, Sung-Chan Kim, and Bok-Hyung Lee. Millimeter-wave monolithic integrated circuit for wireless lan. *Millimeter Wave Technology in Wireless PAN, LAN, and MAN*, page 1, 2008.

[33] D. K. Kharbanda and P. K. Khanna. Design and development of ltcc based package for 3-axis packaging of mems sensors. In *2017 International Conference On Smart Technologies For Smart Nation (SmartTechCon)*, pages 917–920, 2017. doi: 10.1109/SmartTechCon.2017.8358505.

[34] Nouria Belambri, Dominique Dubouil, Christian Talbot, Ammar B Kouki, and Francois Gagnon. Design of a buried hybrid coupler for wideband applications using ltcc technology. In *2011 24th Canadian Conference on Electrical and Computer Engineering (CCECE)*, pages 001101–001104. IEEE, 2011.

[35] Ubaid Ullah, Nor Mahyuddin, Zainal Arifin, Mohd Zaid Abdullah, and Arjuna Marzuki. Antenna in ltcc technologies: a review and the current state of the art. *IEEE Antennas and Propagation Magazine*, 57(2):241–260, 2015.

[36] Li Guo, Ming-Chun Tang, and Mei Li. A low-profile dual-layer patch antenna with a circular polarizer consisting of dual semicircular resonators. *Sensors*, 18(6):1773, 2018.

[37] Steven Yang, Kai-Fong Lee, Ahmed Kishk, and Kwai-Man Luk. Design and study of wideband single feed circularly polarized microstrip antennas. *Progress In Electromagnetics Research*, 80:45–61, 2008.

[38] Boleslav Psota, Martin Klíma, Michal Nicák, and Ivan Szendiuch. Usage of ltcc technology in electronic packaging. In *Proceedings of the 36th International Spring Seminar on Electronics Technology*, pages 206–209. IEEE, 2013.

[39] Henry Lau. *Practical Antenna Design for Wireless Products*. Artech House, 2019.

[40] Marta Gil, Jordi Bonache, and Ferran Martin. Metamaterial filters: A review. *Metamaterials*, 2(4):186–197, 2008.

[41] Muhammad Ali Babar Abbasi, Marco A Antoniades, and Symeon Nikolaou. A compact reconfigurable nri-tl metamaterial phase shifter for antenna applications. *IEEE Transactions on Antennas and Propagation*, 66(2):1025–1030, 2017.

[42] Fengxia Li, Haiyan Chen, Qingting He, Yang Zhou, Li Zhang, Xiaolong Weng, Haipeng Lu, Jianliang Xie, and Longjiang Deng. Design and implementation of metamaterial polarization converter with the reflection and transmission polarization conversion simultaneously. *Journal of Optics*, 21(4):045102, 2019.

[43] Peng Yu, Lucas V Besteiro, Yongjun Huang, Jiang Wu, Lan Fu, Hark H Tan, Chennupati Jagadish, Gary P Wiederrecht, Alexander O Govorov, and Zhim-

ing Wang. Broadband metamaterial absorbers. *Advanced Optical Materials*, 7(3):1800995, 2019.

[44] Yahya Rahmat-Samii and H Mosallaei. Electromagnetic band-gap structures: classification, characterization, and applications. 2001.

[45] Fan Yang and Yahya Rahmat-Samii. *Electromagnetic band gap structures in antenna engineering*. Cambridge university press Cambridge, UK, 2009.

[46] Tianwei Deng and Yue Ping Zhang. *On-Chip Antennas*, pages 1–17. Springer Singapore, Singapore, 2014. ISBN 978-981-4560-75-7. doi: 10.1007/978-981-4560-75-7_56-1. URL https://doi.org/10.1007/978-981-4560-75-7_56-1.

[47] Qammer H Abbasi, Syeda Fizzah Jilani, Akram Alomainy, and Muhammad Ali Imran. *Antennas and Propagation for 5G and Beyond*. Institution of Engineering and Technology, 2020.

[48] Raimi Dewan, MKA Rahim, MR Hamid, MFM Yusoff, Noor Asmawati Samsuri, NA Murad, and K Kamardin. Artificial magnetic conductor for various antenna applications: An overview. *International Journal of RF and Microwave Computer-Aided Engineering*, 27(6):e21105, 2017.

[49] Edward J Rothwell and Raoul O Ouedraogo. Antenna miniaturization: definitions, concepts, and a review with emphasis on metamaterials. *Journal of Electromagnetic Waves and Applications*, 28(17):2089–2123, 2014.

[50] Balamati Choudhury. Metamaterial inspired electromagnetic applications. *NY: Springer*, 162(10.1007):978–981, 2017.

[51] Santosh Tyagi and Kirti Vyas. Bandwidth enhancement using slotted u-shape microstrip antenna with pbg ground. *International Journal of Advanced Technology & Engineering Research*, 3(1), 2013.

[52] Peter H. Siegel. THz instruments for space. *IEEE Transactions on Antennas and Propagation*, 55(11):2957–2965, November 2007. doi: 10.1109/tap.2007.908557. URL https://doi.org/10.1109/tap.2007.908557.

[53] Sasmita Dash and Amalendu Patnaik. Material selection for THz antennas. *Microwave and Optical Technology Letters*, 60(5):1183–1187, April 2018. doi: 10.1002/mop.31127. URL https://doi.org/10.1002/mop.31127.

[54] P. Lu, M. Steeg, K. Kolpatzeck, S. Dulme, B. Khani, A. Czylwik, and A. Stohr. Photonic assisted beam steering for millimeter-wave and THz antennas. In *2018 IEEE Conference on Antenna Measurements & Applications (CAMA)*. IEEE, September 2018. doi: 10.1109/cama.2018.8530567. URL https://doi.org/10.1109/cama.2018.8530567.

[55] M. I. B. Shams, Z. Jiang, J. Qayyum, S. M. Rahman, H.G. Xing, J. L. Hesler, P. Fay, and L. Liu. Characterization of terahertz antennas using photoinduced coded-aperture imaging. *Microwave and Optical Technology Letters*, 57(5): 1180–1184, March 2015. doi: 10.1002/mop.29051. URL https://doi.org/10.1002/mop.29051.

[56] Chao Gu, Steven Gao, and Benito Sanz-Izquierdo. Low-cost wideband low-THz antennas for wireless communications and sensing. In *2017 10th UK-Europe-China Workshop on Millimetre Waves and Terahertz Technologies (UCMMT)*. IEEE, September 2017. doi: 10.1109/ucmmt.2017.8068470. URL https://doi.org/10.1109/ucmmt.2017.8068470.

[57] Thomas Kleine-Ostmann and Tadao Nagatsuma. A review on terahertz communications research. 32(2):143–171, January 2011. doi: 10.1007/s10762-010-9758-1. URL https://doi.org/10.1007/s10762-010-9758-1.

[58] Isha Malhotra, Kumud Ranjan Jha, and Ghanshyam Singh. Terahertz antenna technology for imaging applications: a technical review. 10(3):271–290, February 2018. doi: 10.1017/s175907871800003x. URL https://doi.org/10.1017/s175907871800003x.

[59] Amar Adane, François Gallée, and Christian Person. Bandwidth improvements of 60ghz micromachining patch antenna using gap coupled u — microstrip feeder. In *Proceedings of the Fourth European Conference on Antennas and Propagation*, pages 1–5, 2010.

[60] K. Hettak, G.Y. Delisle, G.A. Morin, S. Toutain, and M. Stubbs. A novel variant 60-GHz CPW-fed patch antenna for broadband short range wireless communications. IEEE, July 2008. doi: 10.1109/aps.2008.4619753. URL https://doi.org/10.1109/aps.2008.4619753.

[61] Imad Ali, Ronald Y. Chang, and Jenny Yi-Chun Liu. Multilayer CPW-fed patch antenna on new AMC ground plane for 60 GHz millimeter-wave communications. IEEE, May 2016. doi: 10.1109/vtcspring.2016.7504357. URL https://doi.org/10.1109/vtcspring.2016.7504357.

[62] Hang Wong, Kung Bo Ng, Kwai Man Luk, Chi Hou Chan, and Quan Xue. Printed millimeter wave vertical patch antenna. IEEE, July 2010. doi: 10.1109/icccas.2010.5581889. URL https://doi.org/10.1109/icccas.2010.5581889.

[63] Syeda Fizzah Jilani and Akram Alomainy. Planar millimeter-wave antenna on

low-cost flexible PET substrate for 5g applications. IEEE, April 2016. doi: 10.1109/eucap.2016.7481680. URL https://doi.org/10.1109/eucap.2016.7481680.

[64] Sandeep Singh and Mridul Chawla. A review on millimeter wave communication and effects on 5g systems. 4(7):28–33, July 2017. doi: 10.17148/iarjset.2017.4705. URL https://doi.org/10.17148/iarjset.2017.4705.

[65] Cihat Seker, Muhammet Tahir Guneser, and Turgut Ozturk. A review of millimeter wave communication for 5g. IEEE, October 2018. doi: 10.1109/ismsit.2018.8567053. URL https://doi.org/10.1109/ismsit.2018.8567053.

[66] Theodore S. Rappaport, Yunchou Xing, George R. MacCartney, Andreas F. Molisch, Evangelos Mellios, and Jianhua Zhang. Overview of millimeter wave communications for fifth-generation (5g) wireless networks—with a focus on propagation models. 65(12):6213–6230, December 2017. doi: 10.1109/tap.2017.2734243. URL https://doi.org/10.1109/tap.2017.2734243.

[67] Adel Barakat, Ramesh Pokharel, and Hala Elsadek. Innovative techniques for 60-GHz on-chip antennas on CMOS substrate. InTech, January 2017. doi: 10.5772/66238. URL https://doi.org/10.5772/66238.

[68] Qing Huo Liu. *Commercial Antenna Design Tools*, pages 67–109. Springer Singapore, Singapore, 2016. doi: 10.1007/978-981-4560-44-3_5. URL https://doi.org/10.1007/978-981-4560-44-3_5.

[69] Thomas Weiland, Martin Timm, and Irina Munteanu. A practical guide to 3-d simulation. *IEEE Microwave Magazine*, 9(6):62–75, 2008.

[70] Vic Grout, Mobayode O Akinsolu, Bo Liu, Pavlos I Lazaridis, Keyur K Mistry, and Zaharias D Zaharis. Software solutions for antenna design exploration: A

comparison of packages, tools, techniques, and algorithms for various design challenges. *IEEE Antennas and Propagation Magazine*, 61(3):48–59, 2019.

[71] Zoltan Cendes. The development of hfss. In *2016 USNC-URSI Radio Science Meeting*, pages 39–40. IEEE, 2016.

[72] Douglas Henry Werner, Micah Dennis Gregory, Zhi Hao Jiang, and Donovan Brocker. Optimization methods in antenna engineering. In *Handbook of antenna technologies*, pages 321–376. Springer Singapore, 2016.

[73] Slawomir Koziel and Stanislav Ogurtsov. *Antenna design by simulation-driven optimization*. Springer, 2014.

[74] James Kennedy. The particle swarm: social adaptation of knowledge. In *Proceedings of 1997 IEEE International Conference on Evolutionary Computation (ICEC'97)*, pages 303–308. IEEE, 1997.

[75] Thomas Bäck, David B Fogel, and Zbigniew Michalewicz. *Evolutionary computation 1: Basic algorithms and operators*. CRC press, 2018.

[76] Rainer Storn and Kenneth Price. Differential evolution–a simple and efficient heuristic for global optimization over continuous spaces. *Journal of global optimization*, 11(4):341–359, 1997.

[77] Li Sun, Gang Ou, Yilong Lu, and Shusen T. Axial ratio bandwidth of a circularly polarized microstrip antenna. In *Advancement in Microstrip Antennas with Recent Applications*. InTech, March 2013. doi: 10.5772/54664. URL https://doi.org/10.5772/54664.

[78] A. Bondarik and D. Sjoberg. Investigation of reconfigurability for a stacked microstrip patch antenna pattern targeting 5g applications. In *2015 IEEE-*

APS Topical Conference on Antennas and Propagation in Wireless Communications (APWC). IEEE, September 2015. doi: 10.1109/apwc.2015.7300200. URL https://doi.org/10.1109/apwc.2015.7300200.

[79] Kai Da Xu, Han Xu, Yanhui Liu, Jianxing Li, and Qing Huo Liu. Microstrip patch antennas with multiple parasitic patches and shorting vias for bandwidth enhancement. *IEEE Access*, 6:11624–11633, 2018. doi: 10.1109/access.2018.2794962. URL https://doi.org/10.1109/access.2018.2794962.

[80] Hua-Juan Lee, Eric S. Li, Huayan Jin, Chung-Yi Li, and Kuo-Sheng Chin. 60 GHz wideband LTCC microstrip patch antenna array with parasitic surrounding stacked patches. *IET Microwaves, Antennas & Propagation*, 13 (1):35–41, October 2018. doi: 10.1049/iet-map.2018.5226. URL https://doi.org/10.1049/iet-map.2018.5226.

[81] Philip Ayiku Dzagbletey and Young-Bae Jung. Stacked microstrip linear array for millimeter-wave 5g baseband communication. *IEEE Antennas and Wireless Propagation Letters*, 17(5):780–783, May 2018. doi: 10.1109/lawp.2018.2816258. URL https://doi.org/10.1109/lawp.2018.2816258.

[82] Hua-Juan Lee, Eric S. Li, Chung-Yi Li, Yu-You Lin, Roger Lu, and Kuo-Sheng Chin. Bandwidth and gain enhancement of LTCC 60-GHz patch antenna by using AMC structure. *Journal of Electromagnetic Waves and Applications*, 33 (11):1463–1476, May 2019. doi: 10.1080/09205071.2019.1614483. URL https://doi.org/10.1080/09205071.2019.1614483.

[83] Mingjian Li and Kwai-Man Luk. Wideband magneto-electric dipole antenna for 60-GHz millimeter-wave communications. *IEEE Transactions on Antennas and Propagation*, 63(7):3276–3279, July 2015. doi: 10.1109/tap.2015.2425418. URL https://doi.org/10.1109/tap.2015.2425418.

[84] Yazan Al-Alem and Ahmed A. Kishk. Simple high gain 60 GHz antenna. In *2018 IEEE International Symposium on Antennas and Propagation & USNC/URSI National Radio Science Meeting*. IEEE, July 2018. doi: 10.1109/apusncursinrsm.2018.8608172. URL https://doi.org/10.1109/apusncursinrsm.2018.8608172.

[85] John L Volakis. *Antenna engineering handbook*. McGraw-Hill Education, 2007.

[86] S. Kundu, A. Chatterjee, S. K. Jana, and S. K. Parui. A compact umbrella-shaped UWB antenna with gain augmentation using frequency selective surface. *Radioengineering*, 27(2):448–454, June 2018. doi: 10.13164/re.2018.0448. URL https://doi.org/10.13164/re.2018.0448.

[87] Sadegh Mansouri Moghaddam, Jian Yang, and Andres Alayon Glazunov. Ultra-wideband millimeter-wave bowtie antenna. In *2017 International Symposium on Antennas and Propagation (ISAP)*. IEEE, October 2017. doi: 10.1109/isanp.2017.8228955. URL https://doi.org/10.1109/isanp.2017.8228955.

[88] Tale Saeidi, Idris Ismail, Wong Peng Wen, Adam R. H. Alhawari, and Ahmad Mohammadi. Ultra-wideband antennas for wireless communication applications. *International Journal of Antennas and Propagation*, 2019:1–25, April 2019. doi: 10.1155/2019/7918765. URL https://doi.org/10.1155/2019/7918765.

[89] Ján SCHNEIDER and Ján GAMEC. Overview of UWB low-profile planar antennas. *Acta Electrotechnica et Informatica*, 14(2):55–59, June 2014. doi: 10.15546/aeei-2014-0019. URL https://doi.org/10.15546/aeei-2014-0019.

[90] M. Du, J. Xu, X. Ding, J. P. Cao, J. H. Deng, and Y. L. Dong. A low-

profile wideband LTCC integrated circularly polarized helical antenna array for millimeter-wave applications. *Radioengineering*, 27(2):455–462, June 2018. doi: 10.13164/re.2018.0455. URL https://doi.org/10.13164/re.2018.0455.

[91] Parisa Shirvani, , and Hamidreza Shirzadfar and. Design a new configuration of micro strip rectangle patch antenna on different thickness substrate for telemedicine applications. *Journal of Nano- and Electronic Physics*, 8(3): 03028–1–03028–4, 2016. doi: 10.21272/jnep.8(3).03028. URL https://doi.org/10.21272/jnep.8(3).03028.

[92] Saadi Djidel, Mohamed Bouamar, and Djamel Khedrouche. A bandwidth enhancement and size reduction of monopole microstrip antenna for ultra wideband application. *World Journal of Engineering*, 2018.

[93] A. Bondarik and D. Sjoberg. Bias network and diode parasitics of a reconfigurable stacked microstrip patch antenna at 60 GHz. In *2016 IEEE-APS Topical Conference on Antennas and Propagation in Wireless Communications (APWC)*. IEEE, September 2016. doi: 10.1109/apwc.2016.7738180. URL https://doi.org/10.1109/apwc.2016.7738180.

[94] Kuo-Sheng Chin, Wen Jiang, Wenquan Che, Chih-Chun Chang, and Huayan Jin. Wideband LTCC 60-GHz antenna array with a dual-resonant slot and patch structure. *IEEE Transactions on Antennas and Propagation*, 62(1):174–182, January 2014. doi: 10.1109/tap.2013.2287294. URL https://doi.org/10.1109/tap.2013.2287294.

[95] Efri Sandi, , Rusmono Rusmono, Aodah Diamah, and Karisma Vinda. Ultra-wideband microstrip array antenna for 5g millimeter-wave applications. pages

198–204, 2020. doi: 10.12720/jcm.15.2.198-204. URL https://doi.org/10.12720/jcm.15.2.198-204.

[96] S. Bouttout, , Y. Bentrcia, S. Benkouda, T. Fortaki, , and and. Parametric study of stacked microstrip patch antenna with dissimilar substrates. *Journal of Nano- and Electronic Physics*, 10(4):04004–1–04004–4, 2018. doi: 10.21272/jnep.10(4).04004. URL https://doi.org/10.21272/jnep.10(4).04004.

[97] Y.P. Zhang and Duixian Liu. Antenna-on-chip and antenna-in-package solutions to highly integrated millimeter-wave devices for wireless communications. *IEEE Transactions on Antennas and Propagation*, 57(10):2830–2841, October 2009. doi: 10.1109/tap.2009.2029295. URL https://doi.org/10.1109/tap.2009.2029295.

[98] Dong Gun Kam, Duixian Liu, Arun Natarajan, Scott Reynolds, and Brian A. Floyd. Low-cost antenna-in-package solutions for 60-GHz phased-array systems. In *19th Topical Meeting on Electrical Performance of Electronic Packaging and Systems*. IEEE, October 2010. doi: 10.1109/epeps.2010.5642554. URL https://doi.org/10.1109/epeps.2010.5642554.

[99] Theodore S. Rappaport, James N. Murdock, and Felix Gutierrez. State of the art in 60-GHz integrated circuits and systems for wireless communications. *Proceedings of the IEEE*, 99(8):1390–1436, August 2011. doi: 10.1109/jproc.2011.2143650. URL https://doi.org/10.1109/jproc.2011.2143650.

[100] Woogeun Rhee, editor. *Wireless Transceiver Circuits*. CRC Press, September 2018. doi: 10.1201/b18162. URL https://doi.org/10.1201/b18162.

[101] Jayashree P. Shinde, Raj Kumar, and Mahadev D. Uplane. Circular polarization in defected hexagonal shaped microstrip antenna. *Wireless Per-*

sonal Communications, 75(2):843–856, September 2013. doi: 10.1007/s11277-013-1394-3. URL https://doi.org/10.1007/s11277-013-1394-3.

[102] Sakshi Srivastava, , Ankit Khandelwal, and Dr. Sandeep Sharma. Microstrip patch antenna: A survey. *IOSR Journal of Electrical and Electronics Engineering*, 9(4):07–13, 2014. doi: 10.9790/1676-09420713. URL https://doi.org/10.9790/1676-09420713.

[103] Antti E. I. Lamminen, Jussi Saily, and Antti R. Vimpari. 60-GHz patch antennas and arrays on LTCC with embedded-cavity substrates. *IEEE Transactions on Antennas and Propagation*, 56(9):2865–2874, September 2008. doi: 10.1109/tap.2008.927560. URL https://doi.org/10.1109/tap.2008.927560.

[104] Wei Liu, Zhi Ning Chen, and Xianming Qing. 60-GHz thin broadband high-gain LTCC metamaterial-mushroom antenna array. *IEEE Transactions on Antennas and Propagation*, 62(9):4592–4601, September 2014. doi: 10.1109/tap.2014.2333052. URL https://doi.org/10.1109/tap.2014.2333052.

[105] Imad Ali, Ronald Y. Chang, and Jenny Yi-Chun Liu. Multilayer CPW-fed patch antenna on new AMC ground plane for 60 GHz millimeter-wave communications. In *2016 IEEE 83rd Vehicular Technology Conference (VTC Spring)*. IEEE, May 2016. doi: 10.1109/vtcspring.2016.7504357. URL https://doi.org/10.1109/vtcspring.2016.7504357.

[106] X. W. Zhu, J. Gao, X. Y. Cao, T. Li, Y. J. Zheng, L. L. Cong, L. R. J, and B. W. Zhu. A novel low-RCS and wideband circularly polarized patch array based on metasurface. *Radioengineering*, 27(1):99–107, April 2019. doi: 10.13164/re.2019.0099. URL https://doi.org/10.13164/re.2019.0099.

[107] Y. Ge, Y. J. Zhao, and J. Q. Chen. Wideband RCS reduction and gain

enhancement for a patch antenna with broadband AMC structure. *Radioengineering*, 27(1):45–52, April 2019. doi: 10.13164/re.2019.0045. URL https://doi.org/10.13164/re.2019.0045.

[108] Mukesh Kumar Khandelwal, Binod Kumar Kanaujia, and Sachin Kumar. Defected ground structure: Fundamentals, analysis, and applications in modern wireless trends. *International Journal of Antennas and Propagation*, 2017: 1–22, 2017. doi: 10.1155/2017/2018527. URL https://doi.org/10.1155/2017/2018527.

[109] Camilla Kärnfelt. *Solutions d'intégration en boîtier de puces MMIC via la technologie LTCC*. PhD thesis, Télécom Bretagne; Université de Bretagne Occidentale, 2016.

[110] S. Kirthiga and M. Jayakumar. Performance studies and review of millimeter wave MIMO beamforming at 60 GHz. *Procedia Technology*, 21:658–666, 2015. doi: 10.1016/j.protcy.2015.10.079. URL https://doi.org/10.1016/j.protcy.2015.10.079.

[111] Djamel Khezzar, Djamel Khedrouche, and Tayeb A. Denidni. 60 GHz broadband LTCC antenna for 5g mobile communication systems. 20(1):1–5, February 2021. doi: 10.18280/i2m.200101. URL https://doi.org/10.18280/i2m.200101.

[112] Kumud Ranjan Jha and G. Singh. Analysis and design of terahertz microstrip antenna on photonic bandgap material. *Journal of Computational Electronics*, 11(4):364–373, August 2012. doi: 10.1007/s10825-012-0416-9. URL https://doi.org/10.1007/s10825-012-0416-9.

[113] G. Jemima Nissiyah and M. Ganesh Madhan. Graphene-based photocon-

ductive antenna structures for directional terahertz emission. *Plasmonics*, 14 (4):891–900, November 2018. doi: 10.1007/s11468-018-0871-7. URL https://doi.org/10.1007/s11468-018-0871-7.

[114] Mohammad Alibakhshikenari, Bal S. Virdee, Chan H. See, Raed A. Abd-Alhameed, Francisco Falcone, and Ernesto Limiti. High-gain metasurface in polyimide on-chip antenna based on CRLH-TL for sub-terahertz integrated circuits. *Scientific Reports*, 10(1), March 2020. doi: 10.1038/s41598-020-61099-8. URL https://doi.org/10.1038/s41598-020-61099-8.

[115] Mohammad Alibakhshikenari, Bal S. Virdee, Chan H. See, Raed A. Abd-Alhameed, and Ernesto Limiti. High performance on-chip array antenna based on metasurface feeding structure for terahertz integrated circuits. In *2019 44th International Conference on Infrared, Millimeter, and Terahertz Waves (IRMMW-THz)*. IEEE, September 2019. doi: 10.1109/irmmw-thz.2019.8874127. URL https://doi.org/10.1109/irmmw-thz.2019.8874127.

[116] Mohammad Alibakhshikenari, Bal S. Virdee, Chan H. See, Raed A. Abd-Alhameed, Francisco Falcone, and Ernesto Limiti. Overcome the limitations of performance parameters of on-chip antennas based on metasurface and coupled feeding approaches for applications in system-on-chip for THz integrated-circuits. In *2019 IEEE Asia-Pacific Microwave Conference (APMC)*. IEEE, December 2019. doi: 10.1109/apmc46564.2019.9038524. URL https://doi.org/10.1109/apmc46564.2019.9038524.

[117] Mohammad Alibakhshikenari, Bal S. Virdee, Chan H. See, Pancham Shukla, Shahram Salekzamankhani, Raed A. Abd-Alhameed, Francisco Falcone, and Ernesto Limiti. Study on improvement of the performance param-

eters of a novel 0.41-0.47 THz on-chip antenna based on metasurface concept realized on 50ţm GaAs-layer. *Scientific Reports*, 10(1), July 2020. doi: 10.1038/s41598-020-68105-z. URL https://doi.org/10.1038/s41598-020-68105-z.

[118] Ádller de O. Guimarães, José P. da Silva, and Jonathan P. P. Pereira. Analysis of a microstrip antenna with variation on substrate PBG hexagonal. *Microwave and Optical Technology Letters*, 58(4):826–831, February 2016. doi: 10.1002/mop.29679. URL https://doi.org/10.1002/mop.29679.

[119] Shen Ting-gen, Zhou Yue-qun, Ge Jun, Yu Feng-chao, Ji Pei-lai, and Wang Gang. Investigation of patch antennas based on drilled PBG structure. *Journal of Russian Laser Research*, 29(3):255–261, May 2008. doi: 10.1007/s10946-008-9014-5. URL https://doi.org/10.1007/s10946-008-9014-5.

[120] Yongxi Qian, D. Sievenpiper, V. Radisic, E. Yablonovitch, and T. Itoh. A novel approach for gain and bandwidth enhancement of patch antennas. In *Proceedings RAWCON 98. 1998 IEEE Radio and Wireless Conference (Cat. No.98EX194)*. IEEE. doi: 10.1109/rawcon.1998.709176. URL https://doi.org/10.1109/rawcon.1998.709176.

[121] Betoven O. de Andrade and Laercio M. de Mendonca. Frequency invariance, gain improvement, and fast design in 3d-printed photonic band gap antennas with quadratic holes. *Microwave and Optical Technology Letters*, 61(10):2295–2305, June 2019. doi: 10.1002/mop.31897. URL https://doi.org/10.1002/mop.31897.

[122] A. Hocini, M.N. Temmar, D. Khedrouche, and M. Zamani. Novel approach for the design and analysis of a terahertz microstrip patch antenna based on

photonic crystals. *Photonics and Nanostructures - Fundamentals and Applications*, 36:100723, September 2019. doi: 10.1016/j.photonics.2019.100723. URL https://doi.org/10.1016/j.photonics.2019.100723.

[123] Jonathan P. P. Pereira, José P. da Silva, Ádller de, and O. Guimarães. Microstrip antennas design based in periodic and quasiperiodic PBG symmetries. *Microwave and Optical Technology Letters*, 57(12):2914–2917, September 2015. doi: 10.1002/mop.29479. URL https://doi.org/10.1002/mop.29479.

[124] Mohamed Nasr Eddine Temmar, Abdesselam Hocini, Djamel Khedrouche, and Mehdi Zamani. Analysis and design of a terahertz microstrip antenna based on a synthesized photonic bandgap substrate using BPSO. *Journal of Computational Electronics*, 18(1):231–240, January 2019. doi: 10.1007/s10825-019-01301-x. URL https://doi.org/10.1007/s10825-019-01301-x.

[125] Mary Ann B. Meador, Sarah Wright, Anna Sandberg, Baochau N. Nguyen, Frederick W. Van Keuls, Carl H. Mueller, Rafael Rodríguez-Solís, and Félix A. Miranda. Low dielectric polyimide aerogels as substrates for lightweight patch antennas. *ACS Applied Materials & Interfaces*, 4(11):6346–6353, November 2012. doi: 10.1021/am301985s. URL https://doi.org/10.1021/am301985s.

[126] Tanzeela Mitha and Maria Pour. Investigation of dominant transverse electric mode in microstrip patch antennas. *IEEE Transactions on Antennas and Propagation*, 67(1):643–648, January 2019. doi: 10.1109/tap.2018.2874765. URL https://doi.org/10.1109/tap.2018.2874765.

[127] Navdeep Singh, Sarabjeet Singh, and R. K Sarin. Effect of photonic band gap structure on planar antenna configuration. In *2010 10th Mediterranean*

Microwave Symposium. IEEE, August 2010. doi: 10.1109/mmw.2010.5605140. URL https://doi.org/10.1109/mmw.2010.5605140.

[128] Y. Rahmat-Samii, J. M. Kovitz, and H. Rajagopalan. Nature-inspired optimization techniques in communication antenna designs. *Proceedings of the IEEE*, 100(7):2132–2144, July 2012. doi: 10.1109/jproc.2012.2188489. URL https://doi.org/10.1109/jproc.2012.2188489.

[129] J.M. Johnson and Y. Rahmat-Samii. Genetic algorithms and method of moments (GA/MoM): A novel integration for antenna design. In *IEEE Antennas and Propagation Society International Symposium 1997. Digest*. IEEE. doi: 10.1109/aps.1997.631495. URL https://doi.org/10.1109/aps.1997.631495.

[130] Bo Liu, Hadi Aliakbarian, Zhongkun Ma, Guy A. E. Vandenbosch, Georges Gielen, and Peter Excell. An efficient method for antenna design optimization based on evolutionary computation and machine learning techniques. *IEEE Transactions on Antennas and Propagation*, 62(1):7–18, January 2014. doi: 10.1109/tap.2013.2283605. URL https://doi.org/10.1109/tap.2013.2283605.

[131] Parvathy P. Chandran and Sanoj Viswasom. Gain and bandwidth optimization of a novel microstrip patch antenna. In *2014 Fourth International Conference on Advances in Computing and Communications*. IEEE, August 2014. doi: 10.1109/icacc.2014.80. URL https://doi.org/10.1109/icacc.2014.80.

[132] Lei Xie, Yong-Chang Jiao, and Gang Zhao. A compact band-notched UWB slot antenna optimized by genetic algorithm. In *2011 IEEE International Conference on Microwave Technology & Computational Electromagnetics*. IEEE,

May 2011. doi: 10.1109/icmtce.2011.5915520. URL https://doi.org/10.1109/icmtce.2011.5915520.

[133] Gohar Varamini, Asghar Keshtkar, and Mohammad Naser-Moghadasi. Compact and miniaturized microstrip antenna based on fractal and metamaterial loads with reconfigurable qualification. *AEU - International Journal of Electronics and Communications*, 83:213–221, January 2018. doi: 10.1016/j.aeue.2017.08.057. URL https://doi.org/10.1016/j.aeue.2017.08.057.

[134] Mohammad Naderi, Ferdows B. Zarrabi, Fereshteh Sadat Jafari, and Speideh Ebrahimi. Fractal EBG structure for shielding and reducing the mutual coupling in microstrip patch antenna array. *AEU - International Journal of Electronics and Communications*, 93:261–267, September 2018. doi: 10.1016/j.aeue.2018.06.028. URL https://doi.org/10.1016/j.aeue.2018.06.028.

[135] Meidyawati Virginia Hidayat and Catur Apriono. Design of 0.312 THz microstrip linear array antenna for breast cancer imaging application. In *2018 International Conference on Signals and Systems (ICSigSys)*. IEEE, May 2018. doi: 10.1109/icsigsys.2018.8372671. URL https://doi.org/10.1109/icsigsys.2018.8372671.

[136] M. S. Rabbani and H. Ghafouri-Shiraz. Fabrication tolerance and gain improvements of microstrip patch antenna at terahertz frequencies. *Microwave and Optical Technology Letters*, 58(8):1819–1824, May 2016. doi: 10.1002/mop.29920. URL https://doi.org/10.1002/mop.29920.